ДОКЛАДЫ
АКАДЕМИИ НАУК СССР

SOVIET PHYSICS

"Doklady"

VOLUME 1 NUMBER 2

A Translation
of the
"Physics Section"
of the
Proceedings of the Academy of Sciences of the USSR

Published by the
AMERICAN INSTITUTE OF PHYSICS
INCORPORATED

SOVIET PHYSICS

"Doklady"

A translation of the "Physics Section" of the Proceedings of the Academy of Sciences of the USSR.

A publication of the

AMERICAN INSTITUTE
OF PHYSICS

Governing Board

Allen V. Astin
Robert F. Bacher
W. S. Baird
H. A. Bethe
R. T. Birge
Frank D. Dexter
I. C. Gardner
S. A. Goudsmit
Charles Kittel
Hugh S. Knowles
R. B. Lindsay
William F. Meggers
Harry F. Olson
R. R. Palmer
R. F. Paton
Eric Rodgers
Ralph A. Sawyer
Frederick Seitz
H. D. Smyth
Mark W. Zemansky

Officers and Staff

Frederick Seitz
Chairman, Governing Board
Henry A. Barton
Director
Wallace Waterfall
Executive Secretary
Mark W. Zemansky
Treasurer
Theodore Vorburger
Advertising Manager
Ruth F. Bryans
Publication Manager
Kathryn Setze
Assistant Treasurer
Alice Mastropietro
Circulation Manager
Eugene H. Kone
Director of Public Relations

American Institute of Physics Advisory Board on Russian Translations

Elmer Hutchisson, *Chairman*
Dwight Gray, Morton Hamermesh, Vladimir Rojansky,
Viktor Weisskopf

Soviet Physics—"Doklady" is a bi-monthly journal published by the American Institute of Physics for the purpose of making available in English reports of current Soviet research in physics as contained in the "Physics Section" of the Proceedings of the Academy of Sciences of the USSR. The Proceedings appears thirty-six times per year and the "Physics Sections" are accumulated and English translations of them are published in six issues per year.

Transliteration of the names of Russian authors follows the system employed by the Library of Congress.

This translating and publishing project was undertaken by the Institute in the conviction that dissemination of the results of research everywhere in the world is invaluable to the advancement of science. The National Science Foundation of the United States encouraged the project initially and is supporting it in large part by a grant. Translation and printing are being handled by Consultants Bureau, Inc.

The American Institute of Physics and its translators propose to translate faithfully all of the scientific material in the "Physics Section" of the Proceedings of the Academy of Sciences of the USSR appearing after January 1, 1956. The views expressed in the translated material, therefore, are intended to be those expressed by the original authors, and not those of the translators nor of the American Institute of Physics.

One volume is published annually. Volume 1 will consist of six issues and will contain all scientific material published in the "Physics Section" of the original Russian journal during the 1956 calendar year.

Subscription Prices:

Per year (6 issues)	
United States and Canada	$25.00
Elsewhere	27.50
Back Numbers	
Single copies	$ 6.00

Subscriptions should be addressed to the American Institute of Physics, 57 East 55th Street, New York 22, N. Y.

Copyright by American Institute of Physics 1956

SOVIET PHYSICS
"Doklady"

A translation of the "Physics Section" of the Proceedings of the Academy of Sciences of the USSR.

VOLUME 1, NUMBER 2 MARCH-APRIL, 1956

ON THE TRUE SHAPE OF X-RAY SPECTRA

M. A. Blokhin

(Presented by Academician A. A. Lebedev August 4, 1955)

The problem of obtaining the true shape of x-ray spectra from the distorted experimental shape has been satisfactorily solved only for dispersive emission lines.

The general problem has been solved in principle by Smith [1]. Smith's method can only be used in connection with work done with a double crystal spectrometer. However, this method was not developed far enough to be of practical use.

In some papers [2, 3] on the true shape of optical spectra, and in particular combination scattering lines, this problem has been solved practically only for certain simple line shapes which are "dome-shaped" and for the simplest types of distortion. The methods developed in these papers do not provide a practical solution for the complicated line shapes which are characteristic of emission and absorption x-ray spectra associated with the outer atomic levels of molecules and solids, especially of elements belonging to transition series.

Let us consider the simplest case when the distortions introduced by the apparatus may with sufficient accuracy be approximated by the dispersion function

$$\psi(x) = \varphi(x-t) = \frac{1}{\pi\gamma}\,\frac{1}{1+\left(\frac{x-t}{\gamma}\right)^2}, \tag{1}$$

where t is the abscissa of the maximum of $\psi(x)$; γ is the half-breadth; and the area of the dispersive curve is taken as unity. In this case for some simple shapes of "true" curves f(x) it is easy to find the shape F(x) distorted by the apparatus. Thus, if $f(x) = f_0/\,[1+(x+\ x/\gamma')^2]$,

$$F(x) = \frac{\gamma'}{\gamma'+\gamma}\,\frac{f_0}{1+\left(\frac{x}{\gamma'+\gamma}\right)}. \tag{2}$$

If $f(x) = (f_0/\pi)\,[\,\pi/2 - \text{arc tan}\,(x/\gamma')]$,

$$F(x) = \frac{f_0}{\pi}\left(\frac{\pi}{2} - \arctan\frac{x}{\gamma'-\gamma}\right). \tag{3}$$

These results follow directly from the well-known equation (see for example, [3]) which defines F(x):

$$F(x) = \int_{-\infty}^{\infty} f(t)\,\varphi(x-t)\,dt. \tag{4}$$

Let the spectrogram in question contain a standard line of dispersive shape in accordance with data obtained with a double crystal spectrometer and with the true half-breadth γ'. If the experimental shape of this line obtained with other apparatus is dispersive the distortion $\varphi(x-t)$ is dispersive. By subtracting γ' from the experimental half-breadth we obtain according to (2) the desired parameter γ of (1). If the standard line is selected to be sufficiently close to the investigated spectral region it may be assumed that $\varphi(x-t)$ will be characterized in this region by the same value of γ.

The graph of F(x) is known from experiment. By employing one of the well-known methods of graphical harmonic analysis F(x) can be represented as a trigonometric series. If the spectral range $0 \le x \le a$ is selected for correction we take a for one fourth of a period and continue F(x) artificially in the remainder of the period in such a way that F(x) will be an odd function with symmetry of the third kind. We then have

$$F(x) = \sum_k B_k \sin \frac{k\pi}{2a} x, \tag{5}$$

where $k = 2n + 1$; $n = 0, 1, 2, \ldots$. We also represent the distortion function $\varphi(x - t)$ as a trigonometric series. For this purpose we take a for a fourth of a period and continue $\varphi(x - t)$ artifically in the remainder of the period in such a way that $\varphi(x - t)$ will be an even function with symmetry of the third kind. We then have

$$a\varphi(x - t) = \sum_l C_l \cos \frac{l\pi}{2a}(x - t), \tag{6}$$

where $l = 2n + 1$. The coefficients C_l can be found with sufficient accuracy (for $a \gg \gamma$) from the formula

$$C_l = \exp\left(-\frac{l\gamma\pi}{2a}\right) - \frac{l\gamma}{2a} \sin \frac{l\pi}{2} \tag{7}$$

We represent the true shape of the spectrum, that is f(t), by the series

$$f(t) = \sum_h A_h \sin \frac{h\pi}{2a} t, \tag{8}$$

where $h = 2n + 1$. f(t) possesses the same symmetry as F(x).

If F(x) represents an emission line and outside of the finite interval (0, a) the value of F(x) does not exceed experimental error, it is evident that for the correct shape it is possible to take $f(t) = 0$ outside the interval $0 \le t \le a$. Then in (1) the finite limits of integration can be taken as 0 and a. If F(x) represents the curve of the absorption spectral intensity and x is proportional to the frequency ν, then taking the lower asymptote as zero intensity it is possible to designate a as the upper limit of values of x outside of which F(x) does not exceed experimental error. We divide the area of the curve F(x) for $x < a$ into two parts (Figure 1a) separated by the inverse tangent curve expressed by

$$F_1(x) = \frac{f_0}{\pi}\left(\frac{\pi}{2} - \arctan \frac{x - b}{\gamma_1}\right), \tag{9}$$

where f_0 is the ordinate of the upper asymptote of F(x); γ_1 and b are arbitrary constants whose choice depends on the magnitude of the portion of F(x) which is subject to correction. The portion of F(x) to the left of $F_1(x)$ can be corrected directly according to (3); after correction it will be bounded by the curve

$$f_1(x) = \frac{f_0}{\pi}\left(\frac{\pi}{2} - \arctan \frac{x - b}{\gamma_1 - \gamma}\right). \tag{10}$$

For correction of the portion of the area of F(x) bounded by F(x) and $F_1(x)$ we find graphically the difference between these functions (Figure 1b). The curve which is obtained is bounded by very small ordinates on both sides; therefore the choice of finite limits of integration is now easy. Thus the problem of correcting the absorption spectrum is practically reduced to a problem which is entirely analogous to the case of emission spectra.

Substituting (5), (6) and (8) in (4) and integrating between the finite limits 0 and 2a we obtain

$$A_k = \frac{B_k}{C_k}. \tag{11}$$

This ratio is the solution of the integral equation (4) with respect to f(t).

It should be noted here that the simple ratio obtained between the coefficients A_k, B_k and C_k holds true only for integration between the given limits 0 and 2a. Doubling the interval of integration compared with the range a in which the function F(x) is given leads to double edge distortion since the functions F(x) and $\varphi(x-t)$ were artificially continued outside the interval (0, a) from considerations of symmetry and orthogonality. However, if $a \gg \gamma$ it is obvious that the edge effect introduces noticeable distortions only at a small distance from the limits of the interval (0, a).

In order to demonstrate graphically the accuracy of the proposed method and to estimate the edge effects a "correction" was made of the artificial curve imitating the spectrum of the transition elements with a characteristic "bump" on the principal absorption edge. The choice of an "artificial" curve results mainly from the fact that in this case it is easy to find the exact shape of the corrected curve; in addition, experimental errors are excluded which after correction of the experimental curve could induce considerable deviation from the correct spectral curve. The curve of F(x) (Figure 1a) is the graph of the function

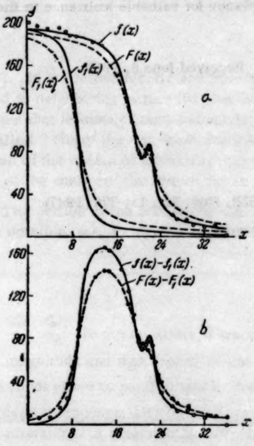

Figure 1.
a) Curves of F(x), f(x), $F_1(x)$ and $f_1(x)$; circles indicate values obtained for f(x).
b) Curves of $F(x) - F_1(x)$ and $f(x) - f_1(x)$; dots indicate the results of summing the series approximately representing $F(x) - F_1(x)$; circles indicate the results of summing the series of odd sinusoids with amplitudes given by (11).

$$F(x) = \frac{200}{\pi}\left(\frac{\pi}{2} - \arctan\frac{x-19}{3}\right) + \frac{25}{1+\left(\frac{x-22}{2}\right)^2}, \tag{12}$$

i.e., it is the superposition of the inverse tangent and dispersion curves whose corrected shapes are easily obtained from (3) and (2):

$$f(x) = \frac{200}{\pi}\left(\frac{\pi}{2} - \arctan\frac{x-19}{2}\right) + \frac{50}{1+(x-22)^2}, \tag{13}$$

where the distortion function is taken in the form (1) for $\gamma = 1$. The auxiliary function $F_1(x)$ is chosen according to (9) for b = 9 and $\gamma_1 = 2$. The corrected shape $f_1(x)$ is determined from (10). The difference $F(x) - F_1(x)$ is shown graphically in Figure 1b. The decomposition of this curve was carried out to the 49th harmonic by Chebyshev's method.

Figure 1b also shows the "corrected" curve $f(x) - f_1(x)$, constructed from the exact analytic expressions for these functions. After correction by the above method in the interval (0; 36) the amplitudes A_k were found. The summation of series (8) at many points, as can be seen from Figure 1b, indicates entirely satisfactory approximation to the correct curve with the exception of the small regions adjacent to the boundaries.

The graphical summation of the calculated ordinates of the function $f(x) - f_1(x)$ with the ordinates of the graph of $f_1(x)$ gave the points of the "corrected" function $f(x)$. These points are indicated in Figure 1a.

The above method is of special value because it enables us to "correct" the shape of the spectrum for the distortion introduced by the outside level of the atom and thus to obtain the correct shape of the energy dependence of the density of states $n(E)$ (more precisely, the product $n(E)p(E)$ where $p(E)$ is the probability of the corresponding transition).

In conclusion I consider it my pleasant duty to thank M. G. Khaplanov for valuable assistance in the development of the above method.

V. M. Molotov Scientific Research Physico-Mathematical
Institute of Rostov State University

Received June 8, 1955

LITERATURE CITED

[1] L. P. Smith, Phys. Rev. 46, 5, 343 (1934).

[2] V. M. Chulanovskii and A. V. Timoreva, Bull. Acad. Sci. USSR, Phys. Ser. 11, 376 (1947).

[3] M. M. Sushchinskii, J. Exptl.-Theoret. Phys. (USSR) 25, 1, 87 (1953).

ON THE INDIRECT EXCHANGE INTERACTION

S. V. Vonsovskii, Corr. Mbr. Acad. Sci. USSR,

and Iu. M. Seiidov

1. In antiferromagnetic and ferromagnetic ionic crystals the magnetic ions of transition metals are not located in neighboring lattice sites but are separated by nonmagnetic ions (oxygen, sulfur, selenium, etc.). We know that ferromagnetism and antiferromagnetism result from the electrostatic interaction of electrons in unfilled shells of the transition elements with resultant spin moment. Special quantum properties of the wave function of the system of electrons (antisymmetry with respect to permutations) lead to considerable dependence of the energy of the system due to the electrostatic interaction on the resultant spin.

The portion of the energy containing the spin dependence is customarily called the exchange energy. In vector notation (see, for example, [1]) the operator of this energy is

$$\hat{H}_{ex} = -\frac{1}{2}\sum_{(i\neq k)} I_k \hat{\vec{\sigma}}_i \hat{\vec{\sigma}}_k, \tag{1}$$

where $\hat{\vec{\sigma}}_i$, $\hat{\vec{\sigma}}_k$ are the operators of electron spin vectors of sites i and k; I_{ik} are the exchange integrals, whose magnitude and sign depend on the specific properties of the system. Depending on the sign of I_{ik} the system tends either to parallel spin orientation ($I_{ik} > 0$) or to antiparallel orientation ($I_{ik} < 0$). The magnitude of I_{ik} depends exponentially on the distance between sites R_{ik}; therefore it is sufficient in (1) to limit oneself to the interaction of nearest neighbors. However in the case of ionic compounds (for example MnO, NiO, Fe_2O_3, etc.) the magnetic ions are not nearest neighbors. Nevertheless, the exchange interaction in these compounds is almost of the same order as in metallic ferromagnetics, where the magnetic ions are nearest neighbors. On the other hand, if in the ionic compounds I_{ik} is understood to be the ordinary exchange integral between next to nearest neighbors among magnetic ions its magnitude would have to be at least 2 to 3 orders smaller. It thus necessarily follows that an essential role in the exchange interaction within ionic crystals is played by the electrons of nonmagnetic ions. The first calculation of this indirect exchange interaction for Tutton's salts and alum was carried out by Kramers [2] following Bloch's suggestion, and developed further for antiferromagnetics [3-6]. It was shown that the indirect exchange arises only in the third approximation of perturbation theory as a result of virtual transfers of electrons from nonmagnetic to magnetic ions. The shortcoming of these calculations is the fact that they solve not the problem of the crystal but that of the triatomic molecule with four electrons, and that the result is then without proof extended to the crystal. There is thus naturally a need for a many-electron calculation of indirect exchange in the crystal.

2. As an initial model it is convenient to use the polar many-electron model of the crystal [7-9]. We shall consider an ionic crystal lattice comprising two kinds of sites: f) sites occupied by nonmagnetic ions (for example, O^{--}) and g) sites occupied by magnetic ions (for example, Mn^{++}). We shall assume that in the normal state each magnetic ion has one s-electron in the unfilled shell and each nonmagnetic ion has two p-electrons with antiparallel spins.* Since the ferromagnetic and antiferromagnetic properties of crystals are

---

*Strictly speaking a magnetic ion, in MnO for instance, has five electrons in an unfilled 3d-shell whose spins are parallel by Hund's rule, and a nonmagnetic ion has six 2p-electrons. We may expect, however, that such a complication will not alter the final result qualitatively.

due principally to spin and not orbital magnetism ("frozen" orbits), for the sake of simplicity of calculation it is entirely permissible in first approximation to consider the electron in the magnetic ions as being not in d- but in s-states. In order to describe the ground state we start with the Hamiltonian of the system expressed in the second quantized representation

$$\hat{H} = \sum_{\alpha,\alpha'} L(\alpha,\alpha')\,\hat{a}^{+}_{\alpha}\hat{a}_{\alpha'} + \frac{1}{2}\sum_{\alpha_1\alpha_2\alpha'_1\alpha'_2} F(\alpha_1,\alpha_2;\alpha'_1,\alpha'_2)\,\hat{a}^{+}_{\alpha_1}\hat{a}^{+}_{\alpha_2}\hat{a}^{1}_{\alpha 2}\hat{a}^{1}_{\alpha 1}; \tag{2}$$

where $L(\alpha, \alpha')$ are additive matrix elements and $F(\alpha_1, \alpha_2; \alpha'_1, \alpha'_2)$ are binary matrices, while $\hat{a}^{+}_{\alpha}$, $\hat{a}_{\alpha}$ are the Fermi operators of the second quantization subject to the commutation relations

$$\hat{a}_{\alpha}\hat{a}^{+}_{\alpha'} + \hat{a}^{+}_{\alpha'}\hat{a}_{\alpha} = \delta_{\alpha\alpha'}, \quad \hat{a}_{\alpha}\hat{a}_{\alpha'} + \hat{a}_{\alpha'}\hat{a}_{\alpha} = 0, \quad \hat{a}^{+}_{\alpha}\hat{a}^{+}_{\alpha'} + \hat{a}^{+}_{\alpha'}\hat{a}^{+}_{\alpha} = 0. \tag{3}$$

The indices α and α' run through the numbers of the f and g lattice sites as well as the two possible values of the spin projection $\sigma = \pm \frac{1}{2}$. Following N. N. Bogoliubov ([8], § 4, Ch. IV) it can be shown that the minimum energy corresponds to the normal state of the model (two electrons at f sites and one electron at g sites).

3. The perturbation calculation is carried out by expanding the operator (2) in terms of a small parameter, the nonorthogonality integral of the atomic wave functions S. In the MnO crystal it is necessary to distinguish: 1) the overlapping of electronic wave functions of neighboring f and g sites; the corresponding integral S will be of the first order in ε since these are nearest neighbors; 2) the overlapping of wave functions of nearest g sites; the corresponding S integral will be of the order ε^2 since the separation ($Mn^{++} - Mn^{++}$) is $\sqrt{2}$ times larger than the separation ($O^{--} - Mn^{++}$) even for nearest g neighbors and the separation of next to nearest g neighbors is 2 times larger than the separation ($O^{--} - Mn^{++}$); 3) the overlapping of wave functions of nearest nonmagnetic neighbors gives an S integral of even higher order since the ($O^{--} - O^{--}$) separation is large and the electrons of a closed O^{--} shell are tightly bound. The wave function of the perturbed system is

$$(\hat{H}_0 + \varepsilon\hat{H}_1 + \varepsilon^2\hat{H}_2 + \varepsilon^3\hat{H}_3 + \varepsilon^4\hat{H}_4 + \ldots - E)\,C = 0, \tag{4}$$

where E is the energy of the system and C is the wave function in the second quantized representation. The terms in (4) above the zero-th order allow for excited states in which there are magnetic sites with two electrons due to transfer of one electron from an f site or in which there are g sites with two electrons and entirely lacking an outer electron due to the transfer of an electron to a nearest neighbor as well as other kinds of excitation. We consider below only the first kind of excitation, which is the most probable type.

We shall designate the increase of energy resulting from one g site with two electrons and one f site with a single electron by $\Delta(f; g)$, and the increase resulting from two such pairs of sites by $\Delta(f_1, f_2; g_1, g_2)$. By using the method of calculation in [8, 9] generalized to the fourth approximation we obtain after some extremely complicated computations for the part of the operator (2) describing the exchange interaction

$$\sum_{g_1 g_2} J(g_1 g_2)\,\hat{a}^{+}_{g_1\sigma}\hat{a}^{+}_{g_1\sigma_1}\hat{a}^{+}_{g_2\sigma_1}\hat{a}_{g_2\sigma}, \tag{5}$$

where

$$\begin{aligned} J(g_1g_2) = \sum_{(f)}\Bigg\{ & \frac{F(g_1g_2; f(1)f(2))\,\Lambda(f(1); g_1)\,\Lambda(f(2); g_2)}{\Delta(g_1; f(1))\,\Delta(g_2; f(2))} + \\ & + \frac{F(g_1f(1); f(1)g_1)\,\Lambda(f(2); g_2)\,\Lambda(g_2; f(2))}{\Delta(f(2); g_2)\,\Delta(g_2; f(2))} + \frac{F(f(1)g_1; g_1f(1))\Lambda(g_2; f(2))\,\Lambda(f(2); g_2)}{\Delta(f(2); g_2)\,\Delta(g_2; f(2))} + \\ & + \frac{F(f(1)f(2); g_2g_1)\Lambda(g_1; f(1))\Lambda(g_2; f(2))}{\Delta(f(1)f(2); g_2g_1)\,\Delta(g_2; f(2))} + \frac{F(g_2g_1; f(2)f(1))\Lambda(f(1); g_1)\Lambda(f(2); g_2)}{\Delta(g_1g_2; f(1)f(2))\,\Delta(g_2; f(2))}\Bigg\} \end{aligned} \tag{6}$$

represents the integral of the indirect exchange interaction for nodes g_1 and g_2 which differs from zero only in the fourth approximation and not in the third approximation as found in previous calculations [2-6]. The quantities Λ (g; f) represent the integrals of transfer of electrons from an f site to a g site, f(1) and f(2) are the numbers of the two electrons of the site. In the normal state of the system for the g sites it is possible to use the conditions of homopolarity [7-8] $a^{+}_{g^{1/2}}\hat{a}_{g^{1/2}} + \hat{a}^{+}_{g-1/2}\hat{a}_{g-1/2} = 1$, which enables us to use spin vector operators in (5):

$$\frac{1}{2}\sum_{g_1g_2} J(g_1g_2)\,[\hat{\sigma}_{g_1}\,\hat{\sigma}_{g_2}]. \tag{7}$$

If we assume that the atomic wave functions are exactly orthogonal we obtain instead of (6) the simpler expression

$$J(g_1g_2) \approx \frac{F(g_1, f(1);\ f(1), g_1)\,\Lambda(f(2);\, g_2)\,\Lambda(g_2;\, f(2))}{\Delta(f(2);\, g_2)\,\Delta(g_2;\, f(2))}, \tag{8}$$

which agrees with the previous expression for the indirect exchange integral; the matrix element $F(g_1, f(1); f(1), g_1)$ is the ordinary exchange integral and the transfer integrals in this instance are equal:

$$\Lambda(f(2);\, g_2) = \Lambda(g_2;\, f(2)) = \Lambda.$$

If in addition we introduce the notation $b = \Lambda/\Delta$ and $A = F$ instead of (8) we obtain

$$J \approx -b^2 A, \tag{9}$$

which agrees with the usual notation of the theory of antiferromagnetism. From (9) it can be seen that the sign of the indirect exchange is determined by the sign of the ordinary exchange integral.

The present deduction is important because it was carried out without certain supplementary assumptions (strong coupling of the electron transferred from the magnetic to the nonmagnetic site with the electrons of the latter, and exact orthogonality of the atomic wave functions). In addition the deduction of equation (5) enables us with complete justification to extend the method of spin waves (ferromagnons) to the case of ferromagnetism and antiferromagnetism of ionic compounds.

Institute of Metal Physics
Ural Branch
Academy of Sciences of the USSR

Received August 18, 1955

LITERATURE CITED

[1] P. Dirac, Quantum Mechanics, Moscow-Leningrad, 1937.

[2] H. A. Kramers, Physica 1, 182 (1933).

[3] P. W. Anderson, Phys. Rev. 79, 350 (1950).

[4] J. H. Van Vleck, J. phys. et radium 12, 262 (1951).

[5] J. Yamashita, Proc. Phys. Soc. Japan 9, 339 (1954).

[6] M. Shimizu, Progr. Theoret. Phys. 8, 416 (1952).

[7] S. P. Shubin and S. V. Vonsovskii, Sov. Phys. 7, 292 (1935).

[8] N. N. Bogoliubov, Lectures on Quantum Statistics, 1949 (Ukrainian).

[9] N. N. Bogoliubov and S. V. Tiablikov, J. Exptl.-Theoret. Phys. (USSR) 19, 256 (1949).

ON THE IMPOSSIBILITY OF EXPLAINING THE STABILITY OF HYPERONS BY THEIR LARGE SPINS

I. I. Gurevich

(Presented by Academician L. A. Artsimovich August 31, 1955)

Hyperons possess unusual stability against decay. The lifetime of hyperons is $\sim 10^{-10}$ seconds, which is 10^{13} times larger than characteristic nuclear lifetimes $\left(\frac{\hbar}{m_\pi c^2} \simeq 10^{-23}\ \text{seconds}\right)$. One may try to explain the metastability of hyperons by their large spins [1, 2]. The pion formed through hyperon decay should then have a large orbital moment and the centrifugal barrier

$$V_l = \frac{\hbar^2 l(l+1)}{2m_\pi r^2} \qquad (1)$$

can decrease the probability of free hyperon decay by the required factor.

The transparency of the centrifugal barrier is given by

$$P_l \cong \frac{(ka)^{2l+1}}{[(2l-1)!!]^2}, \qquad (2)$$

where k is the wave vector of the emerging pion. Taking the radius of the hyperon (nucleon) as $a = 4 \cdot 10^{-14}$ cm [3] and $P_l = 10^{-13}$ it is easily found that for the Λ^0-particle the required value is $l = 5$ [1].

For $l = 5$, $V_l(a) \cong 26$ Bev and the point of passage through the barrier which is determined by the condition $V_l(R) = \epsilon_\pi$ in the case of a Λ^0-particle ($\epsilon_\pi = 31$ Mev) is $R = 1.2 \cdot 10^{-12}$ cm.

The existence of Λ^0-nuclei with lifetimes close to the lifetime of a free Λ^0-particle makes this explanation invalid, as has been noted by I. Ia. Pomeranchuk. The mean separation of nucleons in nuclei:

$$\delta = \left(\frac{4\pi}{3}\right)^{1/3} r_0 \simeq 1{,}8 \cdot 10^{-13}\ \text{см} \quad (r_0 = 1{,}1 \cdot 10^{-13}\ \text{см})$$

is much smaller than R and, consequently, a pion may, with a probability much greater than 10^{-13}, be absorbed by a neighboring nucleon. The probability of absorption of a pion by a nucleon with which it makes "contact" is of the order of unity $\left(\frac{\delta}{\lambda} \sim 1;\ \lambda \text{ is the mean free pion path in the nucleus}\right)$

A detailed calculation of this phenomenon, which may be called the internal conversion of pions, has been performed by I. Iu. Kobzorev and L. B. Okun. It is the intention of the present note to show that this result is not dependent on any specific assumptions but follows from the most general theorems of quantum mechanics and is thus of a fundamental nature.

Let us designate by P_l^* the probability that a pion will penetrate the centrifugal barrier at a distance δ before encountering a neighboring nucleon:

$$P_l(a) = P_l^* P_l(\delta),$$

where $P_l(\delta)$ is given by (2) with a replaced by δ. Hence

$$P_l^* \cong \left[\frac{a}{\delta}\right]^{2l+1}. \tag{3}$$

The fact that P_l^* is independent of the pion energy follows from the fact that $V_l(\delta) \cong 1.3$ Bev $\gg \epsilon_\pi$. Substituting in (3) $\delta = 1.8 \cdot 10^{-13}$ cm, $a = 4 \cdot 10^{-14}$ cm and $l = 5$, we obtain $P_l^* \cong \left(\frac{1}{4.5}\right)^{11} \cong 10^{-7}$. Consequently, Λ^0-nuclei, if the stability of a Λ^0-particle were due to its large spin, would have a lifetime shorter by a factor of $10^{-13}/10^{-7} = 10^{-6}$ than a free Λ^0-particle, which is contrary to experiment. The stability of hyperons is associated with specific selection rules [4, 5].

Received August 4, 1955

LITERATURE CITED

[1] I. I. Gurevich, Doklady Akad. Nauk SSSR 105, 1 (1955).

[2] L. D. Puzikov and Ia. A. Smorodinskii, Doklady Akad. Nauk SSSR 104, 6 (1955).

[3] Ia. A. Smorodinskii, Problems of Modern Physics 7, 22 (1954).

[4] M. Gell-Mann, Conference in Pisa (1955).

[5] A. Pais, Proc. Roch. Conf. (1955).

THE INTERACTION OF 300 MEV π-MESONS WITH PROTONS, DEUTERONS AND NUCLEI IN NUCLEAR EMULSIONS

L. S. Dulkova, T. A. Romanova, I. B. Sokolova, L. V. Sukhov,
K. D. Tolstov and M. G. Shafronova

(Presented by Academician D.V. Skobel'tsyn, July 19, 1955)

Recently a number of papers have been published on the interaction of pions with nuclei and the scattering of mesons on nucleons; principally, the energy range up to 200 Mev was covered. The purpose of the present work was to obtain data on elastic π^--d and π^--p scattering and the interaction of π^--mesons with composite nuclei at 300 Mev. The work was carried out with nuclear track plates. The results are of a preliminary nature and will be more precise after more data is obtained. Type "p" NIKFI plates (Cine-Photography Scientific Research Institute) were used.

Our problem required an increase of the hydrogen content of nuclear emulsions and the introduction of deuterium. For this purpose the plates are usually soaked in ordinary or heavy water [1]. But the hydrogen and deuterium content per cm^3 of the swollen emulsion is increased in this way by only 1.5-1.6 times; further increase is limited by the strong diminution of sensitivity and the non-uniformity of the swelling. Rapid regression is observed as well as a decline of the ratio between the number of grains in the track and the number of grains in the photographic fog. The possibility of drying increases the difficulty of the work and of the control of the quantity of nuclei introduced into the plates. It was therefore advantageous to choose a stable hydrogenous material which would not cause appreciable swelling of the emulsion and provide large grain densities in tracks without any decrease of the number of nuclei introduced into each cm^3 of the emulsion. This substance had to be readily absorbable by gelatin and contain a large amount of hydrogen per molecule. For easy introduction into the emulsion it was desirable that it be soluble in water. The pH of the substance had to be close to the pH of the emulsion. For work with deuterium this substance had to possess a good capacity for replacing hydrogen with deuterium.

We chose lithium acetate $CH_3COOLi \cdot 2H_2O$. By the use of lithium acetate in which hydrogen is easily exchanged for deuterium we were able to introduce deuterium into the plates. This salt possesses all the properties enumerated above. Moreover, loading with lithium acetate also has other advantages.

The presence of the Li enabled us to establish a precise control of the quantity of material introduced by means of spectral or chemical analysis. The registration of α-H_1^3 stars from irradiation with slow neutrons makes it possible to control the uniformity of the emulsion loading. An increase of the pH of the solution will, as is well known, reduce the regression, and this fact was also taken into consideration in the choice of a material (the pH of lithium acetate is 7.4-7.6).

We used a 30% aqueous solution of lithium acetate and heavy lithium acetate.* To increase the amount of the salt introduced and the uniformity of loading we first soaked the plates in water. After loading, the plates were dried in a weak flow of air that had been moistened with ordinary or heavy water. In this way, it was possible to raise the hydrogen content to $0.6 \cdot 10^{23}$ nuclei per cm^3 or to put $0.3 \cdot 10^{23}$ deuterium nuclei into 1 cm^3 of dry emulsion. The loading was uniform. The loaded emulsion was stable. After three days no regression was detected and the number of background grains did not increase. The grain density in minimum ionization tracks increased by 20-30%.

The plates were irradiated by the synchrocyclotron of the Institute for Nuclear Problems of the Academy of Sciences USSR with a beam of π^--mesons, as described in [2]. The beam consisted 97 ± 1.5% of π^--mesons with energy 300 ± 3 Mev [2]. The average energy of the mesons in the plates was 295 ± 8 Mev because of losses in the emulsions and sides of the plateholder. The plates were irradiated horizontally for 5-10 min.; the result was a track density of 10^4-10^5 cm^{-2} with comparatively low background.

---

* The lithium acetate with deuterium was prepared with the cooperation of G. P. Miklukhin, Doctor of Chemical Science, at the Pisarzhevskii Ukrainian Physico-Chemical Institute.

Various methods of scanning were employed. The usual area scanning was performed with enlargement × 945 or × 630. Only events with one or more gray or black prongs were recorded, i.e., cases of meson absorption and inelastic scattering as well as elastic scattering on light nuclei. Stopped mesons and scattering unaccompanied by visible prongs were omitted. In order to expedite the finding of scattering on hydrogen and deuterium another form of area scanning was employed, whereby we first looked for single gray and black tracks beginning in the emulsion and then examined their starting points for the presence of incident and scattered mesons. In this examination only one- and two-pronged events were recorded. A portion of the plates were scanned along the tracks. This was slower scanning but permitted the recording of all kinds of interactions including the scattering of mesons at small angles. The recording efficiency may be considered 100%. Each kind of scanning was carried out in analogous fashion on the H and D plates. Altogether 1580 different interactions with nuclei were found.

Scanning along tracks covered a total of 100.5 m. The mean free path λ_T in the emulsion with respect to all processes including scattering at an angle > 20° was 29.6 ± 1.6 cm for π^--mesons. The geometric path in standard type "p" NIKFI emulsions was 25 cm in the preliminary data and in emulsions loaded with lithium acetate 26 cm. Consequently the total interaction cross section of 300 Mev π^--mesons with emulsion nuclei is 88 ± 5% of the geometric value. For 210 Mev π^--mesons we obtained a mean free path of $\lambda_T = 25.7$ cm [4] which corresponds to 91% of the geometric cross section. According to the data of [5] the total interaction cross section of 450 Mev π^--mesons with C and Cu is, respectively, 61 ± 7% and 77 ± 11.5% of the geometric value. In [6] it is shown that the mean free path of 500 Mev π^--mesons is about twice as large as the geometric value. Thus our result is in good agreement with the results mentioned above and also with the results of [3] and is confirmation of the fact that as the energy is increased from 200 to 500 Mev the π^--meson interaction cross section is reduced.

The mean free paths for different types of interaction obtained by scanning along tracks are given in Table 1, from which it can be seen that the principal contribution to the cross section comes from inelastic scattering processes and meson absorption with star-formation.

By area scanning 1240 stars were found, i.e., cases of absorption or inelastic scattering of a meson with the emission of not less than one charged particle. The mean free path for these processes was $\lambda_I = 43.6 \pm 5$ cm. A comparison of this value with the results of track scanning shows that the efficiency of area scanning for these processes is 80 ± 10%. Among the stars found by area scanning 32 ± 2% contain a minimum ionization track which cannot represent a proton but belongs to a meson, i.e., in 32% of the stars there is inelastic scattering by which the meson loses not more than $^2/_3$ of its energy. Identification of the cases in which the meson loses a larger part of its energy requires additional analysis by the multiple scattering method.

The prong-number distribution of the stars found in track and area scanning is given in Table 2.

The cases of elastic scattering on hydrogen or deuterium were separated according to the characteristics of the collision of the two particles: 1) coplanarity of three prongs; 2) relation between the meson scattering angle and the emission angle of the proton or deuteron; 3) relation between the angle and range of the recoil particle if the range ends in the emulsion. This relation enabled us to distinguish cases of scattering on H and D at small scattering angles.

We found 50 scattering events on hydrogen and 11 on deuterium. The distribution of the scattered mesons should be isotropic in the plane perpendicular to the surface of the emulsion. However, this was not observed experimentally, but this result can be explained by the omission of cases of scattering due to the steepness of the tracks. For the purpose of introducing a correction we constructed a histogram of the number of events as a function of the polar angle in this plane. The correction obtained in this way, which within the limit of statistical error is independent of the scattering angle, amounts to 40%. If, moreover, we take into consideration the scanning efficiency and introduce a correction for the omission of events on the surface of the emulsion of the glass (11%), the elastic scattering cross sections on hydrogen and deuterium are, respectively,

$$\sigma_H = 14 \pm 3.5 \text{ mb and } \sigma_D = 15 \pm 5.5 \text{ mb.}$$

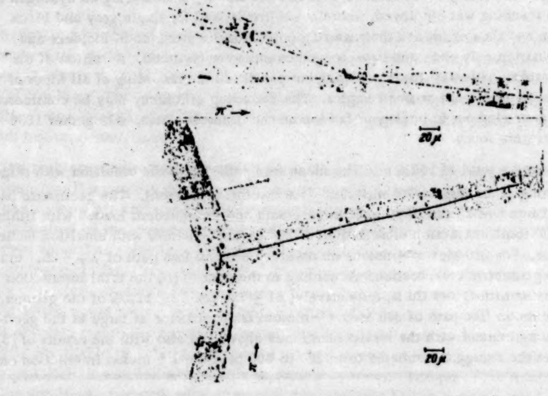

Figure 1. Elastic scattering of π^--mesons on protons.

TABLE 1

Mean Free Path in Nuclear Emulsion

	Mean free path in cm
For scattering at an angle > 20° without emission of charged particles	373 ± 72
For stopping	592 ± 144
For inelastic scattering and absorption with emission of charged particles	34.1 ± 2

Figure 1 contains photographs of scattering on H. Scattering on deuterium is strongly anisotropic – all the observed cases of meson scattering are included in the relative solid angle 0.4, which corresponds to an angular range of 0-80° in the center-of-mass system. The energy transferred by the pion to the recoil deuteron was in the majority of scattering events < 20 Mev and in only one instance 50 Mev.

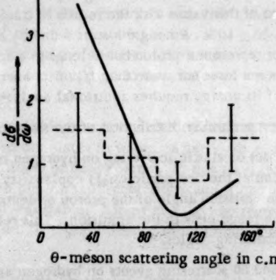

Figure 2. Differential cross section for elastic scattering of π^--mesons by protons.

TABLE 2

Star Distribution by Number of Prongs

Total number of stars	Type of scanning	Number of prongs in stars								
		1	2	3	4	5	6	7	8	9
		Number of stars in %								
1124	Area	9	29	21	19.5	13	6	2	0.5	0.01
267	Along the track	8	22.5	25.5	25.5	11	5	1.5	0.5	0.5

The differential π^--meson scattering cross section on hydrogen in the c.m.s. is given in Fig. 2 as a histogram. The solid curve in Fig. 2 was calculated by L. Pariskaia from a semiphenomenological theory of the interaction of pions and nucleons [7]. The following set of constants was used: $\Delta = 2.1$; $g^2 = 0.14$; $s = 2.0$; $g_1^2 = 0.24$, which differs little from [7] and takes into consideration the most recent experiments on photoproduction of pions. The difference between the theoretical curve and the experimental data at small scattering angles exceeds the statistical error, which is large.however.

In conclusion we wish to express our thanks to I. M. Frank, corresponding member of the Academy of Sciences of the USSR for directing the work and to B. M. Pontecorvo for his assistance.

P. N. Lebedev Physical Institute
Academy of Sciences of the USSR

Received July 10, 1955

LITERATURE CITED

[1] G. Goldhaber et al., Nucl. Sci. Abstr. 7, No. 23, 6559 (1953).

[2] A. E. Ignatenko, A. I. Mukhin, E. B. Ozerov and B. M. Pontecorvo, Doklady Akad. Nauk SSSR 103, 41 (1955).

[3] A. E. Ignatenko, A. I. Mukhin, E. B. Ozerov and B. M. Pontecorvo, Doklady Akad. Nauk SSSR 103, 395 (1955).

[4] A. H. Morrish, Phys. Rev. 90, 674 (1953).

[5] Iyan Lindenbaum, Phys. Rev. 92, 1578 (1953).

[6] M. Blau, M. Caulton, Phys. Rev. 96, 159 (1953).

[7] I. E. Tamm, Yu. A.Gol'fand and V. Ya. Fainberg, J. Exptl.-Theoret. Phys. (USSR) 26, 649 (1954).

AXIALLY SYMMETRIC ELECTRON BEAMS OF A GIVEN SHAPE

V. T. Ovcharov

(Presented by Academician A. I. Berg August 3, 1955)

1. Until recently electron optics has been concerned with the solution of the direct problem of finding electron trajectories in given electric and magnetic fields. But in recent years in connection with the development of ultrahigh frequency devices a beginning has been made of the study of the inverse problem: given an electron trajectory, to find the fields forming that trajectory. However, with the exception of the work of G. A. Grinberg [1] only special cases have been considered. These special cases are not always sufficient for the solution of the beam formation problems encountered in practice. A more general examination of the problem which has been proposed by G. A. Grinberg neglects the effect of space charge; this is not always permissable.

The present paper provides a quite general examination of the problem of forming axially-symmetric electron beams including consideration of the field due to the space charge of the beam itself.

2. We introduce a system of curvilinear coordinates q_1, q_2, q_3 with axial symmetry. q_3 will be the angle of rotation φ around the axis of symmetry. The Lamé coefficients h_1, h_2, h_3 of our coordinate system are independent of q_3.

The electric field is defined in terms of the potential U and the magnetic field in terms of the vector potential **A**; because of the axial symmetry of the fields

$$\frac{\partial U}{\partial \varphi}=0, \quad A_1=A_2=0, \quad A_3=A \tag{1}$$

where A_1, A_2 and A_3 are the components of the vector potential along the q_1, q_2 and $q_3 = \varphi$ axes of our system of coordinates. (We assume that the axes of symmetry of the electric and magnetic fields coincide with the axis of symmetry of the coordinate system).

In view of the above the equations of motion can be written in the form

$$\frac{d}{dq}(h_1^2\dot{q}_1)-\sum_{m=1}^{2} h_m \frac{\partial h_m}{\partial q_1}\dot{q}_m^2=-\frac{\partial Q}{\partial q_1}; \tag{2}$$

$$\frac{d}{dt}(h_2^2\dot{q}_2)-\sum_{m=1}^{2} h_m \frac{\partial h_m}{\partial q_2}\dot{q}_m^2=-\frac{\partial Q}{\partial q_2}; \tag{3}$$

$$h_3^2\dot{\varphi}+\frac{eA}{mc}h_3=C; \tag{4}$$

$$Q=\frac{e}{m}U+\frac{1}{2}h_3^2\dot{\varphi}^2. \tag{5}$$

In Equations (2) to (5), e and m are the electron charge and mass; c is the velocity of light; a dot denotes differentiation with respect to the time t. C in (4) is constant along a given trajectory but differs for other trajectories.

We now add the equation of the conservation of energy:

$$-2\frac{e}{m}U = h_1^2\dot{q}_1^2 + h_2^2\dot{q}_2^2 + h_3^2\dot{q}_3^2. \tag{6}$$

We assume that the potential of the cathode is zero and that electrons leave it with zero velocity, although this limitation is not obligatory.

From (5) and (6) we obtain for Q the following expression:

$$Q = -\frac{1}{2}(h_1^2\dot{q}_1^2 + h_2^2\dot{q}_2^2). \tag{7}$$

3. We now impose the following limitation on the motion of the electrons: let the electron trajectories in the q_1, q_2 plane coincide with lines parallel to the q_1-axis. Then for all electrons

$$q_2 = \text{constant}. \tag{8}$$

Substituting in Equations (3), (6) and (7), we find

$$h_1\frac{\partial h_1}{\partial q_2}\dot{q}_1^2 = \frac{\partial Q}{\partial q_2}; \tag{9}$$

$$Q = -\frac{1}{2}h_1^2\dot{q}_1^2; \tag{10}$$

$$-2\frac{e}{m}U = h_1^2\dot{q}_1^2 + h_3^2\dot{q}_3^2. \tag{11}$$

Eliminating $\dot{q}_1$ from (9) and (10), we obtain an equation which is easily integrated. The result obtained is

$$h_1^2 Q = -P(q_1), \tag{12}$$

i.e., the product $h_1^2 Q$ is a function of the coordinate q_1 alone.

From (10), (11), and (12) we obtain the potential U:

$$U = -\frac{m}{2e}\left[\frac{2P(q_1)}{h_1^2} + \Phi^2\right], \tag{13}$$

where

$$\Phi = h_3\dot{\varphi}. \tag{14}$$

According to (4) this φ-component of the velocity is determined only by the magnetic field.

4. We substitute the potential (13) in Poisson's equation

$$\frac{1}{h_1h_2h_3}\left[\frac{\partial}{\partial q_1}\left(\frac{h_2h_3}{h_1}\frac{\partial U}{\partial q_1}\right) + \frac{\partial}{\partial q_2}\left(\frac{h_1h_3}{h_2}\frac{\partial U}{\partial q_2}\right)\right] = -4\pi\rho, \tag{15}$$

which associates the potential U inside the beam with the density ρ of the space charge. After some simple transformations we obtain

$$f_1\frac{d^2P}{dq_1^2} + f_2\frac{dP}{dq_1} + f_3P + f = \frac{8\pi e}{m}\rho. \tag{16}$$

Here f_1, f_2, f_3 and f are functions of q_1 and q_2 which are defined by the following expressions:

$$
\begin{aligned}
f_1 &= \frac{2}{h_1^4}, \\
f_2 &= \frac{2}{h_1h_2h_3}\left[\frac{h_2h_3}{h_1}\frac{\partial}{\partial q_1}\left(\frac{1}{h_1^2}\right)+\frac{\partial}{\partial q_1}\left(\frac{h_2h_3}{h_1^3}\right)\right], \\
f_2 &= \frac{2}{h_1h_2h_3}\left\{\frac{\partial}{\partial q_1}\left[\frac{h_2h_3}{h_1}\frac{\partial}{\partial q_1}\left(\frac{1}{h_1^2}\right)\right]+\frac{\partial}{\partial q_2}\left[\frac{h_1h_3}{h_2}\frac{\partial}{\partial q_2}\left(\frac{1}{h_1^2}\right)\right]\right\}, \\
f &= \frac{1}{h_1h_2h_3}\left[\frac{\partial}{\partial q_1}\left(\frac{h_2h_3}{h_1}\frac{\partial\Phi^2}{\partial q_1}\right)+\frac{\partial}{\partial q_2}\left(\frac{h_1h_3}{h_2}\frac{\partial\Phi^2}{\partial q_2}\right)\right].
\end{aligned}
\tag{17}
$$

In order to eliminate from (16) the density ρ of the space charge, which is a still unknown function of the coordinates, we multiply (16) by $\dot{q}_1h_1h_2h_3dq_2d\varphi$ and integrate over the cross section of the electron beam. If on the left side we replace $\dot{q}_1$ by

$$\dot{q}_1 = \frac{\sqrt{2P}}{h_1^2}, \tag{18}$$

which is obtained from (10) and (12), after integration we obtain

$$F_1\frac{d^2P}{dq_1^2}+F_2\frac{dP}{dq_1}+F_3P+F=\frac{a}{\sqrt{P}}. \tag{19}$$

In this equation F_1, F_2, F_3 and F are functions of q_1 which are defined in terms of f_1, f_2, f_3 and f by

$$F_n = \frac{1}{2}\int_\alpha^\beta \frac{h_2h_3}{h_1} f_n(q_1; q_2)\, dq_2, \tag{20}$$

where α and β are the values of q_2 which determine the boundaries of the electron beam. We note that α and β are constants since the trajectories coincide with lines parallel to the q_1 axis. The constant a is given by

$$a = \frac{e}{m}\sqrt{2I}. \tag{21}$$

Here I is the current of the electron beam:

$$I = \int_\alpha^\beta\int_0^{2\pi} \rho\dot{q}_1h_1h_2h_3dq_2d\varphi. \tag{22}$$

5. We set boundary conditions for the function $P(q_1)$ which satisfy the differential Equation (19). The cathode has an equipotential surface where, in addition, $\Phi = 0$ due to the conditions which we have assumed. We make the surface of the cathode coincide with $q_1 = q_0 =$ constant. As can be seen from (13), on the cathode surface $U = 0$ when $P(q_0) = 0$. Assuming that the velocity of the electrons emitted by the cathode is zero, we can also assume that on the cathode surface grad $U = 0$. This condition will be satisfied when, in addition to $P(q_0) = 0$, we also have $\left.\frac{dP}{dq_1}\right|_{q_1=q_0} = 0$.

Thus when it is assumed that $U = 0$ and the velocity of the emitted electrons is zero, the boundary conditions for P are

$$P = 0, \quad \frac{dP}{dq_1} = 0 \quad \text{for} \quad q_1 = q_0. \tag{23}$$

If we take into consideration the initial electron velocities or assume that the potential of the cathode differs from zero the boundary conditions on the cathode cannot be satisfied in every system of coordinates but only where the Lamé coefficient h_1 depends only on q_1. This limitation must be kept in mind in choosing the shape of the electron beam and the appropriate system of coordinates.

6. With a given magnetic field we can solve (19) with the boundary conditions (23). The coefficients in (19) are determined by the coordinate system, which, in turn, is determined by the chosen shape of the electron beam. After determining P we obtain from (13) the potential U; then by (15) or (16) we calculate the density ρ of the space charge. Using (18) we can calculate the longitudinal velocity $h_1\dot{q}_1$.

In order to realize an electron beam in practice it is necessary to find the shape of the electrodes and the potential on them for the purpose of obtaining a calculated potential distribution inside the beam. In the design of electron beams the shape of the electrodes is found by using an electrolytic bath in which the edge of the beam is represented by a dielectric plate. However in our general case the magnetic field makes it impossible to represent the edge of the beam by a dielectric plate.

In our case the procedure must be as follows. We calculate the potential which results from the space charge of the beam. Subtracting this potential from the potential V found above we obtain the potential produced inside the beam by the surface charges on the electrodes. It is now possible to make use of the electrolytic bath without a dielectric plate. We select the shape of the electrodes in the bath which will give the potential distribution on the edge of the electron beam that is produced by the electrode surface charges.

Received August 3, 1955

LITERATURE CITED

[1] G. A. Grinberg, Selected Problems of the Mathematical Theory of Electrical and Magnetic Phenomena, Acad. Sci. USSR Press, 1948.

UNUSUAL V^{0}-DECAY

E. Fridlender and S. Bercha*

(Presented by Academician D. V. Skobel'tsyn, November 11, 1955)

In a systematic investigation of V^{0}-decays in Ilford G-5 emulsions irradiated with cosmic rays at 2867 m an unusual V^{0}-decay was discovered [1]** in which the heavier particle was evidently much heavier than a proton. Careful measurements led to the following results.

The light particle (to be designated hereafter as A) was identified by scattering and a blob count as a pion of kinetic energy $T_p = 19.7 \pm 2.6$ Mev.

The heavy particle (B) formed a track whose density was close to saturation ($g^* \geq 10$, where g^* is the normalized blob density). After traversing a visible path of 1925 μ this particle apparently left the emulsion. From this minimum range and the scattering parameters in the initial 1000 μ of the track we obtain the mass (in proton mass units):

$$m \leq (2.5 \pm 0.7), \qquad (1)$$

whereas the minimum value of g^* (equal to 10) gives

$$m \geq (1.5 \pm 0.2). \qquad (2)$$

A more precise estimate of the mass from scattering (average deflection [2]) gives

$$m = 1.97 \pm 0.21 = (3620 \pm 390)\, m_e. \qquad (3)$$

Thus the B particle is most probably a deuteron although a mass value between 1 and 2 (charged hyperon) cannot be excluded. The probability that this particle is a proton is lower than 0.02%. Thus it is very unlikely that this event is an Λ^0-decay.

The residual range of the particle $\underline{r}$ at the point of exit was determined by a method which is a variant of the average deflection method. If $\underline{l}$ is the visible path length,

$$\frac{r}{l} = 1.0 \pm 0.2, \qquad (4)$$

and the total path length of the particle from the point where the V-decay took place is

$$R_B = (3850 \pm 385)\, \mu. \qquad (5)$$

---

* Original spelling: E. Friedländer and S. Bercea.

** First reported at a scientific meeting of the Bucharest University June 10, 1954.

Thus the kinetic energy of this particle T_B is

$$T_B \equiv T_d = (37.1 \pm 2.2)\ \text{Mev}, \qquad (6)$$

if it is a deuteron, and

$$T_B = T_Y = (30.6 \pm 1.8)\ \text{Mev}, \qquad (7)$$

if it is a hyperon $Y^{\pm}$ (2370 m_e [3]).

Since $\cos\Phi = 0$, the mass of the unstable heavy particle should be $(4084 \pm 41)m_e$ if B is a deuteron and $(2692 \pm 27)m_e$ if B is a $Y^{\pm}$-particle. The corresponding values of Q are (38 ± 20) and (24 ± 13) Mev.

The decay is similar to one that was described by the Bombay group (see also [5]). The mass value found by the Bombay group was $(4120 \pm 20)\,m_e$ which is close to ours and makes the Q equal to (56 ± 10) Mev*.

Thus it is very probable that in both instances we were observing the decay of a hitherto unknown "extra-heavy" V^0-particle. Depending on our hypothesis of the nature of particle B we may consider the following decay schemes:

$$V^0 \rightarrow \pi^- + d + Q,\ Q \sim 40\text{-}60\ \text{Mev},\ M \sim 4100\ m_e; \qquad (8)$$

$$V^0 \rightarrow \pi^{\mp} + Y^{\pm} + Q,\ \ Q \sim 20\ \text{Mev},\ M \sim 2700\ m_e. \qquad (9)$$

Since in the event observed by the Bombay group [4] particle B was very definitely identified as a deuteron, scheme (8) is more probable. Since the deuteron is a composite particle it is very unlikely that the observed V^0-particle is a new "elementary" particle. It is more reasonable to assume that in both instances we were observing the mesonic decay of a Λ^0-particle bound to a neutron, i.e., the decay of a Λ^0-dineutron. The observed value of Q is very close to the value (37 ± 3) Mev taken for the Q of a Λ^0-particle [3]; for the binding energy of the Λ^0-particle in the dineutron there remains only the small range of values between 1 and 3 Mev. This is in good agreement with the small values of Λ^0-particle binding energies in Λ^0-tritons [6] and Λ^0 α-particles [7].

In the center-of-mass system the decay products have equal and opposite momentum (in the nonrelativistic approximation):

$$P = \sqrt{\frac{2Qm_Am_B}{m_A + m_B}}. \qquad (10)$$

In the same approximation the recoil energy T_B^* of particle B in the c.m.s. is

$$T_B^* = \frac{Qm_A}{m_A + m_B} \qquad (11)$$

Assuming that the Q is equal to the value (37 Mev) taken for a Λ^0-particle we obtain

$$T_B^* = (2.6 \pm 1.3)\ \text{Mev}. \qquad (12)$$

This value is very close to the binding energy of the deuteron (2.3 Mev). Thus we have the same paradox which arises from the fact that relatively fast deuterons ($T \geq 10^8$ ev) often are emitted in high energy fission [8, 9], although one might expect that such a weakly bound particle would split during a collision.

---

* In [3, 4], probably because of an error in calculation, the erroneous value (89 ± 10) Mev is given for Q.

The specific mechanism by means of which large kinetic energy is imparted to two nucleons at one time (which under normal conditions are weakly bound), requires further investigation. It should be recalled that dineutrons are probably emitted in some fissions induced by the capture of negative pions.

By the use of (11) it can easily be shown that in the events described in [10] both neutrons had to be in the ground state and the rest energy of the pion was insufficient to excite a neutron into a Λ^0-state. If, on the other hand, we assume that in both instances particle B is a charged hyperon, i.e., that the observed decay is the first stage of a decay similar to "neutral" cascade decay [11],

$$Y^{\pm} \longrightarrow \pi^- + \Lambda^0, \quad \Lambda^0 \longrightarrow \pi^- + p, \tag{13}$$

similarly

$$Y^0 \longrightarrow \Lambda^{\pm} + \pi^{\mp}, \quad \Lambda^{\pm} \longrightarrow \mu + \pi^{\pm}, \tag{14}$$

where $m_Y \sim 2700\ m_e$. This value deviates insignificantly from the value of the mass found for decay in [12].

If the interpretation given in (14) is correct and if we consider [3] a Λ^0-particle as an excited state of the neutron, the Y^0-particle described above may be considered to be a neutron at a higher level of excitation.

A charged particle with similar properties was described by Eisenberg [12].

The authors are greatly indebted to Professor Khulubei for the use of laboratory equipment and constant support, and also to Professors Titeika and Auslender for valuable discussions of the results.

Structure of Matter Laboratory, Bucharest University Received July 20, 1955

LITERATURE CITED

[1] C. Bercea, E. Friedländer, Bull. Univ. C. I. Parhon, 1955.

[2] J. Ausländer, C. Bercea, K. Friedländer, Comm. Acad. R. P. R. 5, 2, 343 (1955).

[3] C. F. Powell, Nuovo cimento 11, Suppl. No. 2, 165 (1954).

[4] D. Lal, Yash Pal, B. Peters, Phys. Rev. 92, 439 (1953).

[5] B. Peters, Bagneres Congr., 1953, p. 173, quoted in Problems Mod. Phys. 4, 100 (1955).

[6] A. Bonetti, R. H. Setti, N. Panetti, G. Tomasini, Nuovo cimento 10, 1736 (1953).

[7] J. Crussard, D. Morellet, Bagneres Congr., 1953, p. 180.

[8] P. H. Fowler, Phil. Mag. 41, 169 (1950).

[9] A. Alikhanian and G. Marikian, Doklady Akad. Nauk SSSR 87, 2, 191 (1952).

[10] A. P. Zhdanov, P. I. Likirskii and Z. S. Sokolova, Doklady Akad. Nauk SSSR 80, 5, 729 (1951).

[11] R. B. Leighton, Bagneres Congr., 1920, p. 97.

[12] Y. Eisenberg, Phys. Rev. 94, 629 (1954).

INSTRUMENTAL DISTORTION OF X-RAY SPECTRA

M. A. Blokhin

(Presented by Academician A. A. Lebedev August 4, 1955)

In an earlier paper [1] we developed a method of obtaining the true shape of x-ray spectra for the particular case of dispersive distortions. In order to determine the nature of the distortions it is necessary to record one line as close as possible to the investigated region, whose true dispersive shape and width has been obtained by means of a double crystal spectrometer. This will be called the "standard line". If its shape is found to be nondispersive this will be an indication that the distortions due to the apparatus are nondispersive. In the general case the distortions may be asymmetric.

Let the true shape of the line chosen as the standard be $f_c(x)$:

$$f_c(x) = \frac{1}{\pi\gamma} \frac{S}{1 + (x/\gamma)^2}, \tag{1}$$

where γ is the half-width of the line obtained with a double crystal spectrometer, and S is the area of the dispersion curve. If $F_c(x)$ represents the distorted shape of this line obtained with the apparatus mentioned, S is given by

$$S = \int_{-\infty}^{\infty} F_c(x)\,dx \approx \int_{-\Delta/2}^{\Delta/2} F_c(x)\,dx, \tag{2}$$

where Δ is the length of the portion of the spectrum which is to be corrected. Here it is assumed that the width of the distorted shape of the standard line is considerably smaller than Δ. The integral on the right-hand side of (2) can be obtained graphically.

The functions $F_c(x)$ and $f_c(x)$ are connected by the integral equation

$$F_c(x) = \int_{-\infty}^{\infty} f_c(t)\,\varphi(x - t)\,dt, \tag{3}$$

where $\varphi(x - t)$ is the distortion function, which is normalized by

$$\int_{-\infty}^{\infty} \varphi(z)\,dz = 1. \tag{4}$$

In order to obtain $\varphi(x - t)$ we expand all three functions in (3) in trigonometric series. The interval Δ is taken as half of the period of these functions. In the second half of the period we continue the curves so as to possess symmetry of the third kind; $f_c(t)$ is an even function. We will then have

$$f_e(t) = \sum_h A'_h \cos\frac{h\pi}{\Delta} t, \tag{5}$$

$$F_c(x) = \sum_h \left(B'_k \cos\frac{k\pi}{\Delta} x + b'_k \sin\frac{k\pi}{\Delta} x\right), \tag{6}$$

$$\varphi(x-t) = \sum_{l}\left[C_l \cos\frac{l\pi}{\Delta}(x-t) + c_l \sin\frac{l\pi}{\Delta}(x-t)\right], \tag{7}$$

where h, k and l are odd numbers. The coefficients A'_h (for $\Delta \gg \gamma$) can be obtained with sufficient accuracy from the equation

$$A'_h = \frac{2S}{\Delta}\left[\exp\left(-\frac{h\pi\gamma}{\Delta}\right) - \frac{2h\gamma}{\Delta}\,\mathrm{si}\,\frac{h\pi}{2}\right]. \tag{8}$$

The coefficients B'_k and b'_k are obtained by one of the standard methods of graphic harmonic analysis from the experimental intensity distribution of the standard line. The zero abscissa must be the wavelength of the standard line peak as given by the double crystal spectrometer.

Substituting (5), (6) and (7) in (3) we obtain

$$C_k = \frac{2}{\Delta}\frac{B'_k}{A'_k}; \quad c_k = \frac{2}{\Delta}\frac{b'_k}{A'_k}. \tag{9}$$

This solves the problem of obtaining the shape of the distortions introduced by the apparatus.

For the purpose of verifying the accuracy attained in practice in determining the finite number of coefficients A'_h, B'_k and b'_k the above-described method will be applied to the case in which the given analytic function $F_c(x)$ enabled us to obtain an analytic expression for the distortion function $\varphi(x-t)$. $F_c(x)$ was chosen to be asymmetric:

$$F_c(x) = \frac{400}{3}\left[\frac{1}{1+(x/2)^2} + \frac{0.5}{1+((x+1)/2)^2}\right]. \tag{10}$$

The dispersive curve of equal area which represented the "true shape" of the standard line was taken in the form

$$f_c(t) = \frac{400}{1+t^2} \tag{11}$$

In this case the distortion functions are given by

$$\varphi(x-t) + \frac{2}{3\pi}\left[\frac{1}{1+(x-t)^2} + \frac{0,5}{1+(1+x-t)^2}\right], \tag{12}$$

where (4) is satisfied.

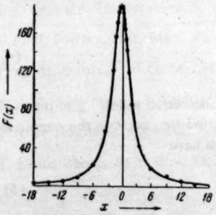

Figure 1. Graph of $F_c(x)$.
The points represent the summation of the series (6) with amplitudes obtained graphically.

The graph of $F_c(x)$ drawn from (10) is given in Figure 1. The graphic harmonic analysis of this curve was carried out by the method of P. L. Chebyshev [2]. We obtained the first 13 pairs of amplitudes B'_k and b'_k for odd k from 1 to 25. From (8) we calculated the A'_k for the same values of k. From the values of C_k and c_k obtained from (9) we summed the series (7) at many points. These points are shown in Figure 2 together with the curve constructed from the exact analytic expression (12) for $\varphi(x-t)$. As can be seen from this figure, even for such a small number of calculated amplitudes the result is entirely satisfactory. The edge effect discussed in reference [1] is extremely small.

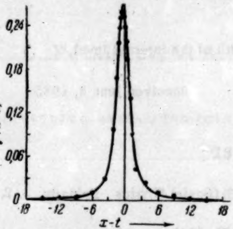

Figure 2. Graph of $\varphi(x-t)$.
The points represent the summation of the series (7) with amplitudes obtained from (9).

We now formulate the problem of obtaining the true shape f(x) of a spectrum whose distorted shape F(x) has been found experimentally. We shall assume that the distortion $\varphi(x-t)$ has been obtained by the above method using the coefficients C_1 and c_1 of (7). F(x) is represented by the trigonometric series

$$F(x)=\sum_k\left(B_k\cos\frac{k\pi}{\Delta}x+b_k\sin\frac{k\pi}{\Delta}x\right), \tag{13}$$

where Δ is the interval used above in which F(x) was given graphically. F(x) is provided with the same symmetry as $F_c(x)$. Δ is taken to be half the period of F(x). In this case the amplitudes of the even harmonics are zero. The zero abscissa is placed at the middle of Δ. In order to avoid appreciable edge effects the interval Δ must be so chosen that near its limits F(x) will have values as small as possible. If this condition cannot be satisfied because of the nature of the spectrum, as in the case of absorption spectra, we represent the portion of the spectrum which interests us by an inverse tangent function as described in [1]. If this inverse tangent is selected sufficiently distant from the absorption edge its correction can be performed approximately assuming dispersive distortions, which do not introduce significant errors into the spectral region which is of interest.

We represent the true shape by the series

$$f(t)=\sum_h\left(A_h\cos\frac{h\pi}{\Delta}t+a_h\sin\frac{h\pi}{\Delta}t\right), \tag{14}$$

where the amplitudes of the even harmonics are also zero. Substituting (13), (14) and (7) in the integral equation

$$F(x)\approx\int_{-\Delta/2}^{\Delta/2}f(t)\,\varphi(x-t)\,dt, \tag{15}$$

we obtain

$$A_k=\frac{2}{\Delta}\,\frac{b_kc_k+B_kC_k}{C_k^2+c_k^2};\qquad a_k=\frac{2}{\Delta}\,\frac{b_kC_k-B_kc_k}{C_k^2+c_k^2}. \tag{16}$$

Summing (14) with the amplitudes A_k and a_k enables us to draw the correct shape of the spectrum.

The above method enables us to obtain any shape of distortion of an x-ray spectrum and to utilize it in order to establish the true shape of the spectrum. It is evident, however, that the shape established by this method will be more accurate and closer to the true shape the greater the resolving power of the apparatus. Thus the distortion may be of any shape but not of any width. If any details of the spectral shape with insufficient resolution become completely "smeared" and do not exceed experimental errors (associated with the quantum nature of the radiation, grain size of the film, etc.) it will be altogether impossible to observe such details.

After establishing the true shape of the spectrum it is possible once more to "correct" it by the width and shape of the internal level with a known dispersive shape as explained in [1]. For emission spectra this problem is, of course, considerably easier. Keeping in mind the additivity of the dispersion distortions, the correction method of [1] can be used once. In this case we can use as $\varphi(x-t)$ the dispersion function with half-width γ which equals the sum of the half-widths of the distortion and internal level.

In treating absorption spectra the correction for the true shape must be performed according to the curve of intensity distribution. From the corrected spectrum the absorption coefficient distribution curve will be constructed. This latter curve can be "corrected" again for the width of the internal level.

V. M. Molotov State University
Rostov on Don

Received June 8, 1955

LITERATURE CITED

[1] M. A. Blokhin, Doklady Akad. Nauk SSSR 107, 1 (1956)(Soviet Physics · Doklady, 1, 2, p. 145.)

[2] P. L. Kalantarov, Theory of Alternating Current, § 79, 1940.

PRIMARY IONIZATION BY FAST MUONS

G. P. Eliseev, V. A. Liubimov and A. M. Frolov

(Presented by Academician A. I. Alikhanov September 24, 1955)

For primary ionization in a medium traversed by a fast charged particle theory predicts a logarithmic rise with increasing particle velocity(for $\beta \sim 1$)[1]. The polarization of the medium resulting from the passage of the charged particle results after a certain momentum is reached in saturation of the ionization and cessation of the increase with particle momentum. In gases under normal conditions a rise of ~30% above the minimum primary ionization can be expected [2].

Some experimental work is to be found which confirms the logarithmic increase with particle velocity [3, 4]. However, the effect of polarization on the primary ionization has not been demonstrated experimentally.

In the present work we obtained the primary ionization spectrum of fast muons in the momentum range $2 \cdot 10^{8} - 3.4 \cdot 10^{10}$ ev/c. The momentum was measured by the curvature of the trajectory in the magnetic field of a mass spectrograph [5]. The ionization was measured by two ten-layered sets of low-efficiency counters filled with a mixture of neon and propane* to a pressure of 30 mm Hg. Each layer had the same efficiency ; thus the entire system was equivalent to one 20-layered set of counters.

The primary ionization, which is the number of primary ion pairs produced in a layer of gas by a charged particle, is related to the probability of triggering of any given layer by the expression:

$$q = \frac{k}{N} = 1 - e^{-n} \quad \text{or} \quad n = n_0 I = \ln N - \ln (N - k),$$

where $\underline{q}$ is the probability of triggering of a layer, or efficiency; N is the total number of counter layers; $\underline{k}$ is the number of triggered layers; I is the relative primary ionization; $\underline{n}$ is the number of primary ion pairs produced in one layer by a charged particle; and n_0 is the number of primary ion pairs produced in a layer by a particle of minimum ionizing power.

The dependence of the relative error in the primary ionization on the efficiency of a layer is shown in Figure 1. The chosen layer efficiency $q = 0.71$ ensured the smallest error over the entire required range of ionization measurements.

Momenta and ionization were measured for 1779 muons. These particles were classified in 10 groups according to momentum; the average momentum and ionization were determined for each group.

For each momentum group the experimental distribution of ionization fluctuations was determined. These distributions possessed considerable asymmetry on the side of large ionization values due to the fact that the instrumental errors in determining the number of triggered layers, which have a normal distribution curve, are transformed nonsymmetrically in the determination of the ionization.

On the assumption that the upper portion of the experimental ionization fluctuation distribution is a symmetrical Gaussian curve we used the following method of treating the experimental data.

In the histogram whose horizontal axis represents ionization and whose vertical axis represents the number of observed events, a dividing line was drawn parallel to the horizontal axis and the weighted mean value of the ionization was found for the distribution lying above this line. We determined the relative fraction of the area α lying below the dividing line on the increase of which the weighted mean did not change. Each group of particles was treated in this way. The largest value of α which was obtained was 0.4. Then for each of the experimental histograms we performed a division at $\alpha = 0.4$ and from the distributions lying above these divisions we determined the average ionization. The statistical error was taken to be

---

*Commercial propane of unknown chemical composition was used.

$$\delta\% = \frac{\sigma_\alpha\%}{\sqrt{(1-\alpha)N}},$$

where $\sigma_\alpha\%$ is the half-width of the distribution lying above the dividing line, and N is the number of ionization counts in a given group.

The method described above enabled us to treat the experimental data with entire correctness and may prove to be useful in determining a probable value when the central portion of the experimental distribution is symmetrical.

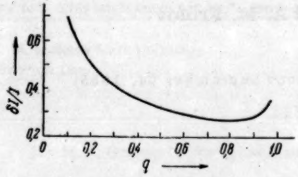

Figure 1. Dependence of the relative error δI/I in determining the ionization with 20-layered low-efficiency counters on the layer efficiency q.

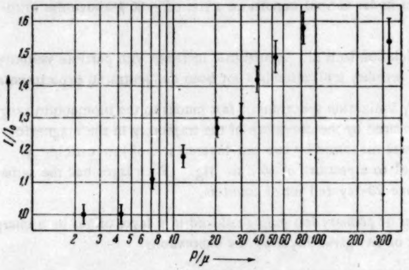

Figure 2. Dependence of primary ionization on particle velocity.

The results of the experiment (see Figure 2) agree qualitatively with the theoretically predicted logarithmic rise of the primary ionization by relativistic particles and confirm the saturation of the primary ionization due to polarization of the medium in the case of muons with momentum $p > 10^{10}$ ev/c.

Received September 20, 1955

LITERATURE CITED

[1] H. A. Bethe, Handb. d. Phys. 24/1, 518 (1933).

[2] P. Budini, G. Poiani, Nuovo cimento 9, 199 (1952).

[3] G. P. Eliseev, V. K. Kosmachevskii and V. A. Liubimov, Doklady Akad. Nauk SSSR 90, 995 (1953).

[4] M. H. Shamos, I. Hyges, Phys. Rev. 84, 1056 (1951).

[5] A. I. Alikhanov and G. P. Eliseev, J. Exptl.-Theoret. Phys. (USSR) 21, 1009 (1951).

DIFFUSION CHAMBER STUDY OF NEGATIVE PION SCATTERING IN HYDROGEN

M. Kozodaev, R. Suliaev, A. Filippov and Iu. Shcherbakov

(Presented by Academician L A. Artsimovich September 7, 1955)

In the present work, which was performed on the synchrocyclotron of the Institute for Nuclear Studies of the Academy of Sciences of the USSR using a diffusion chamber, we have studied the interaction of 330 Mev negative pions with protons. The following reactions are possible:

$$\pi^- + p \longrightarrow \pi^- + p \quad \text{(elastic scattering);} \quad (1)$$

$$\pi^- + P \longrightarrow \pi^0 + n \quad \text{(scattering with charge exchange);} \quad (2)$$

$$\pi^- + p \longrightarrow n + \gamma \quad \text{(radiative capture) .} \quad (3)$$

At such pion energies reactions accompanied by meson production are also possible. The principal aim of our work was the separate measurement of the total cross sections for elastic and charge-exchange scattering. In order to study the elementary scattering of pions by protons we used a diffusion chamber of 270 mm diameter filled with hydrogen at about 20 atmospheres. The bottom of the chamber was cooled by a mixture of dry ice and ethyl alcohol to −65 degrees; the temperature of the upper part was maintained by heaters at from + 10 to + 15 degrees. The required temperature distribution in the operating space was provided by a plexiglass ring 8 mm thick inside the chamber between the bottom and a trough containing methyl alcohol which served as the vapor source. Near the upper boundary of the sensitive layer was located an ion-collecting grid at −1000 volts with respect to the housing of the chamber. Under these conditions the height of the sensitive layer was about 6 cm; and it was illuminated from two sides through plexiglass windows by IPK-400 flash lamps. Particle tracks were photographed by a stereo-camera on 35 mm panchromatic film of 1000 units sensitivity. (All-Union State Standard).

The negative pions were produced in a carbon target inside the accelerator in the path of a circulating beam of 670 Mev protons. Deflected by the edge magnetic field of the accelerator, the pions passed through a steel collimator in a 4 meter concrete shield. The collimated meson beam was deflected by an electromagnet through 22 degrees and then entered the diffusion chamber. The pion energy was determined from a thin conductor model of the trajectory to be 330 ± 6 Mev. The simplicity of the kinematic picture of pion-proton collisions as well as the existence of a sufficiently monochromatic meson beam enabled us in this experiment to analyze each interaction very definitely even without the use of a magnetic field. In addition, the absence of a magnetic field simplified the problem of detecting $\pi - \mu$ decays and made it possible to measure angles with great accuracy.

A diffusion chamber cannot function with a large continuous ion flux; therefore pulses were obtained from the accelerator. The synchronization of the accelerator and of the operating devices of the diffusion chamber was effected by special electronic apparatus with a high-frequency accelerating voltage during one or more cycles for the time intervals required to restore the sensitivity of the diffusion chamber. The time between pulses as well as the number of cycles for each pulse was controlled within wide limits thus making it easy to provide the required mean beam intensity. The time between pulses was 5-6 seconds. Out of each pulse 4 particles on the average passed through the entrance window of the chamber. In 42 hours of operation about 12,000 photographs were obtained.

The photographs were scanned with a stereo-microscope. All cases were selected which could be considered to be pion-proton interactions as well as $\pi-\mu$ decays. The number of tracks of particles passing through the entrance window was recorded and all tracks were rejected which deviated from the principal direction by angles exceeding the angle of divergence of the beam. Elastic scattering was identified by the following criteria: 1) the initial particle is moving in the direction of the beam; 2) all three particle tracks are coplanar; 3) the relation between the scattering angles of the meson and the recoil proton corresponds to elastic scattering. In those instances where the recoil proton was stopped in the gas an additional criterion was the proton recoil energy determined by its range. In addition, in almost all cases it was possible to distinguish the recoil proton from the scattered meson by the ionization which they produced.

The identification of interactions accompanied by loss of the pion charge was very difficult. The principal difficulty was the existence in the diffusion chamber of regions of temporary local insensitivity. The following criteria were employed to determine such instances: 1) the track must be straight, going in the direction of the beam, with a distinct break-off; 2) the ionization at the end of the track must not increase and must be minimal; 3) the break-off of the track must not be at the edge of the illuminated region; 4) in the vicinity of the break-off there should be no detectable deficit of alcohol vapor. The last condition was determined by analyzing neighboring tracks and adjacent frames.

A stereocomparator was used to treat the data from all interactions.

The total pion range in the chamber was determined from the number of $\pi-\mu$ decays and the mean pion lifetime. 183 $\pi-\mu$ decays were recorded.

In order to obtain the total number of decays in the chamber it was necessary to correct for inefficiency of detection. The inefficiency in the detection of decays at angles ≥ 3 degrees was determined by a repeated careful examination of $\frac{1}{5}$ of all photographs to be 89%. A correction for omissions in the small angle range was introduced on the basis of the calculated distribution of decay angles, which is almost isotropic. In order to increase the statistical accuracy of the mapping of the experimental distribution we used the averaged results of both stereo images. The resulting distribution is shown in Figure 1. The sum of the above-mentioned corrections is proportional to the shaded area. Finally, a small correction was made for inefficiency of detection of $\pi-\mu$ decays near the chamber walls.

In computing the total pion range in the chamber the average lifetime of a pion at rest was assumed to be $(2.55 \pm 0.19)\ 10^{-8}$ seconds [1]. From a comparison of the total pion range obtained in this way with the combined trajectories of both particles in the chamber it was found that the admixture of muons and electrons in the beam was about 6%.

The examination of the photographs revealed 11 instances of elastic scatterings of pions by protons, the data for which is collected in Table 1. The total elastic scattering cross section computed from these 11 scatterings and the above-determined total pion range in the chamber is $\sigma_{el} = (11 \pm 4)\ 10^{-27}\ \text{cm}^2$.

The differential cross sections for three angular ranges in the center-of-mass system in units $10^{-27}\ \text{cm}^2/\text{sterad}$ are:

$$\left.\frac{\Delta\sigma}{\Delta\Omega}\right|_{0^\circ}^{60^\circ} = (1.3 \pm 0.7); \quad \left.\frac{\Delta\sigma}{\Delta\Omega}\right|_{60^\circ}^{120^\circ} = (0.3 \pm 0.2); \quad \left.\frac{\Delta\sigma}{\Delta\Omega}\right|_{120^\circ}^{180^\circ} = (1.6 \pm 0.7).$$

So far as these results enable us to judge the angular distribution of elastic pion scattering it can be said that the shape of the distribution changes slightly as the energy rises from 217 Mev to 330 Mev [2].

We also observed 13 cases of break-off of particle tracks. These can be identified with either of the Reactions (2) or (3) or with $\pi^- + p \longrightarrow 2\pi^0 + n$ since all of these give no charged particle in the final state. Experiments on the interaction of pions with nuclei of photographic emulsions [3, 4] as well as the fact that we observed not a single instance which could be identified with the creation of charged mesons indicate that the cross section of the latter reaction, at least, is smaller than $10^{-27}\ \text{cm}^2$. The cross section for radiative capture of pions [Reaction (3)] can be computed by the principle of detailed balancing from the cross section of photoproduction of charged mesons by protons, keeping in mind the approximately equal yield of positive and negative photomesons from deuterium [5, 6]. This computation gives for reaction (3) the value

TABLE 1

Case No.	Pion scattering angle in laboratory system, (deg)	Recoil proton scattering angle in laboratory system, (deg)	Scattering angle in center of mass system, (deg)
1	5.3	83.4	9.3
2	8.8	85.6	12.5
3	14.6	79.2	21.6
4	44.0	57.3	59.9
5	48.4	55.8	65.4
6	96.1	28.0	116.1
7	113.6	24.4	130.9
8	120.0	20.1	136.7
9	127.8	17.7	142.6
10	135.5	14.2	148.5
11	160.1	8.2	166.2

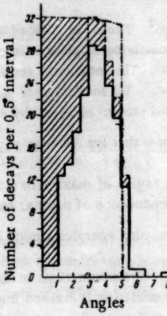

Figure 1. Angular distribution of $\pi - \mu$ decays.

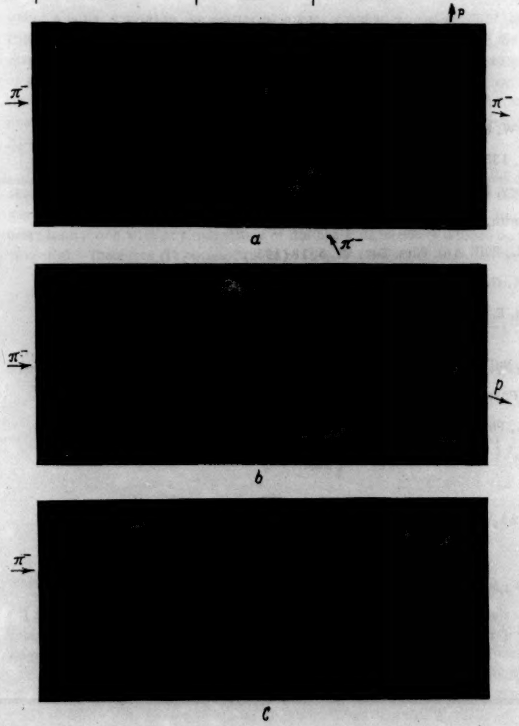

Figure 2. Photographs of interactions between negative pions and protons in a diffusion chamber.
a) Scattering of a negative pion by a proton at 8.8°;
b) scattering of a negative pion by a proton at 96.1°;
c) scattering of a negative pion with charge exchange.

$\sigma_{rad} = 0.2 \cdot 10^{-27}$ cm^2. These values lead us to assume that the break-offs of tracks in the chamber are due principally to the scattering of pions with charge exchange. The cross section found for this reaction is $\sigma_{ch} = (13 \pm 4) \cdot 10^{-27}$ cm^2. The total cross section for the interaction of pions with protons at 330 Mev is $\sigma_t = (24 \pm 5) \cdot 10^{-27}$ cm^2. This result agrees quite well with the measured total cross sections for the interaction of negative pions and protons obtained by a transmission method [7, 8].

The results show that for 330 Mev negative pions the cross section ratio is $\frac{\sigma_{ch}}{\sigma_{el}} = 1.2 \pm 0.5$. At lower pion energies in the region of maximum cross sections this ratio is approximately 2 [2, 9, 10]. From the hypothesis of charge independence of nuclear forces we may conclude that the observed change of the ratio $\frac{\sigma_{ch}}{\sigma_{el}}$ indicates that at pion energies around 330 Mev there is no longer a predominant interaction in a state with isotopic spin $T = {}^3/_2$. The interactions in states with isotopic spins $T = {}^3/_2$ and ${}^1/_2$ at this energy are equally important. A similar conclusion is derived from comparison of the total scattering cross sections of positive and negative mesons by protons at the same energies [7, 8].

In conclusion we wish to thank M. M. Kuliukin and T. N. Tomilina for their assistance with the pulsed operation of the accelerator.

Institute for Nuclear Problems
Academy of Sciences of the USSR

Received September 6, 1955

LITERATURE CITED

[1] R. P. Durbin, H. H. Loar, W. W. Havens, Phys. Rev. 88, 168, 179 (1952).

[2] M. Glicksman, Phys. Rev. 94, 1335 (1954).

[3] N. A. Mitin and E. L. Grigor'ev, Doklady Akad. Nauk SSSR 103, 2 (1955).

[4] M. Blau, M. Caulton, J. E. Smith, Phys. Rev. 92, 516 (1953).

[5] R. F. Backer, J. C. Keek et al., Bull. Am. Phys. Soc. 28, 5, 18 (1953).

[6] R. S. White, M. J. Jacobson, A. G. Schulz, Phys. Rev. 88, 836 (1952).

[7] A. E. Ignatenko, A. I. Mukhin, E. B. Ozerov and B. M. Pontecorvo, Doklady Akad. Nauk SSSR 103, 3 (1955).

[8] C. L. Juan, S. L. Lindenbaum, Bull. Am. Phys. Soc. 28, 6, 13 (1953).

[9] H. Anderson, E. Fermi et al., Phys. Rev. 91, 155 (1953).

[10] E. Fermi, M. Glicksman et al., Phys. Rev. 92, 161 (1953).

THE APPLICATION OF FERMI'S EQUATION TO THE POLARIZATION OF SCATTERED FAST NUCLEONS

I. I. Levintov

(Presented by Academician L. D. Landau October 22, 1955)

In connection with experiments on the polarization of fast protons scattered by nuclei (see experimental work in [1, 10]) Fermi [2] estimated polarization effects in the first Born approximation using a complex potential in the form of a square well with spin-orbit interaction $H_{so} = \frac{a}{r}\frac{dv}{dr}(\mathbf{l}, \vec{\sigma})$ where v is the real part of the potential. The following equation is obtained for the polarization:

$$P(\theta) = (\mathbf{n}\, 2k^2 vwa \sin\theta / v^2 + w^2)(1 + k^4 a^2 v^2 \sin^2\theta / v^2 + w^2)^{-1}, \tag{1}$$

where **n** is the normal to the scattering plane; $\underline{v}$ and $\underline{w}$ are the depth of the real and imaginary parts of the potential; $\underline{a}$ is the spin-orbit coupling constant. Heckrotte [3] showed that (1) is invariant with respect to the shape of the potential well. Both in Fermi's and in Heckrotte's work an important assumption was the smallness of the total nuclear potential, i.e., it was assumed that all phases $\Delta_l^{\pm} \ll 1$. While this assumption can be considered valid to some degree for the lightest nuclei (for example He^4), for medium and certainly for the heaviest nuclei the phases cannot be considered small (even for scattering of 100 Mev neutrons from carbon $\Delta_1 \sim 0.6$ for small $\underline{l}$).

Therefore a number of writers [1, 2, 4] including the author of the present note [5] have expressed doubts about the applicability of Eq. (1). It can be shown, however, that the requirement of smallness of all phases is too strong. To satisfy (1) it is sufficient to require smallness of only the part of a phase which depends on a spin-orbit interaction with any magnitude of the phase shifts which depend on the central part of the complex potential. Therefore (1) corresponds to reality to a larger degree than had been previously thought.

The basis of the proof is Lepore's equation [6]:

$$\mathbf{p} = \mathbf{n}(AB^* + BA^*)(AA^* + BB^*)^{-1}, \tag{2}$$

where A and B are the scattering amplitudes without and with spin inversion:

$$A = \frac{ik}{2}\sqrt{\frac{\theta}{\sin\theta}}\int_0^\infty \left\{2 - e^{2i\Delta_\rho^+} - e^{2i\Delta_\rho^-}\right\} J_0(k\rho\theta)\,\rho\, d\rho, \tag{3}$$

$$B = -\frac{k}{2}\sqrt{\frac{\theta}{\sin\theta}}\int_0^\infty \left\{e^{2i\Delta_\rho^+} - e^{2i\Delta_\rho^-}\right\} J_1(k\rho\theta)\,\rho\, d\rho, \tag{4}$$

where $\Delta_\rho^{\pm}$ are complex phases corresponding to $I = l \pm \frac{1}{2}$; and the $J_{0,1}$ are Bessel functions. Equations (3) and (4) are obtained directly from the corresponding expressions for Lepore's amplitudes [6] with the summation over orbital momenta $\underline{l}$ replaced by integration over the impact parameter $\rho = l/k$, and with the Legendre polynomials replaced by asymptotic expressions given by Fok [7, 8]:

$$P_l = \sqrt{\frac{\theta}{\sin\theta}}\, J_0\left\{\left(l+\frac{1}{2}\right)\theta\right\}; \quad P_l^1 = \sqrt{\frac{\theta}{\sin\theta}}\left(l+\frac{1}{2}\right) J_1\left\{\left(l+\frac{1}{2}\right)\theta\right\}.$$

These expressions can be used for angles $0 \leq \theta \leq \pi/2$.

For the purpose of determining the phases we use the well-known semiclassical expression

$$\Delta_\rho^{\pm} = -\frac{k}{2E}\int_\rho^\infty \frac{V_\rho^{\pm}(r)\, r\, dr}{\sqrt{r^2-\rho^2}} = -\frac{k}{2E}\int_0^\infty V_\rho^{\pm}\left(\sqrt{s^2+\rho^2}\right) ds \tag{5}$$

(the right-hand side of (5) is obtained by conversion to the new variable of integration $s = \sqrt{r^2-\rho^2}$).

The nuclear potential $V_\rho^{\pm}$ is written as

$$V_\rho^{\pm} = A_1 q(r) + \frac{A_2}{r}\frac{dq}{dr}(\mathbf{l}, \vec{\sigma}), \tag{6}$$

where A_1 and A_2 are complex *: $A_{1,2} = V_{1,2}e^{i\alpha_{1,2}}$; q(r) is an arbitrary radial function in the potential. We merely assume that for sufficiently large ρ $\Delta\rho \equiv 0$. From (5) and (6) we have

$$\Delta_\rho^{\pm} = \Delta_\rho^{(0)} \pm \Delta_\rho^{so}, \tag{7}$$

$$\Delta_\rho^{(0)} = A_1\frac{k}{2E}\int_0^\infty q\left(\sqrt{\rho^2+s^2}\right) ds \tag{8a}$$

$$\Delta_\rho^{so} = A_2\frac{k}{2E}\int_0^\infty \frac{k\rho}{\sqrt{\rho^2+s^2}}\,\frac{dq\left(\sqrt{\rho^2+s^2}\right)}{d\left(\sqrt{\rho^2+s^2}\right)}\, ds; \tag{8b}$$

(in (8b) we have replaced the eigenvalues of $(\mathbf{l}\vec{\sigma})$ by $\pm\, k\rho$).

We define $\Delta_\rho^{(0)}$ as the complex phase associated with the part of the potential which is spin-independent and Δ_ρ^{so} as the part of the phase due to the spin-orbit interaction in (6).

By differentiating $\Delta_\rho^{(0)}$ with respect to ρ we find that

$$\Delta_\rho^{so} = k\frac{A_2}{A_1}\frac{d\Delta_\rho^{(0)}}{d\rho}. \tag{9}$$

---

* The complex nature of the spin-orbit interaction was pointed out by L. D. Landau.

We now assume that $\Delta_\rho^{s\,o} \ll 1$ for all values of ρ. Then (3) and (4) can be expanded in terms of $\Delta_\rho^{s\,o}$ and limited to the first term of the series. As a result we have:

$$A = ik\sqrt{\frac{\theta}{\sin\theta}}\int_0^\infty \{1 - e^{2i\Delta_\rho^{(0)}}\} J_0(k\rho\theta)\,\rho\,d\rho; \tag{10}$$

$$B = -2ik\sqrt{\frac{\theta}{\sin\theta}}\int_0^\infty \Delta_\rho^{s\,o} e^{2i\Delta_\rho^{(0)}} J_1(k\rho\theta)\,\rho\,d\rho. \tag{11}$$

Substituting in (11) the value of $\Delta_\rho^{s\,o}$ from (9) we obtain for B after some simple transformations:

$$B = k^2\frac{A_2}{A_1}\sqrt{\frac{\theta}{\sin\theta}}\int_0^\infty J_1(k\rho\theta)\,\rho\,d\left\{1 - e^{2i\Delta_\rho^{(0)}}\right\}. \tag{12}$$

Integrating (12) by parts and using the well-known expression for the Bessel functions $d[xJ_1(cx)] = cxJ_0(cx)dx$, remembering that for $\rho \to \infty$ $\Delta_\rho \equiv 0$, we finally obtain for B

$$B = -k^2\frac{A_2}{A_1}\theta k\sqrt{\frac{\theta}{\sin\theta}}\int_0^\infty \left\{1 - e^{2i\Delta_\rho^{(0)}}\right\} J_0(k\rho\theta)\,\rho\,d\rho, \tag{13}$$

i.e., B differs from A only by the factor $k^2\frac{A_2}{A_1}\theta$.

From (2), (10) and (13) there follows directly

$$\mathbf{P} = -2nk^2\frac{V_2}{V_1}\sin(\alpha_2 - \alpha_1)\,\theta\left\{1 + k^4\left(\frac{V_2}{V_1}\right)^2\theta^2\right\}^{-1}. \tag{14}$$

Eq. (14) is transformed into (1) if we assume (with Fermi) that the spin-orbit interaction is real and use the asymptotic expressions for the Legendre polynomials which are suitable for small angles: $P_1(\cos\theta) = J_0(1\sin\theta)$.

With the aid of (9) we can verify our basic assumption of the smallness of $\Delta_\rho^{s\,o}$. We take the value $A_2 = 5\cdot 10^{-26}$ Mev · cm² from reference [1]. This value of A_2 satisfies the experimental data on polarization of 300 Mev protons scattered at small angles from light nuclei. The effective value is

$$\bar{\Delta}_\rho^{so} = k\frac{A_2}{A_1}\overline{\frac{d\Delta_\rho^0}{d\rho}} \cong k\frac{A_2}{A_1}\frac{\Delta_{\rho=0}^0}{R} \cong c\frac{k^2}{E}A_2,$$

where R is the effective nuclear radius; c = 1/2, 1/4, 1/3, $\pi/4$ for a square, triangular, parabolic and Gaussian well, respectively. Thus we obtain $\bar{\Delta}_\rho^{s\,o} \cong 0.1$ independently of the energy and radius. It is thus seen that the condition $\bar{\Delta}_\rho^{s\,o} \cong 1$ is probably satisfied for all nuclei. It should be noted, however, that for all particles which are scattered by the edge of the nucleus the condition $\Delta_\rho^{s\,o} \ll 1$ may not be satisfied because of the excessively large gradient of q(r) at the edge.

For the experimental verification of (14) we express the parameters in (14) in terms of θ_m and P_m, the angle and magnitude of maximum polarization:

$$\mathbf{P}(\theta) = 2\mathbf{n} P_m x (1 + x^2)^{-1}, \tag{15}$$

where

$$x = \frac{\theta}{\theta_m}, \quad P_m = \sin(\alpha_1 - \alpha_2), \quad \theta_m = \frac{1}{k^2}\frac{V_1}{V_2}. \tag{16}$$

A comparison of (15) and (16) with the available experimental data on the polarization of protons is difficult for two reasons: 1) at angles $\theta < \theta_m$ interference with Coulomb scattering will strongly decrease the magnitude of the polarization compared with the value calculated from (15) [1]; 2) at large angles ($\theta > \theta_m$) the measured values of P will also be decreased by the inseparable admixture of practically unpolarized inelastically scattered particles. An examination of the experimental data confirms the above in general. The nonmonotonic nature of the decrease of polarization which is observed after the first principal maximum is probably due to the fact that for large angles an important contribution comes from particles which are scattered by the edge of the nucleus, for which the condition $\Delta_\rho^{s\,0} \ll 1$ cannot be satisfied.

An estimate of the values of V_2/V_1 and $\sin(\alpha_2 - \alpha_1)$ from experimental data is of course only approximate. This applies especially to $\sin(\alpha_2 - \alpha_1)$ since the measured values of P_m may be diminished due to inelastic processes. The values of $\theta_m = \frac{V_1}{V_2}\frac{1}{k^2}$ are evidently better. This is confirmed by the fact that θ_m is actually inversely proportional to the energy, as follows from (15).

In Table 1 we present the values of V_2/V_1 and of $\sin(\alpha_1 - \alpha_2)$ obtained from (15) and (16) using all the experimental data at our disposal. The data in Table 1 for V_2/V_1 can be compared with an analogous value obtained from the phases of $p-He^4$ scattering at 1-10 Mev [9]. Indeed, the best agreement of experimental and calculated phases is obtained with the Gaussian potential and the ratio $V_2/V_1 = 3.3 \cdot 10^{-27}$ cm²; we arrive at this value by evaluating V_2/V_1 from the one-particle doublets of Pb^{209} [13] and from the doublet $D_{5/2}$-$D_{3/2}$ of O^{17}. We once more [11] call attention to the noteworthy constancy of V_2/V_1 when the energy and atomic weight change by two orders.

TABLE 1

Element	E_p, Mev	P_{max}	θ_{max} in degrees	$\frac{V_2}{V_1} \cdot 10^{27}$ cm²	Source in the literature
He .	315	0.76	17	3.3	(1)
C . .	290	0.72	12	3.4	(1)
C . .	130	0.82	25	3.5	(10)
Be .	315	0.64	12	4	(12)
Be .	130	0.78	25	3.5	(10)
Al .	290	0.64	12	4	(1)
Al .	130	0.72	20	4.6	(10)
Fe .	130	0.63	28	3.3	(10)
Cd .	130	0.63	22	3.9	(10)
In . .	130	0.60	30	3.1	(10)
Bi . .	130	0.41	27	3.5	(10)
U . .	130	0.41	25	3.6	(10)

Fernbach, Lepore and Heckrotte [1] have shown that an interaction such as (6) can be obtained formally if the nuclear potential is considered to result from the averaged interaction of the incident nucleon with the individual nucleons of the nucleus. In such a theory the indicated energy-independence of V_2/V_1 imposes definite conditions on the nature of the nucleon-nucleon scattering amplitude:

$$\langle f \mid t \mid i \rangle = A + A_1 \left(\vec{\sigma}_1 + \vec{\sigma}_2\right) \mathbf{n} + \ldots$$

$\mathrm{Re}\,|A_1/A_2|$ is apparently independent of the energy.

In conclusion we wish to point out that (15) is not in contradiction with Eq. (15) of reference [11], which follows at least from the fact that the only experimental data lead to similar values of the spin-orbit coupling constant. However, the equations of reference [11] are given in a worse approximation than (14) of the present paper.

I am indebted to L. D. Landau for much advice.

Institute for Chemical Physics
Academy of Sciences of the USSR

Received October 13, 1955

LITERATURE CITED

[1] S. Fernbach, W. Heckrotte, J. Lepore, Phys. Rev. 97, 1068 (1955).

[2] E. Fermi, Nuovo cimento 11, 407 (1954).

[3] W. Heckrotte, Phys. Rev. 94, 1797 (1954).

[4] B. Bosco, T. Regge, Nuovo cimento 12, 285 (1954).

[5] I. I. Levintov, Doklady Akad. Nauk SSSR 98, 373 (1954).

[6] J. V. Lepore, Phys. Rev. 79, 137 (1950).

[7] V. A. Fok, Doklady Akad. Nauk SSSR 1, 3, 97 (1934).

[8] K. S. Shifrin, Dispersion of Light in a Turbid Medium, Foreign Lit. Press, 1951.

[9] S. Sack, J. C. Biedenharn, D. T. Breit, Phys. Rev. 93, 321 (1954).

[10] T. M. Dickson, Mr. B. Rose, D. C. Salter, Proc. Phys. Soc. (London) 68A, 361 (1955).

[11] I. I. Levintov, Doklady Akad. Nauk SSSR 103, 215 (1955).

[12] H.G. de Carvalho, T. Marshall,L. Marshall, Phys. Rev 96, 1081 (1954).

[13] R. T. Blin-Stogle, Phil. Mag. 46, 973 (1955).

THE DIFFRACTIVE SCATTERING OF FAST DEUTERONS

A. I. Akhiezer and A. G. Sitenko

(Presented by Academician L. D. Landau October 3, 1955)

1. It is known that the absorption of particles scattered by a nucleus induces destructive interference with the incident wave which results in elastic scattering that is not associated with the formation of a compound nucleus. This elastic scattering which is due to an absorbing scatter is similar in the case of small wave lengths of the incident particles to the diffraction of light from an ideal black sphere and is called diffractive scattering. The diffractive scattering of point particles (such as neutrons) by absorbing nuclei can be investigated by an optical method using Huygens' principle. In the study of diffractive scattering of complex particles (such as deuterons) this method cannot be used directly. The required generalization of the ordinary optical method has been indicated by L. D. Landau.

In order to understand the nature of this generalization we shall consider first of all the simplest case of diffractive scattering of point particles by absorbing nuclei assuming the nuclei to be perfectly black.

The free motion of the particles in a plane perpendicular to the wave vector of the incident particles (the z-axis) is characterized by the wave function $\psi_{\vec{\varkappa}} = \frac{1}{L} e^{i\vec{\varkappa}\vec{\rho}}$, where L is the normalizing length and $\vec{\kappa}$ is the projection of the wave vector on the plane perpendicular to the z-axis. (The functions $\psi_{\vec{\kappa}}$ are normalized by $\int \psi_{\vec{\varkappa}} \psi^*_{\vec{\varkappa}'} d\vec{\rho} = \delta_{\vec{\varkappa}\vec{\varkappa}'}$.) . The wave function $\psi_0 = 1/L$ represents incident particles. An absorbing nucleus results in the "eating away" of a portion of this function when $\rho \le R$ (R is the nuclear radius). The diffraction picture resulting from this "eating away" can be obtained by expanding in terms of the functions $\psi_{\vec{\kappa}}$ the remainder of the wave function which is given by $\Psi = \Omega(\rho)\psi_0$ (where $\Omega(\rho) = 0$ for $\rho \le R$; $\Omega(\rho) = 1$ for $\rho > R$):

$$\Psi = \Omega(\rho)\psi_0 = \sum_{\vec{\varkappa}} a_{\vec{\varkappa}} \psi_{\vec{\varkappa}}. \tag{1}$$

The probability of diffractive scattering in which the wave vector $\vec{\kappa}$ of the scattered particle lies in the interval $d\vec{\kappa}$ is related to $a_{\vec{\kappa}}$ by $dw = |a_{\vec{\varkappa}}|^2 \frac{L^2 d\vec{\varkappa}}{(2\pi)^2}$, and the corresponding differential scattering cross section is

$$d\sigma = \frac{dw}{1/L^2} = |a_{\vec{\varkappa}}|^2 \frac{L^4\, d\vec{\varkappa}}{(2\pi)^2}. \tag{2}$$

If K is the magnitude of the particle wave vector, $\kappa = K \sin\theta$ and $d\vec{\kappa} = K^2 do$, where do is an element of solid angle.

The scattering amplitude $f(\theta)$ is related to the expansion coefficient $a_{\vec{\kappa}}$ by

$$f(\vartheta) = -i \frac{L^2 K}{2\pi} a_{\vec{\varkappa}}. \tag{3}$$

Thus for point particles we obtain the well-known formulas

$$f(\vartheta) = iR \frac{J_1(KR\vartheta)}{\vartheta}, \quad d\sigma = R^2 \frac{J_1^2(KR\vartheta)}{\vartheta^2} do \quad \vartheta \ll 1. \tag{4}$$

The above discussion of the diffraction of point particles allows direct generalization for diffractive scattering of complex particles.

2. We shall first examine elastic diffractive scattering of deuterons by absorbing nuclei assuming $\lambda\!\!\!^{-} \ll R$. We shall neglect effects due to the Coulomb interaction. The deuteron diffraction picture is determined by the series expansion of the "eaten-away" function $\Psi = \Omega(\rho_n)\,\Omega(\rho_p)\,\psi_0(\vec{\rho}_d)\,\varphi_0(r)$ in terms of $\psi_{\vec{\varkappa}}(\vec{\rho}_d)\,\varphi_0(r)$:

$$\Psi = \sum_{\vec{\varkappa}} A_{\vec{\varkappa}}\,\psi_{\vec{\varkappa}}(\vec{\rho}_d)\,\varphi_0(r), \tag{5}$$

where $\varphi_0(r) = \sqrt{\frac{\alpha}{2\pi}}\,\frac{e^{-\alpha r}}{r}$ is the wave function of the deuteron ground state and $\psi_{\vec{\varkappa}}(\vec{\rho}_d) = \frac{1}{L}\,e^{i\vec{\varkappa}\vec{\rho}_d}$ is the wave function of the motion of the center of gravity of the deuteron.

From (5) it follows that

$$f(\vartheta) \equiv -i\,\frac{L^2K}{2\pi}\,A_{\vec{\varkappa}} = iK\Bigg\{\frac{8\alpha}{\varkappa}\,\mathrm{arc\,tg}\,\frac{\varkappa}{4\alpha}\,\frac{RJ_1(\varkappa R)}{\varkappa} -$$

$$-\frac{1}{2\pi}\int\frac{4\alpha}{|2\mathbf{g}-\vec{\varkappa}|}\,\mathrm{arc\,tg}\,\frac{|2\mathbf{g}-\vec{\varkappa}|}{4\alpha}\,\frac{RJ_1(gR)}{g}\,\frac{RJ_1(|\vec{\varkappa}-\mathbf{g}|R)}{|\vec{\varkappa}-\mathbf{g}|}\,d\mathbf{g}\Bigg\}. \tag{6}$$

The differential cross section of elastic diffractive scattering is

$$d\sigma_e = R^2\Bigg|\frac{4p}{\varkappa'}\,\mathrm{arc\,tg}\,\frac{\varkappa'}{2p}\,\frac{J_1(\varkappa')}{\varkappa'} -$$

$$-\frac{1}{2\pi}\int\frac{2p}{|2\mathbf{g}'-\vec{\varkappa}'|}\,\mathrm{arc\,tg}\,\frac{|2\mathbf{g}'-\vec{\varkappa}'|}{2p}\,\frac{J_1(g')}{g'}\,\frac{J_1(|\vec{\varkappa}'-\mathbf{g}'|)}{|\vec{\varkappa}'-\mathbf{g}'|}\,d\mathbf{g}'\Bigg|^2 d\vec{\varkappa}', \tag{7}$$

where $\vec{\kappa}' = R\vec{\kappa}$, $\mathbf{g}' = R\mathbf{g}$ and $p = 2\alpha R = R/R_d$ (R_d is the deuteron radius).

In the limiting case $p \gg 1$ the differential cross section for elastic scattering becomes

$$d\sigma_e = 2\pi R^2\left\{\left(\frac{2p}{\varkappa}\,\mathrm{arc\,tg}\,\frac{\varkappa}{2p}\right)^2\frac{J_1^2(\varkappa)}{\varkappa} + \frac{1}{2p}\,J_1(\varkappa)\,J_0(\varkappa)\right\}d\varkappa, \quad p \gg 1. \tag{8}$$

The integral elastic scattering cross section is then

$$\sigma_e = \pi R^2 + \frac{\pi}{3}(1-\ln 2)\,RR_d, \quad R_d \ll R. \tag{9}$$

3. From knowledge of the elastic scattering amplitude at zero angle it is possible to obtain the total cross section of all processes (both elastic scattering and absorption) [1]:

$$\sigma_t = 4\pi\lambda\!\!\!^{-} J_m f(0). \tag{10}$$

Using (6) we obtain

$$\sigma_t = 4\pi R^2\left\{1 - \int_0^\infty \frac{p}{\xi}\,\mathrm{arc\,tg}\,\frac{\xi}{p}\,\frac{J_1^2(\xi)}{\xi}\,d\xi\right\}, \quad p = \frac{R}{R_d}. \tag{11}$$

In the limiting case $p \gg 1$ the total cross section is

$$\sigma_t = 2\pi R^2 + \pi RR_d, \quad R_d \ll R. \tag{12}$$

4. As a result of the small binding energy of the deuteron a comparatively small change of its momentum in diffractive scattering may result in disintegration of the deuteron at some distance from the nucleus. This process may be called diffractive disintegration of the deuteron.* Both "stripping" and diffractive disintegration result in the liberation of the neutron and proton which compose the deuteron.

The probability amplitude of diffractive disintegration of the deuteron can be determined analogously to the amplitude of elastic diffractive scattering. It is only necessary in the series expansion (5) to replace $\varphi_0(\mathbf{r})$ with the function

$$\varphi_{\mathbf{f}}(\mathbf{r}) = \frac{1}{L^{3/2}}\left(e^{i\mathbf{fr}} + \frac{a}{r}\,e^{-ifr}\right),$$

which describes the relative motion of the neutron and proton which are liberated by deuteron disintegration. Here $\hbar\mathbf{f}$ is the momentum of relative motion of the particles and $a = -\dfrac{1}{\alpha - if}$ is the scattering length of the neutron by a proton in an S-state. The second term in $\varphi_{\mathbf{f}}$ is a spherical ingoing wave which, as is well known, must always be taken into consideration when a new particle appears [3].

Thus the diffractive disintegration cross section is given by the formula

$$d\sigma_f = |A_{\vec{\varkappa}\,\mathbf{f}}|^2 \frac{L^2 d\vec{\varkappa}}{(2\pi)^2}\,\frac{L^3 d\mathbf{f}}{(2\pi)^3}\,L^2, \tag{13}$$

where

$$\begin{aligned} A_{\vec{\varkappa}\,\mathbf{f}} = -\frac{2\pi}{L^2}\sqrt{\frac{\alpha}{2\pi}}\,\frac{1}{L^{3/2}}\,\frac{R^2}{\alpha^2}\Bigg\{&\frac{J_1(\varkappa')}{\varkappa'}\int\frac{e^{-x}}{x}\left(e^{-i\mathbf{ux}} - \frac{1}{1+iu}\,\frac{e^{iux}}{x}\right)e^{i\frac{\vec{\varkappa}'\mathbf{x}}{p}}\,d\mathbf{x} + \\ &+ \frac{J_1(\varkappa')}{\varkappa'}\int\frac{e^{-x}}{x}\left(e^{-i\mathbf{ux}} - \frac{1}{1+iu}\,\frac{e^{iux}}{x}\right)e^{-i\frac{\vec{\varkappa}'\mathbf{x}}{p}}\,d\mathbf{x} - \\ &- \frac{1}{2\pi}\int\frac{J_1(g')}{g'}\,\frac{J_1(|\vec{\varkappa}' - \mathbf{g}'|)}{|\vec{\varkappa}' - \mathbf{g}'|}\left[\int\frac{e^{-x}}{x}\left(e^{i\mathbf{ux}} - \frac{1}{1+iu}\,\frac{e^{iux}}{x}\right)e^{i\frac{2\mathbf{g}' - \vec{\varkappa}'}{p}\mathbf{x}}\,d\mathbf{x}\right]d\mathbf{g}'\Bigg\}, \end{aligned} \tag{14}$$

$$\mathbf{f} = \alpha\mathbf{u}, \quad \vec{\varkappa}R = \vec{\varkappa}', \quad \mathbf{g}R = \mathbf{g}', \quad \alpha\mathbf{r} = \mathbf{x}.$$

In the limiting case of large p the energy distribution of the products of deuteron disintegration is given by

$$d\sigma_f = 2RR_d\left\{1 + \frac{8}{3}(\ln 2 - 1)\frac{1}{1+u^2}\right\}\frac{u^2\,du}{(1+u^2)^2}, \quad p \gg 1. \tag{15}$$

The integral cross section for diffractive disintegration is

$$\sigma_f = \frac{\pi}{3}\left(\ln 2 + \frac{1}{2}\right)RR_d, \quad R_d \ll R. \tag{16}$$

5. From a comparison of the expressions for the cross sections σ_f and σ_e with the total cross section σ_t for p ≫ 1 it can easily be seen that the following relation holds good:

$$\sigma_e + \sigma_f = \frac{1}{2}\,\sigma_t. \tag{17}$$

This relation holds good for all values of p.

---

* The possibility of diffractive disintegration of the deuteron was established independently by E. L. Feinberg.

Since the sum of the cross sections for elastic scattering and diffractive disintegration of the deuteron comprise half of the total cross section the remaining processes also are represented by $\frac{1}{2}\sigma_t$. These processes are "stripping" of the neutron and proton and absorption of both particles by a nucleus. Representing the cross sections of these processes by σ_n, σ_p and σ_a, respectively, we have, consequently,

$$\sigma_n + \sigma_p + \sigma_a = \frac{1}{2}\sigma_t. \tag{18}$$

As we know [2], for $R_d \ll R$

$$\sigma_n = \sigma_p = \frac{\pi}{2} RR_d, \quad R_d \ll R. \tag{19}$$

With regard to the cross section for the absorption of the deuteron by a nucleus, i.e., the cross section for absorption of both particles, it can be shown that for $R_d \ll R$

$$\sigma_a = \pi R^2 - \frac{\pi}{2} RR_d, \quad R_d \ll R. \tag{20}$$

The authors are deeply indebted to Academician L. D. Landau, who suggested the method used in this paper for the study of diffraction problems.

Physico-technical Institute
Academy of Sciences of the USSR
and
A. M. Gorkii Kharkov State University

Received September 8, 1955

LITERATURE CITED

[1] B. Lippman, J. Schwinger, Phys. Rev. 79, 481 (1950).

[2] R. Serber, Phys. Rev. 72, 1008 (1947).

[3] A. Sommerfeld, Atombau und Spektrallinien, 1939.

THE VERTEX PART AT HIGH ENERGIES

V. Z. Blank

(Presented by Academician N. N. Bogoliubov October 4, 1955)

The method developed in reference [1] can be used to investigate the behavior of the vertex part $\Gamma_\alpha(p, q\,|\,\underline{1})$ for $|\underline{1}^2| \gg |p^2|, |q^2| \gg m^2$. This problem was examined by V. V. Sudakov [2] using the method of adding diagrams and for the more general case $|\underline{1}^2| \gg |p^2|, |q^2|$ by A. A. Abrikosov [3]. This case is extremely important for the study of high energy effects.

In order to obtain the vertex part we use the relation between the electron Green's function and the vertex part:

$$\Gamma_\alpha(p, q\,|\,l) = -G^{-1}(q\,|\,0)\left\{\frac{\delta G(p\,|\,A)}{\delta e A_\alpha(l)}\right\}_{A=0} G^{-1}(p\,|\,0). \tag{1}$$

We write the equation for the Green's function of the electron in the impulse representation [1]:

$$\Big\{\hat{p} - m + \int \hat{k} A_\alpha(k)\frac{\delta}{\delta A_\alpha(k)}\,dk + \varepsilon\int \hat{A}(k)\,dk + \\ + i\varepsilon\gamma_\beta\int \mathscr{G}_{\beta\alpha}(k)\frac{\delta}{\delta A_\alpha(k)}\,dk\Big\}\, G(p\,|\,A) = -1, \tag{2}$$

where $\varepsilon = \sqrt{4\pi}e/(2\pi)^2$. We denote the operator which acts on $G(p\,|\,A)$ by $\mathscr{H}$. We take the variational derivative of (2):

$$\mathscr{H}\frac{\delta G(p\,|\,A)}{\delta A_\alpha(l)} = -\frac{\delta\mathscr{H}}{\delta A_\alpha(l)}\, G(p\,|\,A),$$

and for $\delta G(p\,|\,A)/\delta A_\alpha(\underline{1})$ we obtain

$$\Big\{\hat{p} + \hat{l} - m + \int \hat{k} A_\alpha(k)\frac{\delta}{\delta A_\alpha(k)}\,dk + \varepsilon\int \hat{A}(k)\,dk + \\ + i\varepsilon\gamma_\beta\int \mathscr{G}_{\beta\alpha}(k)\frac{\delta}{\delta A_\alpha(k)}\,dk\Big\}\frac{\delta G}{\delta A_\alpha(l)} = -\varepsilon\gamma_\alpha G. \tag{3}$$

We shall solve this equation with respect to $\delta G(p\,|\,A)/\delta A_\alpha(l)$.

We perform the quadrature of (3) setting

$$\frac{\delta G(p\,|\,A)}{\delta A_\alpha(l)} = \Big\{\hat{q} + m + \int \hat{k} A_\alpha(k)\frac{\delta}{\delta A_\alpha(k)}\,dk + \varepsilon\int \hat{A}(k)\,dk + \\ + i\varepsilon\gamma_\beta\int \mathscr{G}_{\beta\alpha}(k)\frac{\delta}{\delta A_\alpha(k)}\,dk\Big\}\,\Delta_\alpha(q, p\,|\,A),$$

where $\hat{q} = \hat{p} + \hat{\underline{1}}$ from conservation of momentum. Unlike [1] we here need a more complete quadrature leaving a minimum number of matrices.

We now go over to proper time:

$$\Delta_\alpha(q, p|\ A) = -\int^{\infty} e^{-\varepsilon\nu} U_\nu(q, p|\ A)\, d\nu.$$

By this method the asymptotic behavior is determined in the region of large ν [1]. This is equivalent to integrating over k only in the region of small momenta. Therefore, in the lowest approximation we neglect all terms proportional to ϵ^2 as well as those proportional to ϵ in which k appears under the integral sign as a factor. Also, in this case $k_1 k_2$ is much smaller than k_1^2 and we shall drop the corresponding term. The resulting equation for $U_\nu(q, p|A)$ is

$$-i\frac{\partial U_\nu}{\partial\nu} = \Big\{q^2 - m^2 + \int (k^2 + 2kq)\, A_\sigma(k)\frac{\delta}{\delta A_\sigma(k)}\, dk + 2\varepsilon\int qA(k)\, dk + + 2i\varepsilon\int q_\sigma \mathscr{F}_{\sigma\tau}(k)\frac{\delta}{\delta A_\tau(k)}\, dk\Big\}\, U_\nu; \quad U_0 = -\varepsilon\gamma_\alpha G(p|A), \tag{4}$$

where $G(p|A)$ of the initial condition is obtained in the same approximation.

Equation (4) may be solved easily:

$$U_\nu(q, p|A) = \exp\Big\{i\nu(q^2 - m^2) + 2i\varepsilon\int_0^\nu d\nu\int qA(k)\exp[i(k^2 + 2kq)\nu]\, dk - - 4i\varepsilon^2\int_0^\nu d\nu\int_0^\nu d\nu\int q_\sigma q_\tau \mathscr{F}_{\sigma\tau}(k)\exp[i(k^2 + 2kq)\nu]\, dk\Big\}\, U_0(p/A^{tr}),$$

where

$$A_\sigma^{tr}(k) = \Big[A_\rho(k) + \frac{2i\varepsilon q_\beta \mathscr{F}_{\beta\sigma}(k)}{k^2 + 2kq}\Big]\exp\{i(k^2 + 2kq)\nu\}.$$

Furthermore

$$G(p|A) = \Big\{\hat{p} + m + \int \hat{k} A_\sigma(k)\frac{\delta}{\delta A_\sigma(k)}\, dk + \varepsilon\int \hat{A}(k)\, dk + + i\varepsilon\gamma_\sigma\int \mathscr{F}_{\sigma\tau}(k)\frac{\delta}{\delta A_\tau(k)}\, dk\Big\}\, \chi(p|A).$$

In our approximation $\chi(p|A)$ is given by:

$$\chi(p|A) = iZ^{-1}\int_0^\infty \exp\Big\{-\delta\mu + i\mu(p^2 - m^2) + + 2i\varepsilon\int_0^\mu d\mu\int pA(k)\exp[i(k^2 + 2kp)\mu]\, dk - - 4i\varepsilon^2\int_0^\mu d\mu\int_0^\mu d\mu\int p_\sigma p_\tau \mathscr{F}_{\sigma\tau}(k)\exp[i(k^2 + 2kp)\mu]\, dk\Big\}\, d\mu$$

and Z is the renormalization constant of the Green's function. The double integrals in the exponential function over μ and ν have been investigated in [1].

When $\delta G/\delta A_\alpha(\underline{1})$ is substituted in (1), the contribution of these terms is canceled by the corresponding terms of $G^{-1}(p|0)$ and $G^{-1}(q|0)$. Thus we shall not write these terms in the expression for $\delta G(p|A)/\delta A_\alpha(\underline{1})$:

$$\left\{\frac{\delta G(p\,|\,A)}{\delta A_\alpha(l)}\right\}_{A=0} = -(\hat{q}+m)\gamma_\alpha(\hat{p}+m)Z^{-1}\varepsilon\int_0^\infty d\nu\int_0^\infty d\mu \exp\{-\varepsilon\nu-\delta\mu+$$

$$+i(q^2-m^2)\nu+i(p^2-m^2)\mu+\Phi(\nu,\mu)\}\,d\mu,$$

where $$\Phi(\nu,\mu) = -4i\varepsilon^2\int_0^\nu d\nu\int_0^\mu d\mu\, q_\sigma \mathscr{D}_{\sigma\tau}(k)\,p_\tau \exp[i(k^2+2kq)\nu+i(k^2+2kp)\mu].$$

We note that the condition $|\underline{l}^2| \gg |q^2|, |p^2|$ is equivalent to $|(pq)| \gg |q^2|, |p^2|$. In order to eliminate divergences at small μ and ν we shall calculate the integrals from $1/(pq)\Lambda^2$ instead of from zero. Consequently Λ^2 approaches infinity and is eliminated by mass and charge renormalization. Assuming $|p^2|, |q^2| \gg m^2$ and eliminating divergences, we obtain

$$\Phi(\nu,\mu) \approx -\frac{e^2}{2\pi}\ln\{\mu(pq)\}\ln\{\nu(pq)\}.$$

Substituting the variables $\mu p^2 = \xi$, $\nu q^2 = \eta$ and selecting Z equal to the integral over ξ and η we obtain the expression for $\{\delta G/\delta A_\alpha(\underline{l})\}_{A=0}$:

$$\left\{\frac{\delta G}{\delta A_\alpha(l)}\right\}_{A=0} = -e\frac{(\hat{q}+m)\gamma_\alpha(\hat{p}+m)}{q^2p^2}\exp\left\{-\frac{e^2}{2\pi}\ln\left|\frac{(pq)}{p^2}\right|\ln\left|\frac{(pq)}{q^2}\right|\right\},$$

and for $\Gamma_\alpha(p,q\,|\,\underline{l})$ we obtain

$$\Gamma_\alpha(p,q\,|\,l) = \gamma_\alpha\exp\left\{-\frac{e^2}{2\pi}\ln\left|\frac{(pq)}{p^2}\right|\ln\left|\frac{(pq)}{q^2}\right|\right\},$$

which agrees with the result obtained by V. V. Sudakov [2].

In conclusion I wish to express my profound gratitude to N. N. Bogoliubov for his guidance.

M. V. Lomonosov Moscow State University Received May 20, 1955

LITERATURE CITED

[1] V. Z. Blank, Doklady Akad. Nauk SSSR 104, 5 (1955).

[2] V. V. Sudakov, Dissertation, Inst. Phys. Prob. Acad. Sci. USSR., 1954.

[3] A. A. Abrikosov, Dissertation, Inst. Phys. Prob. Acad. Sci. USSR, 1955.

THE TEMPERATURE DEPENDENCE OF THE ELASTIC CONSTANTS OF QUARTZ

V. G. Zubov

(Presented by Academician I. K. Kikoin, October 4, 1955)

1. We know [1-5] that measurements of the normal vibrational modes of quartz plates and blocks can be used to obtain the effective elastic coefficients q_1, q_2, q_3 which correspond to quasi-longitudinal and quasi-transverse waves propagating along each of the axes of the quartz. From these values of q_1, q_2, q_3 the fundamental dynamic elastic constants of quartz can be calculated from the Christoffel relationships.

Atanasoff and Hart [1] and Fredericks and Mikhailov [6] using electronic resonance methods have investigated the temperature dependence of q_1 and q_3 for the X and Y axes of quartz. They were thus able to obtain the general form of the temperature dependence of the elastic constants C_{11}, C_{66}, C_{44} and C_{14} of quartz from 0 to 573°.

The impossibility of observing by electronic means the vibrations corresponding to the coefficients q_2 of the X and Y axes and q_1, q_2, q_3 of the Z axis made it impossible for Atanasoff and Hart to investigate the temperature dependence of C_{33}, and made it necessary to calculate C_{44} and C_{14} from fairly complicated equations, which made the values obtained for these quantities unreliable, requiring further verification.

The present article describes the results obtained by a new measurement of the temperature dependence of the normal modes of quartz samples from 20 to 573° by observation of light diffraction on ultrasonic waves (the Bergmann-Schāfer method [7]).

2. Quartz samples in the shape of cubic blocks oriented along the principal axes were subjected to an alternating electric field whose intensity was of the order of 500-1000 v/cm and frequency 8-10 Mc along either the X or the Y axis. A mercury lamp with a green filter was used as the light source. The sample was placed in the path of a parallel beam and the diffraction patterns were observed and photographed in the focal plane of the objective.

The same sample was used to obtain diffraction patterns of the passage of light along each of the axes of the sample and for corresponding directions of the field.

Complete and entirely satisfactory diffraction patterns were obtained in the temperature ranges from 20 to 300° and 510 to 550°. In the range 300-510° individual diffraction points were obtained which correspond to the fundamental forms of vibration that can be excited by a field along the X or Y axis and to the coefficients q_1, q_2, q_3 of the X and Y axes. From the diffraction patterns were calculated the velocities of the quasi-longitudinal and quasi-transverse waves propagating along each axis as well as the values of all nine effective elastic coefficients corresponding to these waves.

3. Figure 1 shows the temperature dependence of the coefficients in the entire range. The curves are marked to show to which q coefficient and to which axis they correspond. The q_1X and q_3Y curves, which give the variation of C_{11} and C_{66}, bear the points obtained in [1]. The satisfactory agreement of our curves with [1] indicates that our method of measurement is reliable.

No data could be found in the literature for the q_1Z and q_2X, q_2Y curves. These curves give a direct determination of C_{44} and C_{33} and simplify the calculation of C_{14}.

As can be seen from Figure 1 at 370° the effective elastic coefficients corresponding to both transverse waves along the Y axis are equal, i.e., with regard to the propagation of transverse waves the Y axis of quartz at 370° resembles the Z axis to a certain extent. When this temperature is approached there is an attenuation of the piezoelectric action of quartz, and at 370° quartz almost ceases to be excited by a field along the Y axis. Above 370° the piezoelectric reaction of quartz to a field along the Y axis is restored and in a certain temperature range there is a gradual increase.

As shown by a preliminary calculation, in the 510-530° range an additional equality holds: $C_{44} = C_{66}$. In this range a considerable increase of piezoelectric activity was observed with respect to a field along the Y axis. At these temperatures the diffraction patterns were similar in completeness and sharpness to those taken at room temperature. It should be noted that the production of the patterns required a fairly strong external field.

The data indicate that at 370° and 510-530° partial changes take place in the elastic and piezoelectric properties of quarts which may be related to changes in other physical properties of the quartz.

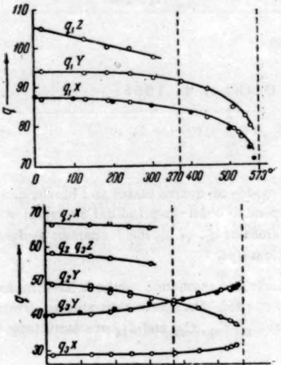

Figure 1.

M. B. Lomonosov Moscow State University

Received September 30, 1955

LITERATURE CITED

[1] J. V. Atanasoff, P. J. Hart, Phys. Rev. 59, 85 (1941).

[2] F. Jona, Helv. Phys. Acta 23, 6-7 (1950).

[3] O. Nomoto, Proc. Phys.-Math. Soc.(Japan) 25, 240 (1943).

[4] W. G. Cady, Piezoelectricity and its Practical Applications, For. Lit. Press, Moscow, 1949.

[5] Christoffel, Ann. di Mat. pura ed appl. II, 8, 193 (1877).

[6] V. Frederiks and G. Mikhailov, Z. Physik 76, 328 (1932).

[7] L. Bergmann, Der Ultraschall, und seine Anwendung in Wissenschaft und Technik, Zurich, 1954.

THE DETERMINATION OF INTERNAL CONVERSION RATIOS FOR THE ISOMERIC TRANSITION OF In^{114}

V. M. Kel'man, R. Ia. Metskhvarishvili, V. A. Romanov,
L. I. Rusinov and K. A. Konoplev

(Presented by Academician A. A. Lebedev, September 22, 1955)

With the aid of a prism beta spectrometer [1, 2] we have studied the spectrum of conversion electrons accompanying an isomeric transition in In^{114} (transition energy 192 kev) and have obtained the internal conversion ratios. These measurements were obtained with an instrumental half width of 0.04% and spectrometer transmission factor 0.02% of 4π. The resolving power of the instrument enabled us to distinguish the conversion electrons from the L subshells as well as M and N shells of In^{114} and to obtain the ratios of the corresponding conversion coefficients. We also repeated the work of various writers (see Table 1) on the conversion ratios in K, L and M shells.

To serve as a source a layer of a natural mixture of stable indium isotopes was evaporated in vacuum on an aluminum backing which was then activated by neutrons. The work was done with sources of varying surface density, of the order of a few tenths of a milligram per sq. cm. The size of the sources was 1×10 mm^2 and the thickness of the aluminum backing about 2μ.

Figure 1 shows the spectrum of internal conversion electrons from the L_I, L_{II} and L_{III} subshells and the M and N shells of In^{114}. Because of the high resolving power of the instrument the weak background formed by electrons of the continuous beta spectrum is practically unnoticeable. Since the separations of the L sublevels of indium are small (the energy difference of L_I and L_{II} is 300 ev, of L_{II} and L_{III} 200 ev [3]) and the energy of the conversion electrons is quite large (for electrons from the L sublevels about 188 kev) and, moreover, there is a considerable background of electrons scattered in the source, the L_I, L_{II} and L_{III} lines were not completely resolved. In order to obtain the ratios of the areas of the lines they were resolved graphically. We endeavored to preserve the geometrical form of the lines corresponding to the various sublevels. The ratio of the L_I and L_{III} line areas was 0.24 ± 0.01; the L_{II}/L_{III} ratio was 1.27 ± 0.02 and the L_I/L_{II} ratio was 0.19 ± 0.01. To obtain the values given here the L shell conversion electron spectrum was taken 12 times, weighted averages were taken of the area ratios and the probable errors were found. Thus the ratio found in this work for the L subshell internal conversion coefficients is $L_I : L_{II} : L_{III} = (0.24 \pm 0.01) : (1.27 \pm 0.02) : 1$.

The L/M and M/N ratios (where L, M, and N are the total internal conversion coefficients for the given shells), obtained by averaging 8 measurements of the conversion electron spectrum, were $L/M = 4.4 \pm 0.1$ and $M/N = 4.6 \pm 0.2$.

We also determined the ratio of the internal conversion coefficients in the K and L shells. The line produced by the conversion electrons from the K shell is shown in Figure 2. Figures 1 and 2 refer to the same source with correction for decay. Since the energy separation of the K and L levels of In^{114} is relatively large (about 24 kev [3]) a correction was introduced in this case for absorption in the windows of the counters (in a coincidence circuit) and of the counting chamber. The window of the chamber was sealed with a 3μ mica sheet. In order to enter the second chamber the electrons had to pass through three counter windows of which the first, the entrance window of the first counter, was open and each of the other two was covered with $1.5\ \mu$ aluminum foil. The last two windows, which belonged to different counters, were very closely situated. The dimensions of all windows were such that electrons scattered through 25° in the mica window of the counting chamber and not absorbed in the aluminum foils still could enter the second counter.*

---

* The same recording system and the same thicknesses of mica and aluminum foil were used in [2].

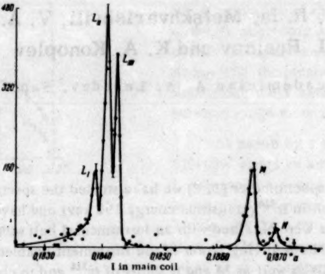

Figure 1. Spectrum of internal conversion electrons from the L, M, and N shells of In^{114}. Transition energy was 192 kev. The horizontal axis gives the current in the main coil of the beta spectrometer; the vertical axis gives the number of coincidence pulses reduced by the counter background.

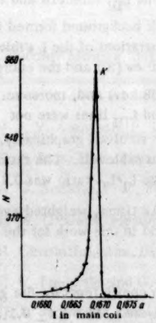

Figure 2. Lines produced by internal conversion electrons in the K shell of In^{114}. Transition energy 192 kev.

TABLE 1

References	K/L	L/M	K/L+M	K/M
[7]	1.0 ± 0.1		0.9 ± 0.1	4.6 ± 0.8
[8]	1.1 ± 0.1			
[9]	1.16			
[10]	1.10 ± 0.05			
[11]	1.30 ± 0.05			
[12]	1.18	5.7	1.00	6.7
this article	1.32 ± 0.02	4.4 ± 0.1	1.08 ± 0.02	5.8 ± 0.2

Since the root mean square scattering angles in the mica covering the chamber window as calculated for conversion electrons from the K and L shells of In^{114} by Williams' [4] formulas are found to be about 1/5 of this value, it may be assumed that scattering in the mica does not affect the measurements of K/L. Absorption in the mica and aluminum foils was calculated from data given in [5, 6]. The difference in window absorption for K and L conversion electrons, comprising 3.5%, was taken into account in determining K/L. Absorption in the material of the counters did not noticeably affect this ratio because of their small thickness. Values of K/L obtained with sources of different thicknesses varying by a factor of 3 were in agreement within the limits of statistical error. The average of ten measurements of K/L was 1.32 ± 0.02.

In determing the above ratios corrections were made for the width of the energy range of the beta spectrometer and for the decay of the source wherever these produced a noticeable effect.

Table 1 gives a comparison of our values for our measurements of the conversion ratios in the K, L and M shells of In^{114} with the data of other writers.

Recently there have appeared very detailed and accurate tables of the internal conversion coefficients for the K shell and L subshells which were compiled by Rose [13] from theoretical calculations. The interpolation of the data in these tables makes it possible to determine the theoretical ratios $L_I : L_{II} : L_{III}$ for the transition energy and atomic number corresponding to the isomeric transition of In^{114} assuming various multipole transitions. Although the accuracy of the values obtained by interpolation is considerably lower than the accuracy of the values given directly in the tables it is still possible by comparing the theoretical and experimental conversion ratios to arrive at an unambiguous determination of the type of transition. The comparison shows that closest to the above experimental ratio for the In^{114} subshells is the theoretical ratio calculated with an E4 isomeric transition in In^{114}. In that case the theoretical ratios are $L_I : L_{II} : L_{III} = 0.25 : 1{,}13 : 1$. This choice of transition type is supported by a comparison of the theoretical values for K/L with the experimental values given in Table 1. The theoretical value of K/L obtained by interpolating data from [13] on the assumption of E4, is 1.2.

The authors wish to thank L. A. Sliv for discussion of the results.

Leningrad Physicotechnical Institute
Academy of Sciences of the USSR

Received July 14, 1955

LITERATURE CITED

[1] V. M. Kel'man, D. L. Kaminskii and V. A. Romanov, Bull. Acad. Sci. USSR,Phys. Ser. 18, 209 (1954).

[2] V. M. Kel'man, V. A. Romanov and R. Ia. Metskhvarishvili, Doklady Akad. Nauk SSSR 103, 4 (1955).

[3] R. D. Hill, E. L. Church, J. W. Mihelich, Rev. Sci. Instruments 23, 523 (1952).

[4] E. J. Williams, Phys. Rev. 58, 292 (1940).

[5] L. H. Martin, A. A. Towsend, Proc. Roy. Soc. (London) A170, 190 (1939).

[6] D. Saxon, Phys. Rev. 81, 639 (1951).

[7] J. L. Lawson, J. M. Cork, Phys. Rev. 57, 982 (1940).

[8] F. Boehm, F. Preiswerk, Helv. Phys. Acta 22, 331 (1949).

[9] V. S. Shpinel and N. V. Forafontov, J. Exptl.-Theoret. Phys. (USSR) 21, 1376 (1951).

[10] R. M. Steffen, Phys. Rev. 83, 166 (1951).

[11] W. C. Kelly, Phys. Rev. 85, 101 (1952).

[12] G. A. Graves, L. M. Langer, R. D. Moffat, Phys. Rev. 88, 344 (1952).

[13] K. Siegbahn, Beta- and Gamma-Ray Spectroscopy, Amsterdam, 1955.

THE EFFECT OF QUANTUM FLUCTUATIONS OF RADIATION ON ELECTRON MOTION IN PERIODIC MAGNETIC SYSTEMS

A. A. Kolomenskii

(Presented by Academician I. E. Tamm, September 15, 1955)

The motion of a relativistic electron in a magnetic field is accompanied by the emission of a spherical electromagnetic wave which, as a rule, can be considered on the basis of classical theory (see, for example, [1, 2]). In special cases, however, it is necessary to take into account the effect of the quantum nature of the radiation on the electron trajectory. An examination of this problem by the application of the Dirac equation to an electron moving in an axially symmetric magnetic field has appeared in papers by A. Sokolov and I. Ternov [3], who have found a "broadening" of the trajectory which is without a classical analog.

However, as shown by A. Lebedev and the author [5, 6] there is strong damping in accelerators which substantially limits the effects of the fluctuations. Therefore the conclusions in [3] regarding relatively large radial fluctuations in accelerators are unfounded.

The purpose of the present article is the examination of the peculiar phenomena resulting from the radiation when electrons move in periodic magnetic systems of accelerators, and especially in accelerators with strong focusing [4]. These phenomena must be kept in mind when studying the results obtained with such instruments which are constructed for energies of the order of a few billion volts and higher.

It must be emphasized that we shall not make use of the complicated method employed in [3], for, as we have already noted [5], the above-mentioned "broadening" of the trajectory can be corrected, derived, and interpreted using the ordinary classical theory of betatron oscillations merely by taking into consideration the statistical nature of the radiation. This method may be incorrect only at energies $E \gtrsim E_{1/2} = mc^2(Rmc/\hbar)^{1/2}$ where R is the orbital radius, which at the usual magnetic field intensities H has the huge value $E \gtrsim 10^{15}$ ev.

Let us consider a system consisting of magnetic field sections and straight fieldless sections forming a closed ring in which the same unit sequence is repeated N times. We introduce the quantity $r(\theta)$ which is the separation from the principal (equilibrium) orbit, where the variable θ (the generalized azimuth) is proportional to the length of arc measured along that orbit. The radial betatron oscillations resulting from radiation are obtained from an equation similar to that of Hill [7].

$$r'' + \frac{\Delta E_{tot} + \Delta W_{tot}}{2\pi E} r' + [1 - n(\theta)]\, r = \frac{R}{E} \int\limits_{init} \left[\sum_i \varepsilon_i \delta(\theta - \theta_i) - W_\theta \right] d\theta, \tag{1}$$

where $n(\theta)$ is the magnetic field index which is a periodic function of θ:

$$n(\theta + \vartheta_0) = n(\theta); \tag{2}$$

ϑ_0 is the azimuthal angle subtended by one periodic element. The right-hand side of (1) describes the effect of radiation fluctuations; $\delta(\theta - \theta_i)$ is a delta function; $\epsilon_i = \hbar\omega_i$ is the energy of the i-th photon emitted; W_θ is the average energy lost through radiation over a path $\theta = 1$ and compensated by the accelerating field. The term with r' causes damping of the betatron oscillations and the term $\Delta E_{tot}/2\pi E$ represents the relativistic increase of the electron mass, while $\Delta W_{tot}/2\pi E$ is the above-mentioned damping [6].

In the absence of radiation the motion of an electron with constant energy is described by

$$r(\theta) = \rho_M(\theta) + \rho(\theta), \quad \rho_M(\theta + \vartheta_0) = \rho_M(\theta); \tag{3}$$

$$\rho(\theta) = ae^{i\mu k} f(\vartheta) + \text{к. с.}, \quad 0 \leqslant \vartheta \leqslant \vartheta_0, \tag{4}$$

where $\rho_M(\theta)$ is the radial deviation of the instantaneous closed periodic orbit around which the betatron oscillations $\rho(\theta)$ take place. Here $\underline{k}$ is the ordinal number of the periodic element; $\underline{a}$ is a constant depending on the initial conditions; k.c. is the conjugate complex quantity. The characteristic number μ determines the frequency of the betatron oscillations, the number of which in one revolution is $N\mu/2\pi$.

The function $\rho_M(\vartheta)$ can conveniently be written as

$$\rho_M(\vartheta) = \frac{R\psi(\vartheta)}{\varkappa^2} \frac{\delta E}{E}, \tag{5}$$

where δE is the deviation of E from the equilibrium value eHR; $\kappa^2 = 1 - n$ in a weak-focusing magnet and $\kappa^2 = |n|$ in a strong-focusing magnet.

$\psi(\vartheta)$ and $f(\vartheta)$ are Floquet functions [7] determined by the parameters of the apparatus. For example, for the simplest case of strong focusing where the subtended angle and the quantity $|n|$ are the same for the focusing and defocusing sectors, $\psi(\vartheta)$ and $f(\vartheta)$ are given by

$$\psi(\vartheta) = \begin{cases} 1 + \dfrac{2\,\text{sh}_{1/2} \cos\sqrt{|n|}\left(\vartheta - \dfrac{\nu}{2}\right)}{\text{s}_{1/2}\,\text{ch}_{1/2} - \text{c}_{1/2}\,\text{sh}_{1/2}} & \textbf{(focus);} \\[2ex] -1 + \dfrac{2\,\text{s}_{1/2} \text{ch}\sqrt{|n|}\left(\vartheta - \dfrac{\nu}{2}\right)}{\text{s}_{1/2}\,\text{ch}_{1/2} - \text{c}_{1/2}\,\text{sh}_{1/2}} & \textbf{(defocus);} \end{cases} \tag{6}$$

$$f(\vartheta) = \left(\frac{\text{sch} - \text{csh}}{\sin\mu}\right)^{1/2} \frac{2}{|n|^{1/4}} \times$$

$$\times \begin{cases} \sin\sqrt{|n|}\,\vartheta + \dfrac{i\sin\mu - \text{ssh}}{\text{csh} - \text{sch}} \cos\sqrt{|n|}\,\vartheta & \textbf{(focus);} \\[2ex] \text{csh}\sqrt{|n|}\,\vartheta + \text{sch}\sqrt{|n|}\,\vartheta - \dfrac{i\sin\mu - \text{ssh}}{\text{csh} - \text{sch}} (\text{ssh}\sqrt{|n|}\,\vartheta - \\ \qquad - \text{cch}\sqrt{|n|}\,\vartheta) & \textbf{(defocus);} \end{cases} \tag{7}$$

where

$$\cos\mu = \text{cch}, \ \text{c} = \cos\sqrt{|n|}\,\nu, \ \text{ch} = \text{ch}\sqrt{|n|}\,\nu, \ \text{c}_{1/2} = \cos\frac{\sqrt{|n|}\,\nu}{2} \ \text{etc.} \tag{8}$$

and for $f(\vartheta)$ normalization is given by

$$ff'^* - f^*f' = \frac{2}{i}, \tag{9}$$

in which the asterisk denotes the conjugate complex quantity.

If at some azimuth $\theta(k, \vartheta)$ a photon of energy $\epsilon = \hbar\omega$ is emitted, then according to (5) this leads to an abrupt change of the position of the instantaneous orbit and of its slope at a given point, and simultaneously to changes of similar characteristics of the betatron oscillations:

$$\delta\rho_M(\vartheta) = -\delta\rho(\vartheta) = -\frac{R\psi(\vartheta)\,\epsilon}{\varkappa^2 E}, \quad \delta\rho'_M(\vartheta) = -\delta\rho'(\vartheta) = -\frac{R\psi'(\vartheta)\,\epsilon}{\varkappa^2 E}. \tag{10}$$

The effect of the radiation and of its fluctuations on the instantaneous orbit in periodic systems has been examined in another paper by this author [8]. Here we shall consider the betatron oscillations. By (4) the greatest displacement of the instantaneous orbit due to these oscillations under the given initial conditions is

$$A = 2\,|\,f\,|_{\max}\,|\,a\,|\,. \tag{11}$$

Due to increases in (10) A also increases. We shall obtain the mean square value $\overline{A^2}$ as a function of time (or electron energy). For this purpose, having solved (1), we then with the aid of (4), (5) and (11) average over all moments (azimuths) of photon emission and over the emission spectrum (see, for example [1, 2]). We thus obtain

$$\overline{A^2} = F\overline{A_0^2}, \tag{12}$$

where $\overline{A_0^2}$ corresponds to the case of an axially symmetric field [6] and the factor F takes into consideration the properties of the systems under consideration which are associated with the dependence of n on θ [2]:

$$F = |\,f\,|^2_{\max}\left(\overline{|\,f'\,|^2}\,\overline{\psi^2} + \overline{|\,f\,|^2}\,\overline{\psi'^2}\right). \tag{13}$$

When averaging the functions in (13) the straight parts may be neglected although, of course, it must be remembered that even these functions depend on the length L of these parts and on their position. The expression for $\overline{A_0^2}$ according to [6] can be obtained in the form (assuming for simplicity that E depends on t or θ linearly)

$$\overline{A_0^2} = \frac{55\sqrt{3}}{72}\,\frac{e^2\hbar c}{\varkappa^4 R\sigma}\,\frac{1}{(mc^2)^7\,\dot{E}E}\int\limits_{E_{\mathrm{init}}}^{E} e^{(W_t(\xi) - W_t(E))\,/\,4\dot{E}}\,\xi^6\,d\xi, \tag{14}$$

where $W_t(E)$ represents energy losses through radiation per unit time; $\sigma = 1 + L/R\,\nu$.

In the limiting case when $W_t(E)/4\dot{E} \gg 1$ the expression (14) becomes

$$\overline{A_0^2} = \frac{55\sqrt{3}}{48}\,\frac{\hbar R}{mc}\,\frac{1}{\varkappa^4}\left(\frac{E}{mc^2}\right)^2. \tag{15}$$

If the inequality is not satisfied the value of $\overline{A_0^2}$ for a given E can only be smaller than (15).

We note that for vertical motion (in the z direction) instead of (13) we obtain

$$F_z = |\,n\,|\,|\,f\,|^2_{\max}\,\overline{|\,f\,|^2}, \tag{13a}$$

and instead of (15) (see [6]) we will have

$$A_{0z}^2 = \frac{13\sqrt{3}}{48}\,\frac{\hbar R}{mc}\,\frac{1}{|\,n\,|}. \tag{15a}$$

Table 1 shows that F as calculated from (6), (7) and (13) is a function of μ, i.e., of the position of the representative point in the stability diagram.

TABLE 1

μ	0	$\pi/8$	$\pi/4$	$3\pi/8$	$\pi/2$	$5\pi/8$	$3\pi/4$	$7\pi/8$	π
$\sqrt{\lvert n\rvert}\,\nu$	0	0.82	1.15	1.39	1.57	1.71	1.80	1.85	1.87
F	∞	1465	375	240	215	260	450	1545	∞

As can be seen from (12-15) a strong-focusing system with variable $n = n(\theta)$ [2] behaves in this case like a system with constant $\underline{n}$ given by $n_{ef} \simeq -|n| / \sqrt{F}$ which, for example, for the center of the region of stability ($\mu = \pi/2$) gives $n_{ef} \simeq -|n| / 14.5$. Since, however, the quantity $|n|$ may in principal be taken quite large, the focusing determined by n_{ef} can be made very much stronger than in a weak-focusing instrument. For example, for $n = 100$ the value of $\sqrt{A^2}$ in a strong-focusing system is smaller than in a weak-focusing system by a factor of about 20.

To show the effect of the straight parts in a strong-focusing system Table 2 gives the dependence of F on $L/R\nu$ assuming that $\mu = \pi/2$.

TABLE 2

$L/R\nu$	0	0.5	1	1.5	2
$\sqrt{\lvert n \rvert}\,\nu$	$\pi/2$	1.14	0.93	0.81	0.73
F	214	100	80	70	65

On the basis of our results we may conclude that at electron energies of the order of several billion electron volts and higher, the amplitude of betatron fluctuations due to radiation fluctuations is small and presents no danger. For example, at $E \simeq 5$ Bev ($H \simeq 10^4$) and $|n| \simeq 100$ the value of $\sqrt{A^2}$ is only a fraction of a centimeter and is of the same order as the amplitude of synchrotron oscillations excited by radiation fluctuations [8, 9].

The above theory may also be applied to a weak-focusing accelerator with straight portions. Since these portions are relatively small the difference of F from unity for this case is of the order of a few per cent.

P. N. Lebedev Physics Institute,
Academy of Sciences of the USSR

Received September 10, 1955

LITERATURE CITED

[1] L. Landau and E. Lifshits, Field Theory, § 73, 1948.

[2] D. Ivanenko and A. Sokolov, Classical Theory of Fields, §§ 39-43, 1949.

[3] A. Sokolov and I. Ternov, J. Exptl-Theoret. Phys. (USSR) 24, 249 (1953); 28, 431 (1955).

[4] E. Courant, M. Livingston, H. Snyder, Phys. Rev. 88, 1190 (1952).

[5] A. Kolomenskii and A. Lebedev, J. Exptl.-Theoret. Phys. (USSR) 30, 1 (1956)

[6] A. Kolomenskii and A. Lebedev, Doklady Akad. Nauk SSSR 106, 5 (1956).

[7] D. Stoker, Nonlinear Fluctuations in Mechanical and Electrical Systems, Foreign Lit. Press, 1952, Ch. VI.

[8] A. Kolomenskii, J. Exptl.-Theoret. Phys. (USSR) 30, 1 (1956).

[9] M. Sands, Phys. Rev. 97, 470 (1955).

FINE AND HYPERFINE STRUCTURE OF PARAMAGNETIC RESONANCE IN BIVALENT EUROPIUM

A. A. Manenkov and A. M. Prokhorov

(Presented by Academician M. A. Leontovich October 12, 1955)

The spin-lattice relaxation times in compounds of the rare-earth elements at room temperature are of the order 10^{-11}-10^{-13} seconds [1, 2], and therefore paramagnetic resonance in the majority of rare-earth compounds can be observed only at low temperatures (liquid hydrogen and helium temperatures).

Compounds of trivalent gadolinium and bivalent europium are exceptions. The ground state of the ions Gd^{3+} and Eu^{2+} is $^8S_{7/2}$. Ions in the S state are only weakly affected by the internal electric fields of the crystal and the principal relaxation mechanism is provided by the magnetic interactions which in this case lead to spin-orbit relaxation times of 10^{-6}-10^{-7} second, thus making it possible to observe paramagnetic resonance at room temperature.

The paramagnetic resonance of Gd^{3+} has been investigated in [3, 4]. The fine structure was observed and interpreted. The absence of hyperfine structure in the spectrum was attributed to the fact that the ^8S state of Gd^{3+} is a pure state with the electron configuration $4f^7$ and not a mixture of states with unpaired s electrons.

The purpose of the present work was the investigation of paramagnetic resonance in Eu^{2+}. We have studied two compounds of bivalent europium, SrS · Eu and CaF_2 · Eu. Both compounds are phosphors in which europium is the activator. The SrS · Eu was in powder form while the CaF_2 · Eu was a single crystal.

The measurements were made with a superheterodyne radiospectroscope at 9341 Mc. The lines were observed on the screen of a cathode-ray tube. The magnetic field was measured by proton resonance.

1. In SrS · Eu the electron transition $M = 1/2 \leftrightarrow -1/2$ is observed, consisting of 12 hyperfine components due to the nuclear spins of the two stable isotopes: $^{151}Eu (I = 5/2)$ and $^{153}Eu (I = 5/2)$.

The spectrum is described by the simple Hamiltonian:

$$\mathcal{H} = g\beta \mathbf{H}\cdot\mathbf{S} + A\cdot\mathbf{S}\cdot\mathbf{I}, \qquad (1)$$

where H is the external magnetic field and S and I are the electron and nuclear spins, respectively. A calculation of the observed spectrum (see Figure 1) using this Hamiltonian and second order perturbation theory gives as hyperfine structure constants for the two isotopes:

$$A_{151} = (30.0 \pm 0.1)\cdot 10^{-4}\ \text{cm}^{-1},$$
$$A_{153} = (13.4 \pm 0.1)\cdot 10^{-4}\ \text{cm}^{-1}.$$

The ratio of the nuclear magnetic moments of ^{151}Eu and ^{153}Eu is obtained from the ratio $\frac{A_{151}}{A_{153}}$ giving $\frac{\mu_{151}}{\mu_{153}} = 2.24 \pm 0.03$ with the g-factor equal to 1.992 ± 0.001. Our values for $\frac{\mu_{151}}{\mu_{153}}$ and g are in agreement with recent data in [5], while the values of the hyperfine structure constants differ. We note that the relative intensities of hyperfine lines due to ^{151}Eu and ^{153}Eu are in agreement with the relative content of ^{151}Eu and ^{153}Eu which is 47.77 and 52.22% [6].

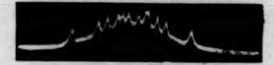

Figure 1. Hyperfine structure of Eu in SrS · Eu. The electron transition is $M = 1/2 \leftrightarrow -1/2$. The magnetic field increases towards the left.

As indicated above the data on paramagnetic resonance in SrS · Eu was obtained from a powder so that only the electron transition $M = 1/2 \leftrightarrow -1/2$ was observed; other transitions are not observed because of strong line broadening due to the random positions of the crystals in the powder.

2. In the single crystal of CaF_2 · Eu we observed 7 fine structure lines each consisting of 12 hyperfine components. Figure 2 shows a photograph of the complete spectrum of CaF_2 · Eu with the external magnetic field parallel to the axis of symmetry of the electric field of the crystal (this axis coincides with one of the crystallographic axès of the third order). The central group of lines corresponds to the electron transition $M = 1/2 \leftrightarrow -1/2$. Both outside groups of lines in the directions of stronger and weaker fields belong to the electron transitions $M = -5/2 \leftrightarrow -7/2$ and $M = 7/2 \leftrightarrow 5/2$ and are well resolved from the lines of other electronic transitions. The groups of hyperfine lines belonging to the electron transitions $M = 3/2 \leftrightarrow 1/2$, $M = 5/2 \leftrightarrow 3/2$ and $M = -1/2 \leftrightarrow -3/2$, $M = -3/2 \leftrightarrow -5/2$ and situated to the right and the left of the central transition $M = 1/2 \leftrightarrow -1/2$ are seen to overlap, with the lines for $M = 5/2 \leftrightarrow 3/2$, $M = -3/2 \leftrightarrow -5/2$ closer to the central transition $M = 1/2 \leftrightarrow -1/2$ than the lines for $M = 3/2 \leftrightarrow 1/2$ and $M = -1/2 \leftrightarrow -3/2$; this follows from the fact that the intensity of the lines of the electron transitions $M = 3/2 \leftrightarrow 1/2$ and $M = -1/2 \leftrightarrow -3/2$ are higher than for $M = 5/2 \leftrightarrow 3/2$ and $M = -3/2 \leftrightarrow -5/2$.

The transition $M = 1/2 \leftrightarrow -1/2$ appears to coincide with the same transition for SrS · Eu (Figure 1). Figure 2 shows the positions of the center of each group of hyperfine lines. We see that the fine structure is not evenly spaced. The number of fine structure lines, 2S, corresponds to the electron spin $S = 7/2$ and thus shows that paramagnetic resonance in CaF_2 · Eu is due to the bivalent europium. The hyperfine structure in each electron transition is nearly isotropic and can be described by the formula

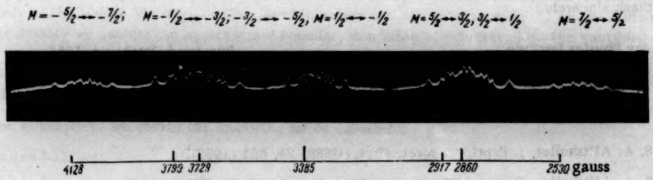

Figure 2. Spectrum of CaF_2 · Eu.

$$h\nu = g\beta H + f(D_i, M) + Am + \frac{A^2}{2g\beta H_0}\{I(I+1) - m^2 + m(2m-1)\}, \qquad (2)$$

where $f(D_i, M)$ is a term describing the fine structure; the D_i are constants depending on the initial splitting of the spin energy levels in the electric field of the crystal; m and M are the nuclear and electron magnetic quantum numbers, respectively; and H_0 is the magnetic field which corresponds to the position of the electron transition lines in the absence of hyperfine structure.

From a comparison of the observed spectrum with (2) we obtained the following values of the constants:

$$g = 1.971 \pm 0.001,$$
$$A_{151} = (34.6_7 \pm 0.1) \cdot 10^{-4}\ \text{см}^{-1},$$
$$A_{153} = (15.4_1 \pm 0.1) \cdot 10^{-4}\ \text{см}^{-1}$$

We see that the hyperfine splitting in $CaF_2 \cdot Eu$ is considerably greater and the g factor smaller than in $SrS \cdot Eu$. The ratio of the magnetic moments of ^{151}Eu and ^{153}Eu is

$$\mu_{151}/\mu_{153} = 2.25 \pm 0.03,$$

which is in good agreement with the values given above from the spectrum of $SrS \cdot Eu$.

Since a few electron transitions are observed in $CaF_2 \cdot Eu$ it is possible to determine the relative signs of A_{151} and A_{153} and thus also the relative signs of the magnetic moments μ_{151} and μ_{153}. Actually, as can be seen from (2), the magnitude of the hyperfine splitting depends on M, i.e., it is not identical for different electron transitions. The separation of the hyperfine components corresponding to $m = {}^5/_2$ and $m = -{}^5/_2$ is

$$\Delta = -5A - {}^5/_2 \frac{A^2}{g\beta H_0}(2M - 1). \quad (3)$$

When A is negative $|\Delta|$ is larger for negative M than for positive. When A is positive $|\Delta|$ is larger for positive M. The observed total hyperfine splitting of the extreme electron transition in the direction of larger magnetic fields for both isotopes of Eu is larger than in the other extreme transition in the direction of smaller magnetic fields. This shows that when A is negative the extreme group of hyperfine lines in the direction of larger magnetic fields belongs to the electron transition $M = -{}^5/_2 \leftrightarrow -{}^7/_2$ and, consequently, the energy level with $M = \pm {}^7/_2$ in zero magnetic field is above the level with $M = \pm {}^5/_2$.

Since it is found that the constants A_{151} and A_{153} have the same sign we conclude that the magnetic moments of ^{151}Eu and ^{153}Eu have the same sign. This supports the optical data in [7].

The phosphors which we investigated were placed at our disposal by Z. A. Trapeznikova and P. P. Feofilov, whom we thank sincerely.

P. N. Lebedev Physics Institute,
Academy of Sciences of the USSR

Received October 4, 1955

LITERATURE CITED

[1] S. A. Al'tshuller, J. Exptl.-Theoret. Phys. (USSR) 24, 681 (1953).

[2] S. A. Al'tshuller, Doctoral Dissertation, Phys. Inst. Acad. Sci. USSR, 1955.

[3] B. Bleaney, H. E. D. Scovil, Proc. Phys. Soc.(London) A, 63, 1369 (1950).

[4] B. Bleaney, R. J. Elliott, H. E. D. Scovil, R. S. Trenam, Phil. Mag. 42, 1062 (1951).

[5] B. Bleaney, W. Low, Proc. Phys. Soc. (London) A, 68, 55 (1955).

[6] G. T. Seaborg and I. Perlman, Table of Isotopes, Foreign Lit. Press, 1951.

[7] P. F. A. Klinkenberg, Revs. Mod. Phys. 25, 63 (1952).

THE THEORY OF THE STRIATED POSITIVE COLUMN

I. M. Chapnik

(Presented by Academician G. S. Landsberg, October 10, 1955)

The theory of the striated positive column has been examined in various papers such as [1-4] and elsewhere but the characteristic dependence of the spacing and damping on the tube radius and on the pressure and nature of the gas [5] was not explained. The present paper considers a set of nonlinear equations describing the longitudinal plasma oscillations as a basis for obtaining equations which relate the spacing and damping to the discharge parameters. The equations considered below are a development of the set of equations advanced by V. L. Granovskii to investigate unstable processes connected with the conduction of electricity through gases [6].

The following assumptions are made: The charge passes through a cylindrical tube with nonconducting walls, whence follows the equality of the electron and ion currents ($j_{er} = j_{pr}$) at the walls. The motion of the electrons and ions is diffusive, i.e., the mean free path λ_e is considerably smaller than the tube radius, which corresponds to the usual conditions in a striated column. The electrons and ions are assumed to have a Maxwellian velocity distribution; the electron temperature T_e and longitudinal field gradient E_x can change along the tube but remain constant in the cross section. The temperature of the ions is assumed to be constant throughout the plasma. Ionization of atoms is assumed to result only from direct collisions. Recombination takes place only at the walls. We neglect alternate ionization and recombination in the space of the tube. For the charge density we assume the approximate boundary condition of Schottky, i.e., the vanishing of electron and ion densities at the walls ($N_e = N_p = 0$). The motion of the charged particles at the walls is considered to be ambipolar diffusion; this is permissible since we consider below the small deviations from the neutral equilibrium state of the plasma.

On these assumptions we obtain the following set of equations:

1. Electron balance:

$$\frac{\partial N_e}{\partial t} + \operatorname{div}(N_e \mathbf{u}_e) - zN_e = 0, \tag{1}$$

where $\mathbf{u}_e$ is the average electron velocity and $\underline{z}$ is the number of ion pairs formed by an electron per second.

2. Equations for longitudinal and radial components of electron velocity [7]:

$$u_{ex} = -b_e E_x - \frac{1}{N_e} D_e \frac{\partial N_e}{\partial x} - \gamma \frac{D_e}{T_e} \frac{\partial T_e}{\partial x} = -b_e\left(E_x + \frac{U_e}{N_e}\frac{\partial N_e}{\partial x} + \gamma \frac{\partial U_e}{\partial x}\right), \tag{2a}$$

$$u_{er} = -\frac{D_a}{N_e}\frac{\partial N_e}{\partial r}. \tag{2b}$$

Here $D_e = b_e U_e$ is the electron diffusion coefficient; $D_a \cong b_p U_e$ is the coefficient of ambipolar diffusion; $U_e = kT_e/e$ is the electron temperature in volts; γ is a numerical coefficient depending on the form of $\lambda_e(c_e)$ [7] for a given gas (c_e is the root mean square electron velocity).

3. Ionization equation:

$$z = \beta\sqrt{U_e}\, e^{-U_i/U_e}. \tag{3}$$

here U_i is the ionization potential of the gas; β is a constant.

4. Energy balance of the electron gas:

$$\frac{\partial U_e}{\partial t} + u_{ex}\frac{\partial U_e}{\partial x} = \frac{2}{3}u_{ex} - H_1(U_e), \tag{4}$$

where

$$H_1(U_e) = \frac{4}{3}\sqrt{\frac{2e}{\pi m}}\frac{\varkappa}{\lambda_e}U_e^{3/2}.$$

Here κ is the average fraction of energy lost by an electron in one collision; e is the charge; m is the mass; λ_e is the mean free electron path; u_{ex} is obtained from (2a).

5. Ion balance:

$$\frac{\partial N_p}{\partial t} + \operatorname{div}(N_p\mathbf{u}_p) - zN_e = 0. \tag{5}$$

6. Equations for longitudinal and radial components of ion velocity:

$$u_{px} = b_pE_x - \frac{1}{N_p}D_p\frac{\partial N_p}{\partial x} = b_p\left(E_x - \frac{U_p}{N_p}\frac{\partial N_p}{\partial x}\right); \quad u_{pr} = -\frac{D_a}{N_p}\frac{\partial N_p}{\partial r}. \tag{6}$$

7. Poisson's equation:

$$\frac{1}{r}\frac{\partial}{\partial r}(rE_r) + \frac{\partial E_x}{\partial x} = 4\pi e(N_e - N_p). \tag{7}$$

8. Radial field component E_r [7]: $E_r = \frac{1}{N_e}\frac{\partial N_e}{\partial r}\frac{D_e - D_a}{b_e + b_p}$. However, $D_e = b_eU_e > D_p = b_pU_p$ and $b_e \gg b_p$; consequently

$$E_r \cong \frac{1}{N_e}\frac{\partial N_e}{\partial r}U_e. \tag{8}$$

In order to simplify (1-8) and reduce to a one-dimensional problem we neglect in first approximation the exact distribution of the parameters along the tube radius. Then it is possible to assume $N_e = n_e(x, t)J_0\left(\frac{\mu}{a}r\right)$ and $N_p = n_p(x, t)J_0\left(\frac{\mu}{a}r\right)$, where $n_e(x, t)$ and $n_p(x, t)$ are the electron and ion concentrations along the tube axis; $J_0\left(\frac{\mu}{a}r\right)$ is the zero-th order Bessel function ($\mu = 2.4$ is its first root). For our purpose it is sufficient to consider the asymptotic form of the set of equations near the tube axis, i.e., for small r, and to employ asymptotic expressions for the Bessel function at small values of the argument $J_0\left(\frac{\mu}{a}r\right) \cong 1$ and $J_1\left(\frac{\mu}{a}r\right) \cong \frac{\mu}{2a}r$. With these assumptions we obtain from (1-8) after some simple transformations the set of equations:

$$\frac{\partial n_e}{\partial t} - b_e\left[\frac{\partial E_x}{\partial x}n_e + E_x\frac{\partial n_e}{\partial x} + (1+\gamma)\frac{\partial U_e}{\partial x}\frac{\partial n_e}{\partial x} + U_e\frac{\partial^2 n_e}{\partial x^2} + \gamma n_e\frac{\partial^2 U_e}{\partial x^2}\right] + \frac{\mu^2}{a^2}b_pU_en_e - \beta\sqrt{U_e}\,e^{-U_i/U_e}n_e = 0;$$

$$\frac{\partial n_p}{\partial t} + b_p\left(\frac{\partial E_x}{\partial x}n_p + E_x\frac{\partial n_p}{\partial x} - U_p\frac{\partial^2 n_p}{\partial x^2}\right) + \frac{\mu^2}{a^2}b_pU_en_p - \beta\sqrt{U_e}\,e^{-U_i/U_e}n_e = 0; \tag{9}$$

$$\frac{\partial U_e}{\partial x} - b_e\left(E_x + \frac{U_e}{n_e}\frac{\partial n_e}{\partial x} + \gamma\frac{\partial U_e}{\partial x}\right)\frac{\partial U_e}{\partial x} = \frac{2}{3}b_e\left(E_x + \frac{U_e}{n_e}\frac{\partial n_e}{\partial x} + \frac{\partial U_e}{\partial x}\right)E_x - H_1(U_e);$$

$$\frac{\partial E_x}{\partial x} + \frac{\mu^2}{a^2}U_e = 4\pi e(n_e - n_p)\,. \tag{9}$$

It is hardly possible to obtain a general solution of the set (9) of nonlinear equations. There is a particular stationary solution which is independent of the x-coordinate. In order to obtain a solution which depends on x we linearize (9) assuming that this solution differs little from the stationary solution. For this purpose we set as usual:

$$n_e = n_c(1 + \bar{\nu}_e e^{kx}); \quad n_p = n_c(1 + \bar{\nu}_p e^{kx}); \quad E_x = E_{xc}(1 + \bar{\chi}e^{kx});$$
$$U_e = U_{ec}(1 + \bar{\varepsilon}e^{kx}). \tag{10}$$

Substituting (10) in (9) we obtain (after eliminating χ) for the stationary solution:

$$(kE_{xc} + U_{ec}k^2 + 4\pi en_c)\bar{\nu}_e - 4\pi en_c\bar{\nu}_p + \left(\gamma U_{ec}k^2 - \frac{\mu^2}{a^2}U_{ec}\right)\bar{\varepsilon} = 0;$$
$$\left(4\pi en_c - \frac{\mu^2}{a^2}U_{ec}\right)\bar{\nu}_e + \left(E_{xc}k - U_{pc}k^2 + \frac{\mu^2}{a^2}U_{ec} - 4\pi en_c\right)\bar{\nu}_p - \frac{\mu^2}{a^2}U_{ec}\frac{U_i}{U_e}\bar{\varepsilon} = 0;$$
$$\left(4\pi en_c - \frac{1}{2}U_{ec}k^2\right)\bar{\nu}_e - 4\pi en_c\bar{\nu}_p + \left(\frac{3+2\gamma}{4} - \frac{3}{4b_eE_{xc}}\frac{\partial H_1}{\partial U_e}k - \frac{\mu^2}{a^2}\right)U_{ec}\bar{\varepsilon} = 0. \tag{11}$$

The condition for the existence of nontrivial solutions of this set of homogeneous linear equations is the vanishing of the determinant of the coefficients, the expansion of which leads to an algebraic equation with respect to the wave number $k = \delta + \sigma i$.

In a striated discharge usually $n_c \geq 10^9$ cm^{-3}; $\sigma \sim \frac{2\pi}{a}$ and $\delta < \sigma$. If we also consider that in a gas discharge $E_{xc} \sim 0.01 - 0.1$ CGSE, $U_{pc} \ll U_{ec}$, $U_{ec} \sim 0.01$ CGSE and $\frac{1}{b_eE_{xc}}\frac{\partial H_1}{\partial U_e} \ll 10$, we may then neglect terms which do not contain n_c, thus obtaining

$$\pi en_c\left[U_{ec}k^3 + 4\gamma E_{xc}k^2 + 2\frac{\mu^2}{a^2}\left(\frac{U_i}{U_e} - \frac{1}{2}\right)U_{ec}k + 4\frac{\mu^2}{a^2}\left(\frac{U_i}{U_{ec}} - \frac{1}{2}\right)E_{xc}\right] \cong 0. \tag{12}$$

Separating real and imaginary parts we obtain two equations for σ and δ:

$$U_{ec}(\delta^3 - 3\delta\sigma^2) + 4\gamma E_{xc}(\delta^2 - \sigma^2) + 2\frac{\mu^2}{a^2}\left(\frac{U_i}{U_{ec}} - \frac{1}{2}\right)U_{ec}\delta -$$
$$- 4\frac{\mu^2}{a^2}\left(\frac{U_i}{U_{ec}} - \frac{1}{2}\right)E_{xc} \cong 0; \tag{13}$$

$$U_{ec}(3\delta^2\sigma - \sigma^3) + 8\gamma E_{xc}\delta\sigma + 2\frac{\mu^2}{a^2}\left(\frac{U_i}{U_{ec}} - \frac{1}{2}\right)U_{ec}\sigma \cong 0. \tag{14}$$

Assuming that for a striated column $\delta < \sigma$ we obtain in first approximation the following relations for the periodic spacing $\underline{l} = \frac{2\pi}{\sigma}$ and the logarithmic decrement δ:

$$l \cong \frac{2\pi a}{\mu}\sqrt{\frac{2\gamma U_{ec}}{2U_i - U_{ec}}}\,, \tag{15}$$

$$\delta \cong \frac{\mu^2(2U_i - U_{ec})(3 - 2\gamma)}{16a^2E_{xc}\gamma^2}\,. \tag{16}$$

If we make the approximate assumption that the variation of λ_e with c_e is expressed by a power function $\lambda_e = \Lambda c_e^{\tau}$ and that the distribution is Maxwellian we obtain positive values for γ (with $\tau > -1$). Then the quantity $3 - 2\gamma$ in (16) will be positive for $\tau < 2$ and negative for $\tau > 2$. From (15) and the known dependence of the electron temperature T_e on $\underline{pa}$ [8] it follows that the ratio $\underline{l}/a$ is a decreasing function of $\underline{pa}$, as is actually the case [5].

As can be seen from Table 1* (15) agrees with experiment.

TABLE 1

Gas	n_{ec} (cm^{-5})	T_e (°K)	U_{ec} (v)	U_i (v)	P (mm Hg)	(a) (cm)	$\underline{l}_{theor}$	$\underline{l}_{exper}$	Reference
N_2	$2 \cdot 10^8$	$3 \cdot 10^4$	2.4	14.5	0.16	3.9	5	6	[9]
H_2	$4 \cdot 10^9$	$1.2 \cdot 10^4$	1	13.5	0.63	1.1	0.8	0.9	[11]

From (16) it follows that if the mean free path for electrons is a rapidly increasing function of c_e (i.e., $\tau > 2$ in relation to $\lambda_e = \Lambda c_e^{\tau}$ and, consequently, $3 - 2\gamma < 0$), the striations induced by the inhomogeneity of charged particle distribution and electron temperature at the cathode end of the positive column [8, 9] are practically damped out in a few centimeters, as has actually been observed experimentally in discharges through Hg, Cd, Cs and Na vapors [10].

In conclusion I take this opportunity to express my deep gratitude to Professor V. L. Granovskii for suggesting the problem and for valuable comments during discussions.

Received July 16, 1955

LITERATURE CITED

[1] J. J. Thomson, Phil. Mag. 8, 1 (1929).

[2] M. J. Druyvestein, Physica 1, 273 (1934).

[3] A. A. Vlasov, Many Particle Theory, 1950.

[4] M. F. Shirokov, Doklady Akad. Nauk SSSR 89, 837 (1953).

[5] N. A. Kaptsov, Electrical Phenomena in Gases and Vacuum, 1950.

[6] V. D. Granovskii, Doklady Akad. Nauk SSSR 26, 873 (1940); 28, 41 (1940).

[7] V. L. Granovskii, Electric Currents in Gases, 1952.

[8] A. Engel and M. Steinbeck, Physics and Technology of Electrical Discharges in Gases, Moscow-Leningrad, 1936, Vol. 2.

[9] D. Oettingen, Ann. Physik 19, 519 (1934).

[10] B. N. Kliarfel'd, J. Exptl.-Theoret. Phys. (USSR) 22, 66 (1952).

[11] H. Paul, Z. Physik 97, 330 (1935).

---

* In the calculation of $\underline{l}_{theor}$ from (15) it is assumed that $\tau = 1$. In this case, $\gamma = 1$.

THE SUBLIMATION OF SILVER STUDIED WITH RADIOACTIVE TRACERS AND A MASS SPECTROMETER

Iu. V. Kornev and E. Z. Vintaikin

(Presented by Academician G. V. Kurdiumov, October 13, 1955)

The measurement of vapor pressure over metals and alloys is of great theoretical and practical importance. An understanding of certain properties and of certain processes in metals and alloys is impossible without a knowledge of the changes of partial internal polar energy and of the activity of the alloy components as a function of the relative composition and temperature. All these thermodynamic quantities can be obtained from experimental determination of the vapor pressure over a metal or alloy. It is also known that when certain metals are refined by vacuum distillation the correct technology requires a knowledge of the rate of evaporation, which is determined by the vapor pressure.

In the present work we have measured the vapor pressure of silver over pure silver and Au-Ag alloy with 30% atomic silver. It was our purpose on the one hand to make a deeper study of the sublimation of pure metals and, on the other hand, to determine the thermodynamic properties of a solid solution through the use of radioactive tracers.

An analysis of the existing methods of measuring vapor pressures led us to the conclusion that the most suitable method of measuring the partial vapor pressures of components over solid solutions is that of measuring the rate of flow of a saturated vapor through a small aperture into a high vacuum as was proposed by Knudsen [1]. In the present work this method has been employed in two versions: in the first the rate of flow of the vapor was measured by the use of a condensation target and radioactive Ag^{110} [2]; in the second version a mass spectrometer was used.

For the preparation of specimens we used chemically pure silver (99.99%). The radioactive isotope was introduced by metallurgical means. The gold alloy with 30% atomic silver was homogenized for 3 hours at 950°C. The Knudsen vessel was made of alumina fired at 1700°C. The samples in the form of filings were loaded into the vessel through an effusion aperture. The temperature was measured with a Pt–PtRh thermocouple which was calibrated at the melting point of silver.

The experimental results are given in Tables 1 and 2.

TABLE 1

Vapor pressure of pure (99.99%) silver from 721° to 956°C

T (°K)	Vapor pressure (mm Hg)	T (°K)	Vapor pressure (mm Hg)
994	$3.32 \cdot 10^{-6}$	1134	$2.08 \cdot 10^{-4}$
1033	$1.05 \cdot 10^{-5}$	1184	$8.28 \cdot 10^{-4}$
1044	$1.53 \cdot 10^{-5}$	1204	$1.21 \cdot 10^{-3}$
1102	$8.84 \cdot 10^{-5}$	1229	$2.32 \cdot 10^{-3}$

By the method of least squares we obtained equations for the temperature dependence of the vapor pressure over pure silver:

$$\log P(\mathrm{mm}) = -\frac{68{,}100}{2.303RT} + 9.465,$$

and over the Au-Ag (30% atomic Ag) alloy:

$$\log P\ (\mathrm{mm}) = -\frac{69{,}800}{2.303\ RT} + 8.993.$$

Graphs of the temperature dependence of the vapor pressure of silver over pure silver and the alloy are presented in Figure 1.

TABLE 2

Partial vapor pressure of silver over Au-Ag (30% atomic Ag) from 747° to 880°C.

T (°K)	Vapor pressure (mm Hg)
1020	$1.16 \cdot 10^{-6}$
1049	$3.12 \cdot 10^{-6}$
1050	$2.62 \cdot 10^{-6}$
1051	$2.84 \cdot 10^{-6}$
1090	$9.27 \cdot 10^{-6}$
1090	$9.27 \cdot 10^{-6}$
1097	$1.12 \cdot 10^{-5}$
1098	$1.29 \cdot 10^{-5}$
1122	$2.80 \cdot 10^{-5}$
1129	$3.01 \cdot 10^{-5}$
1153	$5.74 \cdot 10^{-5}$

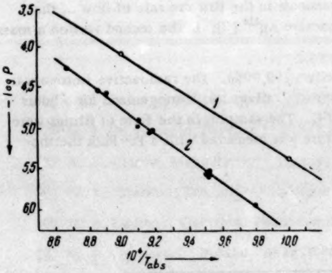

Figure 1. Temperature dependence of vapor pressure. 1) Over pure silver; 2) over Au-Ag alloy (30% atomic Ag).

In the present work for the purpose of determining the heat of sublimation of pure silver we used a MS-2 domestic mass spectrometer. The ion source was equipped with a special effusion crucible and thermocouple.

We obtained experimentally the temperature dependence of the silver line intensities for masses 107 and 109. In order to be certain that lines of the vacuum background did not interfere we measured the isotopic ratio in the entire temperature range, obtaining complete agreement with the tabulated values. We attempted to detect multiatomic clusters in the silver vapor. However, in the range up to 600 mass units no lines were detected which corresponded to multiatomic formation. The operating conditions of the instrument were as follows: ionization potential 30 v, cathode emission current 2 ma, accelerating voltage 2000 v, pressure in ion region 10^{-6} mm Hg and in analyzer 10^{-7} mm Hg.

We performed 6 experiments to determine the heat of sublimation of pure (99.99%) silver. As an illustration Figure 2 contains a graph of the temperature dependence of line intensities obtained from one of the experiments. The heat of sublimation of the silver was calculated from the data of each experiment. The average of the 6 measurements was 68 kcal/g-at.

A few papers have recently appeared on the vapor pressure of pure silver vapor [4, 5].

The distinguishing feature of our measurements is the determination of the heat of sublimation of silver in a wider temperature range by two methods. Both the effusion method with radioactive isotopes and the mass-spectrographic method gave the same value of 68 kcal/g-at for the heat of sublimation.

The radiochemical method used to obtain the weight of the condensate is more sensitive than the weighing method used in [5, 6]. The minimum silver vapor pressure measured in our work was 10^{-6} mm Hg whereas in [5, 6] the minimum was above 10^{-4} mm. It must be noted that the vapor pressure of 10^{-6} mm is not the limit of sensitivity of the method since there are ways of increasing the specific activity of the sample.

The use of radioactive isotopes considerably broadens the possibilities of Knudsen's method. The radioactive isotopes enable us to determine the heat of sublimation for pure metals and the thermodynamic activity of the components of alloys without calculating the absolute vapor pressure, but measuring in the first case only the radioactivity of the condensation target as a function of temperature and in the second case comparing the radioactivity of the target for pure metal and of the alloy at constant temperature.

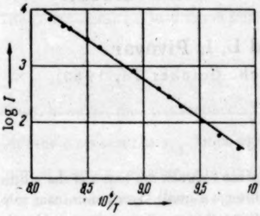

Figure 2. Temperature dependence of silver line intensities obtained with the mass spectrograph.

The coefficients of thermodynamic activity of silver γ_{Ag} for the Au − 0.3 Ag alloy as calculated from our data correspond to the equation $\gamma_{Ag} = \exp(-1700/RT)$, which indicates similarity of a solid and ordinary solution.

Our mass-spectrographic method enabled us to broaden the possibilities for the study of metal sublimation. It was found that in the solid phase silver is evaporated in the form of a monatomic vapor. This is of special interest in connection with [7] in which multiatomic clusters were observed when silver was evaporated from the liquid phase.

We were assisted by Ia. M. Pogosian.

Central Scientific Research Institute for Ferrometallurgy

Received September 1, 1955

LITERATURE CITED

[1] M. Knudsen, The Kinetic Theory of Gases, 1952.

[2] Iu. V. Kornev and V. N. Golubkii, Problems of Metallography and the Physics of Metals, 4th collection, 1955, p. 432.

[3] E. Z. Vintaikin, P. L. Gruzin and S. N. Fedorov, Factory Lab. 7 (1955).

[4] H. M. Schadel, C. E. Birchenall, J. Metals 188, 1134 (1950).

[5] C. L. McCabe, C. E. Birchenall, J. Metals 5, 707 (1953).

[6] C. L. McCabe, H. M. Schadel, C. E. Birchenall, J. Metals 5, 709 (1953).

[7] A. W. Searcy, R. D. Treeman, M. C. Michel, J. Am. Chem. Soc. 76, 4050 (1954).

APPLICATION OF THE DETAILED BALANCING RATIO $\frac{\sigma_{12}\sigma_{31}\cdot\sigma_{23}}{\sigma_{21}\sigma_{13}\cdot\sigma_{32}} = 1$ TO AN ION BEAM OF FIXED COMPOSITION

M. I. Korsunskii, Kh. L. Leviant and L. I. Pivovar

(Presented by Academician L. A. Artsimovich, October 16, 1955)

When an ion beam passes through matter charge exchange takes place between the ions and the atoms of the medium. If the ion beam is initially homogeneous in the passage through a small layer a dominant role is played by processes leading to a decrease of the number of ions of the given charge. Thus, a beam of singly-charged ions which collide with atoms will (as a result of loss of electrons) begin to become enriched with ions of two, three and higher charges and also (because of electron capture) with neutral particles, which lack charge. As the thickness of the traversed layer of matter increases the role of reverse processes is enhanced, leading to the restoration of singly-charged ions. At sufficiently large thicknesses the direct and reverse processes are in equilibrium. Under such conditions the charge composition of the ion beam will remain unchanged while penetrating the medium.

We shall characterize the processes of charge exchange by cross sections. Then the composition of the ion beam can be defined by the relationships

$$\begin{aligned}
\frac{dN_k}{dn} &= -(\sigma_{kl} + \sigma_{km} + \ldots)\, N_k + \sigma_{lk} N_l + \sigma_{mk} N_m + \ldots, \\
\frac{dN_l}{dn} &= -(\sigma_{lk} + \sigma_{lm})\, N_l + \sigma_{kl} N_k + \sigma_{ml} N_m + \ldots, \\
\frac{dN_m}{dn} &= -(\sigma_{mk} + \sigma_{ml} + \ldots)\, N_m + \sigma_{km} N_k + \sigma_{lm} N_l + \ldots, \\
&\ldots\ldots\ldots\ldots\ldots\ldots\ldots\ldots\ldots\ldots\ldots\ldots
\end{aligned} \tag{1}$$

where N_k, N_l and N_m designate the numbers of ions of the respective charges; σ_{kl} is the cross section for the probability of transition of an ion through collision from charge state $\underline{k}$ to charge state $\underline{l}$; $\underline{n}$ is the number of atoms in a layer of the medium of 1 cm^2 area.

If we confine ourselves to three charge states: k =1, l = 2, m = 3 the solution of (1) for stationary ion ratios will be

$$\begin{aligned}
\frac{N_2^{\bullet}}{N_1^{\bullet}} &= \frac{\sigma_{12}}{\sigma_{21}} \frac{\sigma_{31} + \sigma_{32} + \frac{\sigma_{13}\sigma_{32}}{\sigma_{12}}}{\sigma_{31} + \sigma_{32} + \frac{\sigma_{31}\sigma_{23}}{\sigma_{21}}}, \\
\frac{N_3^{\bullet}}{N_2^{\bullet}} &= \frac{\sigma_{13}}{\sigma_{31}} \frac{\sigma_{21} + \sigma_{23} + \frac{\sigma_{12}\sigma_{23}}{\sigma_{13}}}{\sigma_{21} + \sigma_{23} + \frac{\sigma_{32}\sigma_{21}}{\sigma_{31}}},
\end{aligned} \tag{2}$$

where $N_1^{\bullet}$, $N_2^{\bullet}$, $N_3^{\bullet}$ are the relative numbers of ions of corresponding charge for the stationary state.

Since there is detailed balancing for the process of charge exchange [1], for thermal equilibrium the following relations should hold

$$^{\bullet}N_1 \overset{\bullet}{\sigma}_{12} = {}^{\bullet}N_2 \overset{\bullet}{\sigma}_{21}, \quad {}^{\bullet}N_1 \overset{\bullet}{\sigma}_{13} = {}^{\bullet}N_3 \overset{\bullet}{\sigma}_{31}, \quad {}^{\bullet}N_2 \overset{\bullet}{\sigma}_{23} = {}^{\bullet}N_3 \overset{\bullet}{\sigma}_{32}, \tag{3}$$

where $^{\bullet}N_1$, $^{\bullet}N_2$, $^{\bullet}N_3$ are the numbers of ions in equilibrium and $\overset{\bullet}{\sigma}_{12}$, $\overset{\bullet}{\sigma}_{13}$ . . . . are the cross sections (for the respective charge changes of the ions under conditions corresponding to thermal equilibrium.

The conditions in (3) lead to the following relationship of the cross sections:

$$\frac{\sigma^*_{12}\sigma^*_{23}\sigma^*_{31}}{\sigma^*_{21}\sigma^*_{32}\sigma^*_{13}} = 1. \tag{4}$$

Since, however, the cross sections σ^*_{kl} for charge transformations under thermal equilibrium do not agree with the cross sections σ_{kl} for charge changes resulting from the interaction of ion beams (of high energy) with atoms at room temperature, a relationship such as (4) is not obligatory for the cross sections σ_{kl}. For this reason (4) is not used in calculating from experimental data the charge exchange cross sections. However, there must be some relation between the direct cross section σ_{ik} and the reverse cross sections which is not provided for in (2).

Since the nature of this relationship is undetermined we have made an attempt to determine whether (4) is also satisfied by cross sections for charge exchange between ion beams and matter at room temperature. When the relation

$$\frac{\sigma_{12}\sigma_{23}\sigma_{31}}{\sigma_{21}\sigma_{32}\sigma_{13}} = 1 \tag{5}$$

holds good the same will be true for the relations

$$\frac{N^*_2}{N^*_1} = \frac{\sigma_{12}}{\sigma_{21}}\,; \quad \frac{N^*_3}{N^*_1} = \frac{\sigma_{13}}{\sigma_{31}}\,; \quad \frac{N^*_3}{N^*_2} = \frac{\sigma_{23}}{\sigma_{32}}\,, \tag{6}$$

i.e., the ratios of the numbers of ions of different charge (when stationary) will be the ratios of the loss and capture cross sections of electrons by ions.

Unfortunately in the literature on charge exchange we have found no direct data (direct and reverse cross sections) which would enable us to determine whether (6) holds; therefore we have resorted to an indirect check of (5) and (6).

Reference [2] contains data on the change of composition of a beam of singly-charged nitrogen ions with energies from 400 to 1100 kev during passage through various layers of air. These measurements were continued right up to the formation of a stationary ratio. We determined both the cross sections $\sigma_{12}, \sigma_{13}, \sigma_{14} \ldots$ and the stationary ratios of the ions of different charges.

In order to determine the validity of (5) and (6) we proceeded as follows. From (1) one can derive that

$$\frac{d}{dn}\left(\frac{1}{N_1}\frac{dN_1}{dn}\right) = \sigma_{21}\frac{d}{dn}\left(\frac{N_2}{N_1}\right) + \sigma_{31}\frac{d}{dn}\left(\frac{N_3}{N_1}\right) + \sigma_{41}\frac{d}{dn}\left(\frac{N_4}{N_1}\right) + \ldots, \tag{7}$$

Assuming that for n → 0

$$\frac{d}{dn}\left(\frac{N_2}{N_1}\right) = \sigma_{12}; \qquad \frac{d}{dn}\left(\frac{N_3}{N_1}\right) = \sigma_{13},$$

we obtain

$$\frac{d}{dn}\left(\frac{1}{N_1}\frac{dN_1}{dn}\right)_{n\to 0} = \sigma_{21}\sigma_{12} + \sigma_{31}\sigma_{13} + \sigma_{41}\sigma_{14} + \ldots \tag{8}$$

It is easier to obtain $\frac{d}{dn}\left(\frac{1}{N_1}\frac{dN_1}{dn}\right)_{n \to 0}$ because the curve is linear for small n and because the straight line intersects the axis $n = 0$ at the point $\frac{1}{N_1}\frac{dN_1}{dn} = \sigma_{12} + \sigma_{13} + \sigma_{14} + \ldots$. As for the right-hand side of (8) the cross sections σ_{1k} are obtained from the initial slopes of the curves $\frac{N_k}{N_1} = f_k(n)$ (the initial slope of these curves is also linear). The cross sections σ_{21}, σ_{31} etc., are unknown. However, if (6) holds, these cross sections can be calculated from (6) from experimental data for the $\frac{N_k^*}{N_1^*}$ ratios.

Substituting in (8) the values calculated from (6) for the cross sections σ_{21}, σ_{31} . . . we obtain

$$\frac{d}{dn}\left(\frac{1}{N_1}\frac{dN_1}{dn}\right)_{n\to 0} = \sigma_{12}^2\frac{N_1^*}{N_2^*} + \sigma_{13}^2\frac{N_1^*}{N_3^*} + \sigma_{14}\frac{N_1^*}{N_4^*} + \dots \qquad (9)$$

The fulfillment of (9) was also verified. Table 1 shows that the value of $\frac{d}{dn}\left(\frac{1}{N_1}\frac{dN_1}{dn}\right)_{n\to 0}$ obtained from the initial slope of $N_1 = \varphi(n)$ is in good agreement with the value of the sum $(\sigma_{12}\sigma_{21} + \sigma_{13}\sigma_{31} + \dots)$ in which σ_{21}, σ_{31} are calculated using (6). At first glance the accuracy of agreement of the data (the discrepancy does not exceed 6%) in the different columns of Table 1 may be surprising since the values for the cross sections themselves are obtained only to within a factor of 1.5-2. But it must be kept in mind that the principal error in determining the cross section is the inaccuracy in the determination of the number n. Since the error in n appears in the same factor of both $\frac{d}{dn}\left(\frac{1}{N_1}\frac{dN_1}{dn}\right)_{n\to 0}$, and $\left(\sigma_{21}^2\frac{N_1^*}{N_2^*} + \sigma_{31}^2\frac{N_1^*}{N_3^*} + \dots\right)$, this error does not appear in the comparison of data contained in Table 1. The agreement of $\frac{d}{dn}\left(\frac{1}{N_1}\frac{dN_1}{dn}\right)_{n\to 0}$ and $(\sigma_{21}\sigma_{12} + \sigma_{31}\sigma_{13} + \dots)$ can be considerably more accurate than the value of any of the cross sections.

TABLE 1

Energy of ions N$^+$ (kev)	$\frac{d}{dn}\left(\frac{1}{N_1}\frac{dN_1}{dn}\right)_{n\to 0}$	$\sigma_{12}^2\frac{N_1^*}{N_2^*} + \sigma_{13}^2\frac{N_1^*}{N_3^*} + \dots$
485	$14.5 \cdot 10^{-32}$	$14.36 \cdot 10^{-32}$
850	$15.0 \cdot 10^{-32}$	$15.85 \cdot 10^{-32}$
985	$23.2 \cdot 10^{-32}$	$22.3 \cdot 10^{-32}$

TABLE 2

Energy (kev)	$\sigma_{21} \cdot 10^{16}$	$\sigma_{31} \cdot 10^{16}$	$\sigma_{41} \cdot 10^{16}$	$\sigma_{51} \cdot 10^{16}$	$\sigma_{61} \cdot 10^{16}$
485	3.85	4.1	5.2	—	2.85
850	3.16	3.43	3.87	4.0	—
985	4.61	3.65	5.45	5.17	—

The agreement of the data in Table 1 indicates that for the cross sections characterizing the charge exchange between a beam of fast ions and matter at room temperature (5) and (6) are satisfied with sufficient accuracy.

Using (6) and the experimental values of the electron loss cross sections σ_{12}, σ_{13}, σ_{14} as well as N_1^*/N_2^*, N_1^*/N_3^*, N_1^*/N_4^* it is possible to determine the electron capture cross sections σ_{21}, σ_{31}, σ_{41}.

Table 2 gives the cross sections for electron capture by nitrogen ions calculated using (6) from the experimental data in [2]. It is of interest that the cross sections σ_{21}, σ_{31}, σ_{41} . . . differ very little among themselves and agree approximately with cross sections obtained from the kinetic theory of gases. In the indicated energy range, these cross sections undergo little change.

V. I. Lenin
Kharkov Polytechnical Institute

Received October 6, 1955

LITERATURE CITED

[1] N. Bohr, The Penetration of Atomic Particles Through Matter, Foreign Lit. Press, 1950, p. 84 (Translation).

[2] M. I. Korsunskii, Kh. L. Leviant, A. T. Markus and L. I. Pivovar, Doklady Akad. Nauk SSSR 103, 339 (1955).

NUCLEAR REACTIONS OF HIGH ENERGY PROTONS IN COPPER

N. M. Kocharian, G. S. Saakian, M. T. Aivazian, Z. A. Kirakosian
and A. S. Aleksanian

(Presented by Academician V. A. Ambartsumian, October 14, 1955)

The magnetic spectrometer which was described in our previous paper [1] was used to measure the total inelastic cross section of interactions between protons averaging up to 12 Bev and copper atoms. A graphite absorber of about 40 g/cm^2 thickness was placed above the magnet; cosmic ray neutrons produced protons and pions. We afterwards studied the nuclear reactions of these particles in copper absorbers placed below the magnet gap. The data needed to determine the cross section for the interaction of negative pions was the basis of reference [1].

The positive particles produced by neutrons can be protons or positive pions. The total cross section was obtained both for the total flux of positively charged particles and for the protons. We of course had no means of accurately separating the protons from the positive pions, but this separation can be achieved approximately by using the data for negative pions. It has been shown in [2] that in the energy region studied by us the numbers of positive and negative pions produced by neutrons in graphite are approximately equal. Thus in order to derive the number of protons from the total number of positive particles we subtracted the number of negative pions. Consequently it was assumed that the cross sections for inelastic nuclear interactions of pions of both signs in the given energy region are equal.

The trajectories of individual particles were treated by a method described in detail in [1]. The interaction length of the particles was calculated first from the number of nuclear interactions in the first copper absorber Π_1 of 10.6 g/cm^2 thickness, then from the number of interacting particles for absorbers Π_1 and Π_2 together and with a combined thickness of 29 g/cm^2, etc. As a result we obtained several values for the nuclear interaction lengths λ_1, λ_2, etc. We then introduced statistical weights W_k inversely proportional to the squares of the statistical errors $\Delta\lambda_k$ of each separate determination. Then from the formula $\lambda = \sum \lambda_k W_k / \sum W_k$ we calculated the mean free path λ and from $\Delta\lambda = [\sum W_k(\Delta\lambda_k)^2 / n \sum W_k]^{1/2}$ the mean error [3] was obtained.

All the data related to the above is shown in Table 1. The first column contains the deflections of the particles in the magnetic field, which are related to the particle momentum P by $\delta = 6.36/P$, where P is measured in units Bev/c.

For the first energy range $0.91 \leq E \leq 1.38$ Bev the lengths λ_1, λ_2 and λ_3 calculated from the number of nuclear interactions in the absorbers Π_1, $\Pi_1+\Pi_2$ and $\Pi_1+\Pi_2+\Pi_3$, differ strongly among each other. Therefore for this energy range the mean free path was calculated for the absorber $\Pi_1+\Pi_2+\Pi_3$ using

$$\lambda = \frac{52}{\ln \frac{N_0}{N_0 - N_1}},$$

where N_0 is the number of particles on the surface of absorber $\Pi_1+\Pi_2+\Pi_3$ and N_1 is the number of interacting particles in these absorbers. The length λ_1 calculated from the number of nuclear interactions in Π_1 for the energy range $5.5 \leq E < \infty$ differs strongly from the values of λ_2, λ_3, λ_4 and λ_5 as calculated for $\Pi_1+\Pi_2$; Π_2 $\Pi_1+\Pi_2+\Pi_3$; $\Pi_1+\Pi_2+\Pi_3+\Pi_4$ and $\Pi_1+\Pi_2+\Pi_3+\Pi_4+\Pi_5$. Therefore λ_1 was rejected in accordance with Chauvenet's criterion.

For the purpose of comparing our data with the data of other writers we shall indicate that in [4] the value of the inelastic cross section for the interaction of 0.87 Bev protons in copper was found to be $\sigma_{Cu} = 0.85 \cdot 10^{-24}$ cm². In [5] for 1.4 Bev neutrons $\sigma_{Cu} = 0.755 \cdot 10^{-24}$ cm². In [6] for a nuclear photoemulsion and 2.2 Bev protons the cross section was $\sigma \approx 0.8\,\sigma_0$ where σ_0 is the geometric cross section. In [7] for 2.2 Bev protons $\sigma_{Cu} = 0.8 \cdot 10^{-24}$ cm².

Our data for the corresponding energy ranges are in agreement with those quoted.

From the above we can draw the following conclusions:

1. The total inelastic cross section for the interaction of protons in copper in the energy range $1 \lesssim E \lesssim 5$ Bev evidently changes slowly and is equal approximately to $0.75\sigma_0$ ($\sigma_0 = 0.98 \cdot 10^{-24}$ cm² is the geometric cross section).

2. In this energy region $E \gtrsim 5$ Bev the cross section is equal to the geometric cross section.

3. From this and from our earlier work it follows that the inelastic cross section for pion-copper interactions is larger than the cross section for protons and for energies $E \gtrsim 1$ Bev equals σ_0.

The authors wish to thank A. I. Alikhanian for making it possible to perform the measurements.

Physics Institute, Received October 6, 1955
Academy of Sciences
Armenian SSR

LITERATURE CITED

[1] N. M. Kocharian, G. S. Saakian et al., Doklady Akad. Nauk SSSR 105, 6 (1956).

[2] N. M. Kocharian, G. S. Saakian et al., Bull. Acad. Sci. USSR, Phys. Ser. 19, 5 (1955).

[3] A. Worsing and G. Heffner, Methods of Treating Experimental Data, 1953.

[4] F. F. Chew, C. P. Leavitt, A. M. Shapiro, Bull. Am. Phys. Soc. 29, 47 (1954).

[5] G. A. Snow, T. Coor, D. A. Hill et al., Bull. Am. Phys. Soc. 29, 54 (1954).

[6] L. W. Smith, C. P. Leavitt et al., Bull. Am. Phys. Soc. 28, 15 (1953); Phys. Rev. 92, 851 (1953).

[7] G. Friedlander, J. M. Miller et al., Phys. Rev. 94, 727 (1954).

TABLE 1

Total Cross Sections of Inelastic Interactions of Protons in Copper

Ranges of deflection δ	Ranges of proton energy (Bev)	Average proton energy (Bev)	Absorbers		Total No. of particles		Number of noninteracting particles after each absorber										Mean free paths of the nuclear interaction		Proton cross sections for nuclear interactions in units
			designation	total thickness (g/cm²)	p + π⁺	π⁻	Π_1		Π_2		Π_3		Π_4		Π_5		for p + π⁺	for protons	10^{-24} cm²
							p + π⁺	π⁻	p + π⁺	π⁻	p + π⁺	π⁻	p + π⁺	π⁻	p + π⁺	π⁻			
4—3	0.91—1.38	1.1	Π_1—Π_3	52	226	40	216	34	191	29	150	22	—	—	—	—	127 ± 18	140 ± 25	0.755±0.14
3—2	1.38—2.38	1.8	Π_1—Π_4	88.6	178	40	167	36	146	26	115	19	92	15	—	—	133 ± 8	156 ± 17	0.676±0.07
2—1	2.38—5.50	3.4	Π_1—Π_5	141	103	25	92	20	79	16	70	10	48	8	34	5	109 ± 12	141 ± 17	0.750±0.09
1—0	5.50— ∞	12	Π_1—Π_6	141	60	30	51	27	44	22	38	16	22	12	18	8	100 ± 14	104 ± 20	1.01±0.19

THE EFFECT OF RADIATION ON BETATRON OSCILLATIONS IN STRONG-FOCUSING SYNCHROTRONS

A. N. Matveev

(Presented by Academician N. N. Bogoliubov October 3, 1955)

1. A. A. Sokolov and I. M. Ternov [1, 2] have shown that when an electron moves in a constant axially symmetric magnetic field, because of the quantum nature of the radiation there should arise radial and axial betatron oscillations which increase with increasing electron energy. Sands [3] has examined the effect of radiation on synchrotron oscillations and has found very considerable phase oscillations resulting from the radiation.

The importance of these papers is due primarily to their practical significance. They show that at electron energies lying within the limits of contemporary technical possibilities and discussed in the literature, such large radial and phase oscillations must be generated that the operation of weak focusing cylindrical accelerators with reasonable parameters becomes impossible. From the theoretical point of view this phenomenon is interesting as an example of quantum-mechanical excitation of macroscopic oscillations. The generation of these oscillations resulting from the quantum nature of the oscillations is as inevitable as is the radiation from an accelerated charge. Therefore the limit imposed by these oscillations on the energies attainable for accelerated electrons in cyclical accelerators with weak focusing is a serious difficulty.

The present note reports the results of a study of the approximate effect of radiation on radial betatron oscillations of electrons in strong-focusing synchrotrons. Axial betatron oscillations can be examined by a similar method but since the square of their amplitude is $(E/mc^2)^2$ times smaller than for the radial oscillations, stricter criteria do not result.

2. We designate by $n_1 \gg 1$ and $n_2 \ll -1$ the indices of magnetic field decrease, respectively, in the radial focusing and defocusing portions of the sectors $\left(n_i = -\frac{r}{H_i}\frac{dH_i}{dr}\right)$. Then the equations of radial motion in the defocusing and focusing portions of the k-th sector are

$$\frac{d^2\rho_k^{(1)}}{d\theta^2} - (n_1-1)\,\rho_k^{(1)} = 0, \quad \frac{d^2\rho_k^{(2)}}{d\theta^2} + (|n_2| + 1)\,\rho_k^{(2)} = 0, \tag{1}$$

where θ designates the azimuthal angle increasing in the direct of motion. The subtended angles of the focusing and defocusing portions of the sector are designated by $\nu^{(2)}$ and $\nu^{(1)}$, respectively, so that the subtended angle of the entire sector is $\nu^{(2)} + \nu^{(1)} = 2\pi/N$, where N is the total number of sectors.

When a photon of energy ΔE is emitted there is an instantaneous change of the radius of the equilibrium orbit by the amount $\Delta x = R(1-n)^{-1}(\Delta E/E)$, where R is the radius of the equilibrium orbit. This motion of the oscillation center is mathematically equivalent* to the corresponding change of ρ in the solution of (1), which takes place abruptly at the instant of emission. Since the equations are linear their exact solution can be represented as a sum of two terms. The first term accounts for all factors such as the processes at the accelerating gaps and the radiation energy losses, but does not account for the quantum nature of these radiation losses. The second term takes the quantum nature of the radiation into consideration. We are interested only in the latter term, which will be considered below.

---

* These are equivalent, of course, from the mathematical point of view. The actual trajectory is continuous within the limits of the uncertainty principle and the Schrödinger Zitterbewegung.

In consideration of the above the solution of the betatron portion of the oscillations induced by radiation may be represented in the form

$$\begin{aligned}\rho_k^{(1)} &= A_k^{(1)} \operatorname{sh} \sqrt{n_1 - 1}\,\theta + B_k^{(1)} \operatorname{ch} \sqrt{n_1 - 1}\,\theta + \\ &+ \sum_i \varepsilon(\theta, \theta_i)\, \Delta x_{ki}^{(1)} \operatorname{ch} \sqrt{n_1 - 1}\,(\theta - \theta_i), \\ \rho_k^{(2)} &= A_k^{(2)} \sin \sqrt{|n_2| + 1}\,\theta + B_k^{(2)} \cos \sqrt{|n_2| + 1}\,\theta + \\ &+ \sum_j \varepsilon(\theta, \theta_j)\, \Delta x_{kj}^{(2)} \cos \sqrt{|n_2| + 1}\,(\theta - \theta_j),\end{aligned} \tag{2}$$

where $\epsilon(\theta, \theta_i) = 1$ for $\theta > \theta_i$ and $\epsilon(\theta, \theta_i) = 0$ for $\theta < \theta_i$, and the summations are extended over the radiative emissions in the defocusing and focusing portions of the k-th sector.

From the continuity of ρ and its derivative at the boundary between the focusing and defocusing portions, we obtain for A_k and B_k the equations

$$A_{k+2} - 2 \cos q\, A_{k+1} + A_k = N_k, \tag{3}$$

where

$$\cos q = bd - \frac{1 - \eta^2}{2\eta}\, ac, \qquad a = \operatorname{sh} \sqrt{n_1 - 1}\, \nu^{(1)}, \qquad b = \operatorname{ch} \sqrt{n_1 - 1}\, \nu^{(1)},$$
$$c = \sin \sqrt{|n_2| + 1}\, \nu^{(2)}, \quad d = \cos \sqrt{|n_2| + 1}\, \nu^{(2)}, \quad \eta = [(n_1 - 1)/(|n_2| + 1)]^{1/2}.$$

In order to conserve space the expression for N_k is not given.

The solution of (3) is

$$A_k = A_k^{(0)} \sin qk + B_k^{(0)} \cos qk + \frac{1}{\sin q} \sum_{m=0}^{k-2} \sin q(k - m - 1)\, N_m. \tag{4}$$

where $A^{(0)}$, $B^{(0)}$ are determined from the initial conditions. Without limiting generality we may assume that $A^{(0)} = B^{(0)} = 0$.

3. By definition we must calculate the quantity

$$\overline{(\Delta r)^2} = {}^1\!/_2\, [(A^{(2)})^2 + (B_k^{(2)})^2] \tag{5}$$

for very large values of k in order to evaluate the mean square deviation. From (4), using the statistical nature of the quantities $\overline{\Delta X_{ki}^{(2)}}$ and $\Delta X_{kj}^{(1)}$, and considering that the amplitudes of the oscillations are damped, subject to the law $[\Delta X(t)]^2 = [\Delta X(t')]^2\, [E(t')/E(t)]$, but that radiation damping is insignificant, and keeping in mind that the probability of emission of a quantum with energy $hc\zeta/R$ per unit time is

$$W_\zeta = \frac{1}{\pi \sqrt{3}}\, \frac{e^2}{hR} \left(\frac{mc^2}{E}\right)^2 \int\limits_{\frac{2}{3}\left(\frac{mc^2}{E}\right)^3 \zeta}^{\infty} K_{5/3}(x)\, dx, \tag{6}$$

we obtain the calculated expression

$$\overline{[\Delta r(t)]^2} = Q\,\frac{55}{48\sqrt{3}}\,\frac{hc^2 r_0}{RE}\int_0^t \left(\frac{E}{mc^2}\right)^6 dt, \tag{7}$$

where

$$Q = \frac{N\xi}{2\pi\sin^2 q}\left[\frac{\nu^{(2)}\xi}{c^2} - \frac{1}{2}\,\frac{a}{\sqrt{|n_2|+1}}\,\frac{1+\eta^2}{\eta}\right]\frac{1}{(|n_2|+1)^2} + \frac{N\xi}{2\pi\sin^2 q}\left[\frac{\nu^{(1)}\epsilon}{ac}\,\eta + \frac{1}{2}\,\frac{a}{\sqrt{n_1-1}}(1+\eta^2)\right]\frac{1}{(n_1-1)^2}$$

$\xi = b - d\cos q$, $\epsilon = d - b\cos q$. $r_0 = (e^2/mc^2)$ is the classical electron radius. (7) gives the effect of radiation on the radial betatron oscillations of electrons in a strong-focusing synchrotron.

4. We shall first write (7) for the case of a circular accelerator without sections and with weak focusing. For this purpose it is clearly necessary in (7) to set $N = 1$, $\nu^{(2)} \rightarrow 2\pi$, $\nu^{(1)} \rightarrow 0$ and to replace $|n_2| + 1$ by $1 - n_M$. We then obtain

$$\overline{[\Delta_W r(t)]^2} = \frac{55}{48\sqrt{3}}\,\frac{hc^2}{(1-n_W)^2}\,\frac{r_0}{ER}\int_0^t \left(\frac{E}{mc^2}\right)^6 dt, \tag{8}$$

which agrees with the equation obtained by A. A. Sokolov and I. M. Ternov [2].

A comparison of (7) and (8) shows that with the same law of increase of magnetic field, and the same maximum fields and energies there results

$$\left|\frac{\Delta_s r}{\Delta_W r}\right| = Q^{1/2}(1 - n_W). \tag{9}$$

From the point of view of strong focusing it is necessary to select values of $|n_s|$ as large as possible. It is seen from (9) that with sufficiently large $|n_s|$ it would be possible to decrease $|\Delta_s r|$ very considerably by comparison with $|\Delta_W r|$. However, as we know (see, for example, [4]) from a number of considerations connected with injection and technical conditions, it is impossible to use very large values of $|n_s|$; we must limit ourselves to the order of a few hundred in the case of proton accelerators and to the order of tens in the case of electron accelerators. Under these conditions the efficiency of strong focusing from the point of view of combatting the radial oscillations induced by radiation is considerably lowered.

As an example we consider the simplest case, when

$$\nu^{(2)} = \nu^{(1)}, \quad |n_2| + 1 = n_1 - 1 \equiv n_s, \quad q = \pi/2, \quad N = 2\sqrt{n_s}.$$

Then (7) is rewritten as

$$\overline{(\Delta_s r)^2} = \frac{\operatorname{ch}^2(\pi/2)}{2}\,\frac{55}{48\sqrt{3}}\,\frac{hc^2}{n_s^2}\,\frac{r_0}{ER}\int_0^t \left(\frac{E}{mc^2}\right)^6 dt, \tag{10}$$

and (9) becomes

$$\left|\frac{\Delta_s r}{\Delta_W r}\right| = \frac{\operatorname{ch}(\pi/2)}{\sqrt{2}}\,\frac{1-n_W}{n_s} \approx 1.77\,\frac{1-n_W}{n_s}. \tag{11}$$

With $n_W = 0.6$, $n_s = 25$ we obtain $|\Delta_s r/\Delta_W r| = 2.8 \cdot 10^{-2}$, i.e., strong focusing gives quite large attenuation of the oscillations.

Assuming, furthermore, as an example, that the change of energy follows the law $E(\omega t) = E_0 \sin \omega t$ and $E(\pi/2) = E_0 = 1000$ Mev we obtain from (10) for $n_s = 25$; $R = 3.5$ m that $|\Delta_s r| \simeq 0.12$ cm. This value is quite acceptable in practice. With weak focusing under the same conditions $\Delta_W r = 4.4$ cm, which is worse, since twice the amplitude of the corresponding oscillations equals approximately 12.4 cm.

Under the previous conditions but with $E(\pi/2) = 3$ Bev and $R = 10$ m we find that $|\Delta_W r| = 40.5$ cm, $|\Delta_s r| = 1.14$ cm. Thus under these conditions weak focusing is entirely unacceptable, but strong focusing gives very good results. This shows that at higher energies in order to cope with radial oscillations induced by radiation it may be necessary to employ strong focusing. It should be noted, however, that the limitation of possible values of $|n_s|$ does not permit us to thus shift the limit of highest attainable energies as far as we wish. Therefore we must also keep in mind the other possible methods of combatting the radial oscillations due to radiation which are seen directly from (7). These are, first, the change to smaller maximum magnetic fields and corresponding increase of injection energy, and, secondly, the shortening of the acceleration period.

I am indebted to Professor A. A. Sokolov for discussions.

M. V. Lomonosov Moscow State University

Received October 1, 1955

LITERATURE CITED

[1] A. A. Sokolov and I. M. Ternov, Doklady Akad. Nauk SSSR 92, 537 (1953); J. Exptl.-Theoret. Phys. USSR 25, 698 (1953).

[2] A. A. Sokolov and I. M. Ternov, Doklady Akad. Nauk SSSR 97, 823 (1954); J. Exptl.-Theoret. Phys. (USSR) 28, 431 (1955).

[3] M. Sands, Phys. Rev. 97, 470 (1955).

[4] G. Salvini, Nuovo cimento, Suppl. 11, 1, 442 (1955).

Note in Proof: We have now constructed an exact stochastic theory of the phenomenon under consideration. This theory shows that if by $|\Delta_s r|$ in (11) we understand the square root of the exact value of the mean square deviation with allowance for the anharmonicity of the oscillations in the focusing sectors and of the contribution from the defocusing sectors, this equation should contain 5.4 instead of 1.77. The value calculated in the text also follows from the exact theory, to be sure, but does not take all factors into consideration and is of the nature of an estimate.

OPALESCENCE IN THE PHASE TRANSITION OF QUARTZ

I. A. Iakovlev, T. S. Velichkina and L. F. Mikheeva

(Presented by Academician M. A. Leontovich October 21, 1955)

In order to obtain a detailed picture of the molecular mechanism involved in phase transitions of solids it is important to carry out experimental studies of these phenomena at temperatures which are as close as possible to phase transition points. The experiments should embrace a broad range of molecular processes accompanying phase transitions and should not merely aim at studying the behavior of thermodynamic parameters during a phase transition, to which a large number of papers have already been devoted. It is important to include among the problems investigated in connection with phase transformations the molecular scattering of light as well. Indeed, the basic characteristics of scattered light (intensity, state of polarization, spectral composition) provide important material concerning statistical fluctuations in the scattering medium, elastic properties, and other properties of the medium. On the other hand for the large chapter of molecular optics which deals with the scattering of light, it is of interest to introduce among the topics studied the states of solids close to their phase transformation temperatures. In fact, the well-known temperature variation of the refractive index and isothermal elastic constants of crystals close to the λ-points makes us expect to find interesting properties of light scattering in the immediate vicinity of phase transition points.

In accordance with the above considerations we have investigated the temperature dependence of molecular light scattering in quartz from 15 to 600° in which the $\alpha \rightleftarrows \beta$ transition is found (573°). The choice of this subject of investigation was determined by the known high quality of quartz single crystals, which have been very well studied with regard to a great diversity of phenomena [1, 2] and providing an object for classical studies of molecular scattering of light in solids [3-5]. It was established by Perrier and Mandrot [6] that the elastic modulus of quartz passes through a sharp minimum close to the phase transition, which leads us to expect an increase of scattered light intensity in a quartz crystal which is undergoing a phase transition. In the $\alpha \rightarrow \beta$ transition quartz is transformed from a low-temperature phase which belongs to the trigonal crystal class to a high-temperature phase which belongs to the hexagonal class of crystals. The first phase has the symmetry elements $A_3\ 3\ A_2$, the second phase has $A_6\ 6\ A_2$, i.e., it is less strongly ordered. From this it follows that the phase transition in quartz may be a λ-point [7]. The direct calorimetric solution of this problem up to the present time has not been completely unambiguous [8, 9]. It is clear, however, that the jump in entropy between the two phases, if it exists, is very small. The investigations by P. G. Strelkov of the temperature dependence of the specific volume of quartz also enable us to draw conclusions regarding how close this is to a phase transition of the second order [10].

In our experiments an intense light beam from a mercury lamp was propagated along one of the quartz crystal axes (a parallelepiped 40 × 20 × 20 mm), which was placed in a special furnace. The vertical temperature gradient in the region of the crystal did not exceed 0.01°/mm; the horizontal gradient in the direction of propagation of the light beam was 0.03°/mm. The complete cycle of the continuous experiment (15° → 600° → 15°) lasted more than 72 hours. Near the phase transition point the temperature changed at the rate of ≈ 0.3°/hr. These temperature changes were fully adequate for obtaining the results given below*.

---

* The authors are greatly indebted to V. A. Sokolov for valuable advice regarding the thermal conditions of the experiment.

Light scattered by the quartz at an angle of 90° to the primary light beam impinged on a photomultiplier used for the measurement of light scattering intensities. Nicols and light filters enabled us to regulate the polarization and spectral composition of the primary and scattered light. The experimental results for light which was not decomposed spectrally are given in Fig. 1. Along the vertical axis are given values of the ratio of polarized light intensity I_T scattered at temperature T, to the intensity I_{20° of light scattered at 20°. The temperature is given along the horizontal axis. The slope of the linear portion of the curve up to 500° agrees to within 6% with the data [5] up to 250°. Above 500° we were the first to detect a sharp λ-type peak of scattered light intensity corresponding to a phase transition of the solid.

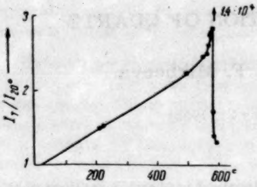

Fig. 1.

In addition to this peak we observed another optical phenomenon in the immediate neighborhood of the phase transition point. When one of the ends of the quartz single crystal reached the phase transition temperature a band of intensely scattered optically inhomogeneous scattered light appeared at that end. This inhomogeneity which had the external appearance of a fog zone, moved towards the other end of the crystal as the temperature was raised. The contours of the zone coincided with the isothermal cross sections of the quartz single crystal in the furnace. Along the primary light beam on both sides of the fog zone were transparent portions of the crystal which scattered light only weakly. These corresponded to the α phase and β phase of the crystal, respectively. The linear thickness of the fog zone, which cut through the entire 20× 20 mm cross section of the crystal, was from 1 to 3 mm. This thickness corresponds to a temperature interval of ≃ 0.1. We were able to show that the thickness of the fog zone increased when the horizontal temperature gradient in the crystal was diminished.

The intensity of the scattered white light in the fog zone was $\simeq 1.4 \cdot 10^4$ times higher than the intensity of light scattered by quartz at room temperature (indicated by a vertical arrow in the figure). Thus it was established that during a phase transition in a crystal opalescence may occur which is more intense than at the critical point of other measured substances [11].

Throughout the entire temperature range that was studied the comparative measurements of scattered light intensities at various wave lengths showed that the dimensions of optical inhomogeneities in quartz (including the fog zone) are small compared with the wave length (the $1/\lambda^4$ law is satisfied). The depolarization of the light scattered by the fog was ≃6%, which is considerably lower than the depolarization of light scattered by quartz outside the temperature region of the phase transition.

The entire course of the observed phenomena is reversible and is not accompanied by temperature hysteresis. Each crystal studied can go through numerous phase transitions. Samples of entirely different origin give identical results. The x-ray patterns before and after the experiments were identical.

The authors are grateful to G. P. Motulevich for interesting discussions during the course of the work.

M. V. Lomonosov Moscow State University Received September 3, 1955

LITERATURE CITED

[1] R. B. Sosman, The Properties of Silica, N. Y., 1927.

[2] A. V. Shubnikov, Quartz and its Uses, Acad. Sci. USSR Press, 1940.

[3] G. S. Landsberg, Z. Physik 43, 773; 44, 442 (1927).

[4] G. S. Landsberg and L. I. Mandel'shtam, J. Russ. Phys. Chem. Soc. 60, 335 (1928).

[5] G. P. Motulevich, Trans. Phys. Inst. Acad. Sci. USSR 5 (1950).

[6] A. Perrier, R. Mandrot, Compt. rend., 175, 622 (1922).

[7] L. D. Landau and E. M Lifshits, Statistical Physics, 1951.

[8] H. Moser, Physik. Z., 37, 737 (1936).

[9] N. N. Sinel'nikov, Doklady Akad. Nauk SSSR 92, 2 (1953).

[10] P. G. Strelkov, Bull. Akad. Sci. USSR, Phys. Ser. 17, 3 (1953).

[11] W. H. Keesom, Ann. Phys., 35 (340), 591 (1911).

[12] V. L. Ginzburg, Doklady, Akad. Nauk SSSR 105, 2 (1955).

Note in Proof: While our article was being printed there appeared an article by V. L. Ginzburg [12] which showed independently the possibility of the anomalous scattering of light at the quartz λ-point.

THE RELATIVISTIC KINETIC EQUATION

S. T. Beliaev and G. I. Budker

(Presented by Academician M. A. Leontovich October 13, 1955)

I. Transformation Properties of the Distribution Function

1. The behavior of the distribution function under Lorentz transformations was examined in [1] assuming invariance of the number of particles in a given element of phase space. In actuality, however, this quantity is not invariant (just as, for example, the product of ordinary density by a tridemensional volume is not invariant) since in different coordinate systems different particles will be considered to be located simultaneously in a given volume*.

The ordinary distribution function depending on 4 coordinates and 3 momenta is not in relativistically invariant form. In [2] a function was introduced which is a function of 4 coordinates and 4 momenta normalized in 8-dimensional space including a time interval, as a result of which the physical meaning of the function is completely obscure.

Thus the problem of a relativistically invariant form of the kinetic equation and of the transformation properties of the distribution function cannot be considered solved.

2. The relativistically invariant form of the distribution function in coordinate and momentum space can be obtained by using a vector F_k, which depends on 4 coordinates x_k and 4 momenta p_k such that $\int F_k d^4p = j_k$ $(k = 1, 2, 3, 4)$, where j_k is the ordinary 4-vector of the flux and density of particles.

It is easily seen that the fourth component of this vector is a distribution function which depends on 8 variables and signifies the number of particles located at a given instant of time in a unit tri-dimensional volume of spatial coordinates and of four-dimensional momentum space. The remaining 3 components represent the current vector in phase space.

The vector F_k is parallel to the 4-velocity of the particles $u_k(x, p)$ since each particle contributes to the flux in the direction of its velocity $F_k = Fu_k$. The scalar $F(x, p)$ will be called the scalar distribution function although it does not represent the particle density in any space.

These functions in addition to their relativistically invariant form are distinguished by the fact that they describe a system of particles with different (in general continuously distributed) values of rest mass. If the rest mass of all particles is the same the function F contains a δ-function: $F(x, p) = icf(x, p)\delta\left(\sqrt{-\left(p_1 - \frac{e}{c}A_1\right)^2} - mc\right)$. The scalar $f(x, p)$ which because of the δ-function can be considered to be a function of 3 (and not 4) momenta coincides with the ordinary distribution function (as can easily be shown from the definition of F). Thus the ordinary distribution function f is invariant with respect to Lorentz transformations*.

---

* The number of particles in a volume is invariant, generally speaking, only when the particles do not cross the boundaries of the volume.

** This differs from the result obtained in [1], where f in various systems differs by a factor which is velocity dependent.

3. We shall use an invariant form of Hamilton's equations:

$$\frac{dp_k}{ds} = -\frac{\partial\mathcal{H}}{\partial x_k}; \quad u_k \equiv \frac{dx_k}{ds} = \frac{\partial\mathcal{H}}{\partial p_k}; \quad \mathcal{H}(x, p) = -\sqrt{-\left(p_l - \frac{e}{c}A_l\right)^2}. \tag{1}$$

In accordance with the conservation of the number of particles and the physical meaning of F_4 we have:

$$\frac{\partial F_4}{\partial t} + \frac{\partial}{\partial x_\alpha}\left(\frac{dx_\alpha}{dt}F_4\right) + \frac{\partial}{\partial p_k}\left(\frac{dp_k}{dt}F_4\right) = 0 \quad (\alpha = 1, 2, 3). \tag{2}$$

Substituting $F_4 = Fu_4$ and using (1) we obtain a relativistically invariant equation for F which describes a system of interacting particles in an electromagnetic field:

$$[\mathcal{H}F] \equiv u_k\frac{\partial F}{\partial x_k} - \frac{\partial\mathcal{H}}{\partial x_k}\frac{\partial F}{\partial p_k} = 0. \tag{3}$$

II. The Kinetic Equation for tne Coulomb Interaction

1. The appropriate equation for the nonrelativistic case was obtained by L. D. Landau [3]. A similar equation can be obtained for the relativistic case when the particle energy $E \ll \sqrt{137\,L}\,mc^2$, where L is the Coulomb logarithm. At high energies a dominant role is played by bremsstrahlung and pair production.

Utilizing the smallness of deflections in Coulomb collisions it is possible to write for F_4 an equation of the Fokker-Planck type in the symmetric form given in [3]:

$$\frac{1}{ic}\frac{\partial F_4}{\partial t} + \frac{1}{ic}\frac{\partial}{\partial x_\alpha}\left(\frac{dx_\alpha}{dt}F_4\right) + \frac{1}{ic}\frac{\partial}{\partial p_k}\left(\frac{dp_k}{dt}F_4\right) = -\frac{\partial J_k}{\partial p_k}, \tag{4}$$

where

$$J_k(p) = \frac{1}{(ic)^2}\int d^4p'\left(F_4\frac{\partial F_4'}{\partial p_k'} - F_4'\frac{\partial F_4}{\partial p_k}\right)\frac{\Delta_i\Delta_k}{2}w(p, p', \Delta, \Delta')\,d\tau_\Delta$$
$$(d\tau_\Delta = d^4\Delta d^4\Delta'), \tag{5}$$

$\Delta_i \equiv \Delta p_i$; $\Delta_i' \equiv \Delta p_i'$ are the momentum changes due to collisions and $w(p, p', \Delta, \Delta')$ is the probability of such a change. We have assumed that the external fields are not very strong so that their effect on the collisions can be neglected.

Average deflections $\int \Delta_i\Delta_k w\,d\tau_\Delta$ can easily be calculated in the system of coordinates where an unprimed particle is at rest: $u_i = (0, 0, 0, i)$, and a primed particle is moving along the x_1 axis:

$u'_i = \left(\frac{v'\gamma'}{c}, 0, 0, i\gamma'\right)$; $\gamma = \left(1 - \frac{v^2}{c^2}\right)^{-1/2}$ In this system the integrand with d^4p' in (5) (which, as can easily be shown, is a 4-vector) is given by

$$i_1 = i_4 = 0, \quad i_2 = -\frac{2\pi e^2 e'^2 L}{v' c^2}\left(F_4 \frac{\partial F'_4}{\partial p'_2} - F'_4 \frac{\partial F_4}{\partial p_2}\right),$$
$$i_3 = -\frac{2\pi e^2 e'^2 L}{v' c^2}\left(F_4 \frac{\partial F'_4}{\partial p'_3} - F'_4 \frac{\partial F_4}{\partial p_3}\right), \tag{6}$$

which by using the vectors u_i, u'_i and the scalar F can be written in invariant form as

$$i_i = \frac{2\pi e^2 e'^2 L}{c^2} W_{ik}\left(F \frac{\partial F'}{\partial p'_k} - F' \frac{\partial F}{\partial p_k}\right), \tag{7}$$

where

$$W_{ik} = \frac{(u_l u'_l)^2}{c\,[(u_l u'_l)^2 - 1]^{3/2}}\{[(u_l u'_l)^2 - 1]\,\delta_{ik} - u_i u_k - u'_i u'_k - u_l u'_l\,(u_i u'_k + u'_i u_k)\},$$
$$u_i\,(p, x) = \partial\mathscr{H}\,(p, x)/\partial p_i = -\,[p_i - \frac{e}{c} A_i\,(x)]/\mathscr{H}\,(p, x). \tag{8}$$

As a result the invariant form of the kinetic equation for a relativistic gas is

$$[\mathscr{H}F] = -\frac{\partial J_k}{\partial p_k}; \quad J_k = \frac{2\pi e^2 e'^2 L}{c^2}\int d^4p'\,W_{kl}\left(F \frac{\partial F'}{\partial p'_l} - F' \frac{\partial F}{\partial p_l}\right). \tag{9}$$

It is easily seen that the function $F^0 = \chi\,(\mathscr{H}\,(p, x))\exp\,(p_k q_k)$, where χ is an arbitrary scalar function and q_k is an arbitrary vector, makes the right-hand side of (9) vanish identically. F^0 is an invariant form of the Maxwell distribution at arbitrary temperature $\theta = c(-q_k^2)^{-1/2}$, hydrodynamic velocity $v^0_\alpha = icq_\alpha/q_4$ and arbitrary distribution of particles with respect to mass χ (mc).

2. From (9) it is possible to obtain a relativistic equation for the ordinary function f, which, however, is not in relativistically invariant form:

$$\frac{\partial f}{\partial t} + [Hf] = -\frac{\partial j_\alpha}{\partial p_\alpha}; \quad j_\alpha = 2\pi e^2 e'^2 L\int d^2p\,\frac{W_{\alpha\beta}}{\gamma\gamma'}\left(f \frac{\partial f'}{\partial p'_\beta} - f' \frac{\partial f}{\partial p_\alpha}\right), \tag{10}$$

where now H is the ordinary Hamiltonian function:

$$W_{\alpha\beta} = \frac{\gamma^2\gamma'^2(1 - \beta_\sigma\beta'_\sigma)^2}{c\,[\gamma^2\gamma'^2(1 - \beta_\sigma\beta'_\sigma)^2 - 1]^{3/2}}\{[\gamma^2\gamma'^2\,(1 - \beta_\sigma\beta'_\sigma)^2 - 1]\,\delta_{\alpha\beta} - \gamma^2\beta_\alpha\beta_\beta -$$
$$-\,\gamma'^2\beta'_\alpha\beta'_\beta + \gamma^2\gamma'^2\,(1 - \beta_\sigma\beta'_\sigma)\,(\beta_\alpha\beta'_\beta + \beta'_\alpha\beta_\beta)\}. \tag{11}$$

($c\beta_\alpha$ (p, x); $c\beta'_\alpha$ (p', x') are the particle velocities expressed in terms of momenta).

(10) differs from the corresponding equation of Landau [3] only in the form of the $W_{\alpha\beta}$, which now are no longer only functions of velocity differences.

III. Transfer of Energy and Momentum from One Gas to Another

1. Multiplying (9) by p_i and integrating over the 4-dimensional momentum volume of a definite group of particles, we obtain after some simple transformations: $\frac{\partial T_{ik}}{\partial x_k} - \frac{e}{c} F_{ik} j_k = I_i$, where $T_{ik} = \int \mathscr{H} u_i u_k F \, d^4 p$ – is the tensor of kinetic energy and momentum of this group of particles; F_{ik} is the electromagnetic field tensor. The 4-vector $I_i = \int J_i d^4 p$ is the density of force and work associated with collisions. From (9)

$$I_i = \frac{2\pi e^2 e'^2 L}{c^2} \int d^4 p \, d^4 p' \, W_{ik} \left(F \frac{\partial F'}{\partial p'_k} - F' \frac{\partial F}{\partial p_k} \right) \tag{12}$$

(the integrals with respect to p' and p can only be taken for different particles, since integration with respect to the same particle vanishes identically). (12) is the energy-momentum flux (in unit proper time of the center of mass system of unprimed particles) which passes to an unprimed group of particles in collision with primed particles.

2. Substituting in (12) the ion distribution function F' in the form $F' = icn' \delta(p'_1 - Mc\beta_0\gamma_0)\delta(p'_2)\delta(p'_3)$ $\delta(\mathscr{H}' + Mc)$, where n, M, $\beta_0 c$ are, respectively, the density, mass and ordered ion velocity, we obtain the transfer of energy and momentum from a straight beam of monochromatic relativistic ions to a relativistic electron gas at rest. Integrating over p' and the angles of the electron momenta we obtain as a function of the absolute value of nonrelativistic electron velocity

$$\begin{aligned} \frac{\partial p}{\partial t} &= \frac{4\pi e^2 e'^2 Lnn'}{mc^2\beta_0^2}\left(1 + \frac{m}{M\gamma_0}\right), & \frac{d\varepsilon}{dt} &= \frac{4\pi e^2 e'^2 Lnn'}{mc\beta_0} \quad (\beta < \beta_0); \\ \frac{dp}{dt} &= 0, & \frac{d\varepsilon}{dt} &= -\frac{4\pi e^2 e'^2 Lnn'}{mc\beta} \quad (\beta > \beta_0), \end{aligned} \tag{13}$$

and for relativistic velocities

$$\frac{dp}{dt} = \frac{4\pi e^2 e'^2 Lnn'}{mc^2\gamma\beta_0^2}, \quad \frac{d\varepsilon}{dt} = \frac{4\pi e^2 e'^2 Lnn'}{mc}\left(\frac{1}{\beta_0\gamma} - \frac{m}{M\beta\gamma_0}\right). \tag{14}$$

The discontinuity at $\beta = \beta_0$ in the nonrelativistic region and the fact that ions with ordered velocity $c\beta_0$ do not transfer momentum to an electron gas at rest when $\beta_0 < \beta$ is an interesting consequence of the Coulomb collision law. For relativistic velocities the discontinuity practically disappears ($\sim 1/\gamma_0^2$).

Substituting for the electrons the relativistic Maxwell distribution and integrating over the absolute value of the electron velocities, we obtain ($m/M \ll 1$)

$$\frac{dp}{dt} = \frac{1}{\beta_0 c}\frac{d\varepsilon}{dt} = \frac{4\pi e^2 e'^2 Lnn'}{\beta_0^2} \frac{K_1(mc^2/\theta)}{\theta K(mc^2/\theta) + mc^2 K_0(mc^2/\theta)}, \tag{15}$$

where k_0 and K_1 are Macdonald functions.

3. Substituting in (12)

$$F = icAn\exp\left(\frac{icp_4}{\theta}\right)\delta(\mathscr{H}+Mc); \quad F' = icA'n'\exp\left(\frac{icp_4'}{\theta'}\right)\delta(\mathscr{H}+mc), \tag{16}$$

we obtain the energy transfer from one gas to the other (each gas is in thermodynamic equilibrium at a temperature different from the temperature of the other gas). After integrating by parts we obtain

$$I_4 = \frac{2\pi e^2 e'^2 Lnn'}{ic}\left(\frac{1}{\theta}-\frac{1}{\theta'}\right)\int d^4p\, d^4p' FF' W_{44}. \tag{17}$$

Averaging W_{44} over the nonrelativistic Maxwellian ion distribution and the relativistic electron distribution we obtain in this case

$$\frac{d\varepsilon}{dt} = \frac{4\pi e^2 e'^2 Lnn'}{Mc\theta'}\,\frac{1+2\dfrac{mc^2}{\theta'}+2\left(\dfrac{mc^2}{\theta'}\right)^2}{\dfrac{2\theta'}{mc^2}K_1\left(\dfrac{mc^2}{\theta'}\right)+K_0\left(\dfrac{mc^2}{\theta'}\right)}(\theta'-\theta). \tag{18}$$

Received August 9, 1955

LITERATURE CITED

[1] A. A. Vlasov, Many Particle Theory, 1950.

[2] Iu. L. Klimontovich, Doklady Akad. Nauk SSSR 87, 927 (1952).

[3] L. D. Landau, J. Exptl.-Theoret. Phys. (USSR) 7, 2, 203 (1937).

SHOCK WAVE EMERGENCE AT A STELLAR SURFACE

G. M. Gandel'man and D. A. Frank-Kamenetskii

(Presented by Academician V. N. Kondrat'ev October 22, 1955)

Internal disturbances which induce supersonic movements may lead to the production of shock waves in the interior of a star. The emergence of such a wave at the stellar surface where the density vanishes should be accompanied by peculiar effects, which we shall examine here.

We know (see, for example [1]) that on a stellar surface the density drops to zero according to a power law:

$$\rho = bx^n, \tag{1}$$

where x is the distance to the surface (measured inside the star); n is the peripheral index of the polytropic curve, which is equal to the ratio of the temperature and density indices in the law of radiant heat conductivity. Our problem is the investigation of the passage of a shock wave through a medium with such a density distribution. For this purpose the ordinary theory of "progressing" shock waves may be used [2-4].

We shall limit ourselves to the simplest case, in which the wave moves normal to the surface. Close to the instant of emergence the curvature becomes insignificant and both the wave and the surface may be assumed to be plane. Then the process is described by a set of one-dimensional equations of gas dynamics:

$$\frac{\partial\rho}{\partial t} = -u\frac{\partial\rho}{\partial x} - \rho\frac{\partial u}{\partial x}, \tag{2a}$$

$$\frac{\partial u}{\partial t} + u\frac{\partial u}{\partial x} = -\frac{1}{\rho}\frac{\partial p}{\partial x} + g, \tag{2b}$$

$$\frac{\partial}{\partial t}p\rho^{-\gamma} + u\frac{\partial}{\partial x}p\rho^{-\gamma} = 0. \tag{2c}$$

We shall consider a strong wave for which the gravitational acceleration g can be neglected. Let the wave front be at a distance X from the surface and move with the velocity

$$D = \frac{dX}{dt}. \tag{3}$$

The density of matter at a point directly in front of the wave will be denoted by ρ_0 We introduce the dimensionless density δ, velocity η and pressure π which are associated with the corresponding dimensional quantities by the relationships

$$\rho = \rho_0 \delta, \tag{4}$$

$$u = D\eta, \tag{5}$$

$$p = \rho_0 D^2 \pi. \tag{6}$$

In the last stage of the emergence of the strong wave on the surface the values of δ, η, π at a point x distant from the surface will depend only on the dimensionless separation

$$\xi = \frac{x}{X}. \tag{7}$$

Directly behind the wave front at $\xi = 1$ these quantities for a strong wave will assume the values

$$\delta(1) = h = \frac{\gamma + 1}{\gamma - 1}, \tag{8}$$

$$\eta(1) = \pi(1) = \frac{h - 1}{h} = \frac{2}{\gamma + 1}, \tag{9}$$

where γ is the index of the adiabatic curve.

A specific "progressing wave" solution is obtained for a power-law dependence of X on time:

$$|X| = C|t|^b, \tag{10}$$

from which

$$D \sim X^{\frac{b-1}{b}}. \tag{11}$$

The calculational problem is the determination of the specific index b.

Substituting (4)-(7) in (2) and neglecting g we obtain a set of ordinary differential equations:

$$(\xi - \eta) \frac{d \ln \delta}{d\xi} = n + \frac{d\eta}{d\xi}, \tag{12a}$$

$$(\xi - \eta) \frac{d\eta}{d\xi} = \frac{b - 1}{b} \eta + \frac{1}{\delta} \frac{d\pi}{d\xi}, \tag{12b}$$

$$(\xi - \eta) \frac{d \ln \sigma}{d\xi} = \beta, \tag{12c}$$

where

$$\sigma = \pi \delta^{-\gamma}, \tag{13}$$

$$\beta = \frac{d \ln D^2 \rho_0^{1-\gamma}}{d \ln X} = 2\frac{b - 1}{b} - (\gamma - 1) n. \tag{14}$$

Equations (12a) and (12c) give the first integral:

$$\frac{\sigma^{n+1}}{[\delta(\xi - \eta)]^{\beta}} = \text{const.} \tag{15}$$

The index b is an eigenvalue of the set (12). To obtain it new variables are convenient:

$$\varphi = \frac{\eta}{\xi} \tag{16}$$

and the dimensionless velocity of sound C defined by

$$C^2 = \gamma \frac{\pi}{\delta \xi^2}. \tag{17}$$

Eliminating δ and σ from (12) we obtain a set of equations

$$\frac{d\varphi}{d \ln \xi} = \frac{C^2\left[\varphi + \frac{1}{\gamma}\left(n + 2\frac{b-1}{b}\right)\right] - \varphi(1-\varphi)\frac{1-b\varphi}{b}}{(1-\varphi)^2 - C^2}, \tag{18a}$$

$$(1-\varphi)\frac{d \ln C}{d \ln \xi} =$$

$$= \frac{C^2\left[\frac{1-b\varphi}{b} + \frac{\gamma-1}{2\gamma}\left(n + 2\frac{b-1}{b}\right)\right] - (1-\varphi)\left[\varphi^2 - \left(\frac{\gamma+1}{2} + \frac{3-\gamma}{2b}\right)\varphi + \frac{1}{b}\right]}{(1-\varphi)^2 - C^2}. \tag{18b}$$

These equations are integrated subject to the initial condition: for $\xi = 1$ $\varphi = \frac{2}{\gamma+1}$; $C^2 = \frac{2\gamma(\gamma-1)}{(\gamma+1)^2}$.

The eigenvalue b is found from the condition that the integral curve passes through a singularity of the set (18) in which both the numerators and denominators of both equations vanish. The vanishing of the denominator corresponds to a transition from sonic flow to supersonic flow (with respect to the wave front).

Numerical integration by the method of successive approximations gives for n = 13/4 and γ = 5/3 the value b = 0.590. The value b < 1 shows that the wave velocity and the temperature at the wave front increase without limit as the surface is approached. The unbounded temperature rise is due to the fact that a finite quantity of heat is supplied to an ever-diminishing quantity of matter (cumulative effect).

At the instant of emergence everywhere except at the front $\xi = \infty$. The distribution at this instant is easily found from the condition that it should cease to depend on X. Hence we obtain the asymptotic curve:

$$\eta(\infty) \sim \xi^{-\frac{1-b}{b}}, \tag{19}$$

$$\delta(\infty) \sim \xi^{n}, \tag{20}$$

$$\pi(\infty) \sim \xi^{n-2\frac{1-b}{b}}. \tag{21}$$

For the distribution of physical quantities at the instant of emergence we obtain

$$u \sim x^{-\frac{1-b}{b}}, \tag{22}$$

$$\rho \sim x^{n} \sim \rho_0, \tag{23}$$

$$p \sim x^{n-2\frac{1-b}{b}}. \tag{24}$$

The temperature distribution is

$$T - \frac{p}{\rho} \sim x^{-2\frac{1-b}{b}}. \tag{25}$$

Thus in the gas-dynamical approximation the temperature of the surface becomes infinite at the instant of emergence of the wave. In actuality of course the temperature is limited due to radiation but for strong waves even black body radiation permits very high temperatures which are entirely adequate for nuclear reactions, for example.

At the surface itself the radiation mean free path and the range of the particles become infinite so that the gas-dynamical approximation is no longer fitting. Our equations must be "cut off" at distances from the surface of the order of the free path. Phenomena which take place at shorter distances may already be of a nonthermal nature and must be considered by gas-kinetic methods.

The above effect of cumulative concentration of energy when a shock wave passes through the surface of a star may be used to explain a number of astrophysical phenomena, and especially the radiation from novae, the profound significance of which has been noted by V. A. Ambartsumian [5].

Institute for Chemical Physics,
Academy of Sciences of U.S.S.R.

Received October 14, 1955

LITERATURE CITED

[1] D. A. Frank-Kamenetskii, Doklady Akad. Nauk SSSR 80, 185 (1951).

[2] L. I. Sedov, Similarity and Dimensional Methods in Mechanics (3rd Ed.), Moscow, 1954, Ch. IV.

[3] K. P. Staniukovich, Theory of Irregular Motions in Gases, Moscow, 1948.

[4] R. Courant and K. Friedrichs, Supersonic Flow and Shock Waves, For. Lit. Press, 1950, 160.

[5] V. A. Ambartsumian, Reports of the Biurakansk Observatory, 1954.

CHRONOMETRIC INVARIANTS AND FRAMES OF REFERENCE IN THE GENERAL THEORY OF RELATIVITY

A. L. Zel'manov

(Presented by Academician V. A. Fok November 2, 1955)

1. Cosmological applications of the general theory of relativity lead to the consideration of arbitrary deformations of a gravitational medium (metagalaxies) using its attached frame of reference. Coordinate systems which are at rest with respect to the same frame of reference are related by transformations of the form $\tilde{x}^0 = \tilde{x}^0 (x^0, x^1, x^2, x^3)$, $\tilde{x}^i = \tilde{x}^i (x^1, x^2, x^3)$, $\partial \tilde{x}^i / \partial x^0 = 0$. Therefore in the attached frame of reference of a medium among the quantities which are not covariant with respect to the general transformations $\tilde{x}^\alpha = \tilde{x}^\alpha (x^0, x^1, x^2, x^3)$, the more important physical quantities are invariant with respect to the transformation $\tilde{x}^0 = \tilde{x}^0 (x^0, x^1, x^2, x^3)$ (or, as we shall say, chronometrically invariant) and covariant with respect to the transformations $\tilde{x}^i = \tilde{x}^i (x^1, x^2, x^3)$, $\partial \tilde{x}^i / \partial x^0 = 0$. (Greek indices run through the values 0, 1, 2, 3; Latin indices run through only 1, 2, 3). These quantities can be considered to be tridimensional tensors and, in particular, as tensors in a tridimensional and, generally speaking, nonholonomic space which is everywhere orthogonal to time lines.

We shall assume that all x^α are real, $x^0 = ct$, $ds^2 = g_{\mu\nu}\, dx^\mu dx^\nu$, in Galilean coordinates $ds^2 = (dx^0)^2 - (dx^1)^2 - (dx^2)^2 - (dx^3)^2$, that the $g_{\mu\nu}$ are continuous in the x^α together with the first and second derivatives with respect to these coordinates and that otherwise all quantities satisfy the usual conditions assumed in the general theory of relativity. When we refer to tridimensional tensors we shall omit mention of the number of dimensions.

2. Let $Q^{ik\ldots p}_{00\ldots 0}$ be components of a world tensor of rank $\underline{n}$ with all superscripts different from zero and all subscripts, numbering $\underline{m}$, equal to zero. Then the quantities $T^{ik\ldots p} = (g_{00})^{-m/2}\, Q^{ik\ldots p}_{00\ldots 0}$ from a (tridimensional) contravariant tensor of rank n-m which is chronometrically invariant (ch. i.). For ch. i. metric tensors h^{ik} and h_{ik} of the fundamental determinant $h = |h_{ik}|$ and the line element du we obtain $h^{ik} = -g^{ik}$; $h_{ik} = -g_{ik} + g_{0i} g_{0k} (g_{00})^{-1}$; $h = -g\, (g_{00})^{-1}$, where $g = |g_{\mu\nu}|$; $du^2 = h_{ik} dx^i dx^k$. For the ch. i. time interval $d\tau$ we obtain $c\, d\tau = (g_{00})^{-1/2} g_{0\alpha} dx^\alpha$. Clearly, $ds^2 = c^2 d\tau^2 - du^2$. For the ch. i. velocity of a point we have: $v^i = dx^i / d\tau$. Ch. i. differential operators will be denoted by asterisks. Then

$$\frac{{}^*\partial}{\partial t} = \frac{c}{\sqrt{g_{00}}} \frac{\partial}{\partial x^0}, \qquad \frac{{}^*\partial}{\partial x^i} = \frac{\partial}{\partial x^i} - \frac{g_{0i}}{g_{00}} \frac{\partial}{\partial x^0}, \tag{1}$$

$$\frac{{}^*\partial^2}{\partial x^i \partial t} - \frac{{}^*\partial^2}{\partial t\, \partial x^i} = \frac{F_i}{c^2} \frac{{}^*\partial}{\partial t}, \qquad \frac{{}^*\partial^2}{\partial x^i \partial x^k} - \frac{{}^*\partial^2}{\partial x^k \partial x^i} = \frac{2A_{ik}}{c^2} \frac{{}^*\partial}{\partial t}. \tag{2}$$

The expressions for the ch. i. vector F_i and the ch. i. tensor A_{ik} follow clearly from (1) and (2). We note the identity

$$\frac{{}^*\partial A_{ik}}{\partial t} + \frac{1}{2}\left(\frac{{}^*\partial F_k}{\partial x^i} - \frac{{}^*\partial F_i}{\partial x^k}\right) = 0. \tag{3}$$

The identical fulfillment of the equation $F_i = 0$ in the four-dimensional region under consideration is the exact (necessary and sufficient) condition for the possibility of everywhere transforming g_{00} into 1 and all $\partial g_{0i}/\partial x^0$ into 0 by a transformation of the coordinate x^0. The identical fulfillment of $A_{ik} = 0$ in the same region is the exact condition for the possibility of everywhere transforming all g_{0i} into 0 by transforming x^0 i.e., the exact condition for the existence of an integrable factor of $d\tau$ or, what amounts to the same, for a holonomic frame of reference. At each world point we introduce a local 4-dimensional geodesic system Σ whose velocity with respect to the given frame of reference is zero at that world point. Then F_i with reversed sign is the acceleration vector of the frame of reference with respect to Σ and A_{ik} is the tensor of the angular rotational velocity of the frame of reference with respect to Σ. We denote by D_{ik} the ch. i. tensor of the rates of deformation of the frame of reference with respect to Σ. (We omit "with respect to Σ" hereafter). Then

$$D_{ik} = \frac{1}{2}\frac{{}^*\partial h_{ik}}{\partial t}, \quad D^{ik} = -\frac{1}{2}\frac{{}^*\partial h^{ik}}{\partial t}, \quad D = \frac{{}^*\partial \ln\sqrt{h}}{\partial t} \tag{4}$$

($D = D^j_j$). Replacing the ordinary derivatives with respect to x^i in the expressions of the three-dimensional Christoffel symbols formed from the h_{ik} and for the corresponding operator of tridimensional covariant differentiation ∇_i by ch. i. derivatives we obtain expressions for ch. i. Christoffel symbols $\Delta_{ij,k}$ and Δ^k_{ij} for the ch. i. operator of covariant differentiation ${}^*\nabla_i$. Then, if Q_i is a vector,

$$({}^*\nabla_{ik} - {}^*\nabla_{ki})\, Q_l = \frac{2A_{ik}}{c^2}\frac{{}^*\partial Q_l}{\partial t} + H_{lki}^{\cdot\cdot\cdot j} Q_j, \tag{5}$$

$$H_{lki}^{\cdot\cdot\cdot j} = \frac{{}^*\partial \Delta^j_{il}}{\partial x^k} - \frac{{}^*\partial \Delta^j_{kl}}{\partial x^i} + \Delta^m_{il}\Delta^j_{km} - \Delta^m_{kl}\Delta^j_{im}. \tag{6}$$

We introduce $C_{lkij} = \frac{1}{4}(H_{lkij} - H_{jkil} + H_{klji} - H_{iljk})$, $C_{lk} = C_{lki}^{\cdot\cdot\cdot i}$ and $C = C^k_k$. If $A_{mn} = 0$ or $D_{mn} = 0$, then $H_{lkij} = C_{lkij}$.

3. Let m_0 be the rest mass of a particle; $p^a = m_0 dx^a/ds$ and Ξ^a are the world vectors of momentum and force; E is the ch. i. energy of the particle; p^i is the ch. i. momentum; ξ^i is the ch. i. nongravitational force (see also Section 5). Then $c^2 P_0 (g_{00})^{-1/2} = E = mc^2$, $cP^i = p^i = mv^i$; the ch. i. mass $m = m_0(1 - v_j v^j/c^2)^{-1/2}$, $c^3 \Xi_0 (g_{00})^{-1/2} = \xi_1 v^1 (1 - v_j v^j/c^2)^{-1/2}$, $c^2 \Xi^i = \xi^i (1 - v_j v^j/c^2)^{-1/2}$. For constant m_0 the world equations of motion become

$$\frac{dE}{d\tau} + mD_{ij}v^iv^j - mF_iv^i = \xi_i v^i, \tag{7}$$

$$\frac{dp^k}{d\tau} + \Delta^k_{ij} p^i v^j + 2m\left(D^k_i + A_i^{\cdot k}\right) v^i - mF^k = \xi^k. \tag{8}$$

We now consider the propagation of light in a vacuum. Let K^a be the world wave vector, and ω the ch. i. angular frequency. Then $cK_0 (g_{00})^{-1/2} = \omega$, $cK^i = \omega a^i$, $a^i = dx^i/du$, $c\, d\tau = du$. We have

$$\frac{1}{\omega}\frac{d\omega}{du} + \frac{1}{c} D_{ij}\alpha^i\alpha^j - \frac{1}{c^2} F_i \alpha^i = 0, \tag{9}$$

$$\frac{1}{\omega}\frac{d(\omega\alpha^k)}{du} + \Delta^k_{ij}\alpha^i\alpha^j + \frac{2}{c}\left(D^k_i + A_i^{\cdot k}\right)\alpha^i - \frac{1}{c^2} F^k = 0. \tag{10}$$

In (7) and (8) we note the presence of inertial force associated with the deformation of the reference frame and energy change of the moving particle. This nonrelativistic effect is similar, as can be seen from (9) and (10) to the Doppler effect resulting from the deformation of the reference system.

4. Let $T_{\mu\nu}$ be the world tensor of energy and momentum; ρ the ch. i. mass density; J^i the ch. i. density of mass flow which is equal to the momentum density (ρc^2 is the energy density, $J^i c^2$ the density of energy flux); U^{ik} is the density of momentum flux, $U = U^j_j$. Then $T_{00}(g_{00})^{-1} = \rho$, $c\, T^i_0 (g_{00})^{-1/2} = J^i$, $c^2 T^{ik} = U^{ik}$. The energy-momentum law becomes

$$\frac{{}^*\partial\rho}{\partial t} + D\rho + \frac{1}{c^2} D_{ij} U^{ij} + \left[\left({}^*\nabla_i - \frac{1}{c^2} F_i\right) J^i\right] - \frac{1}{c^2} F_i J^i = 0, \tag{11}$$

$$\frac{{}^*\partial J^k}{\partial t} + DJ^k + 2\left(D^k_i + A_i^{\cdot k}\right) J^i + \left[\left({}^*\nabla_i - \frac{1}{c^2} F_i\right) U^{ik}\right] - \rho F^k = 0. \tag{12}$$

The square brackets contain expressions for the physical divergence of J^i and U^{ik}. The Einstein equations for the gravitational field, solved with respect to the contracted world tensor of curvature can be written as

$$\frac{{}^*\partial D}{\partial t} + D_{jl} D^{lj} + A_{jl} A^{lj} + {}^*\nabla_j F^j - \frac{1}{c^2} F_j F^j = -\frac{\varkappa}{2}\left(\rho c^2 + U\right) + \Lambda c^2, \tag{13}$$

$${}^*\nabla_j\left(h^{ij} D - D^{ij} - A^{ij}\right) + \frac{2}{c^2} F_j A^{ij} = \varkappa J^i, \tag{14}$$

$$\begin{aligned} \frac{{}^*\partial D_{ik}}{\partial t} - \left(D_{ij} + A_{ij}\right)\left(D^j_k + A_k^{\cdot j}\right) + DD_{ik} - D_{ij} D^j_k + 3A_{ij} A_k^{\cdot j} + \\ + \frac{1}{2}\left({}^*\nabla_i F_k + {}^*\nabla_k F_i\right) - \frac{1}{c^2} F_i F_k - c^2 C_{ik} = \frac{\varkappa}{2}\left(\rho c^2 h_{ik} + 2U_{ik} - U h_{ik}\right) + \Lambda c^2 h_{ik}, \end{aligned} \tag{15}$$

where κ is the Einstein gravitational constant and Λ is the cosmological constant.

5. Hereafter we shall use coordinate systems fixed in the medium (in particular the metagalaxy) and shall neglect the energy flux with respect to the medium and nongravitational mass forces. Then $J^i = 0$, $U_{ik} = p h_{ik} - \epsilon_{ik} = p_0 h_{ik} - \sigma_{ik}$, where p is the true pressure, p_0 is the equilibrium pressure, $\epsilon_{ik} = \sigma_{ik} - \frac{1}{3} \sigma h_{ik}$, $\sigma = \sigma^j_j$, σ_{ik} is the viscous stress tensor (all quantities are ch. i.); $\epsilon_{jl} D^{jl} \geq 0$, $\sigma D \geq 0$.

We note the following deductions.

From (3), (11) and (12) we obtain the equations of change of a vortex. In the absence of ordinary (first) viscosity ($\epsilon_{ik} = 0$) they can become

$$\frac{{}^*\partial}{\partial t}[A_{ik}(E+pV)] = \frac{E+pV}{2(\rho+p/c^2)^2}\left(\frac{{}^*\partial\rho}{\partial x^i}\frac{{}^*\partial p}{\partial x^k} - \frac{{}^*\partial\rho}{\partial x^k}\frac{{}^*\partial p}{\partial x^i}\right), \tag{16}$$

and (11) and (12) can be written as $dE + pdV = 0$ (with $\epsilon_{ik} \neq 0$, $dE + pdV = \epsilon_{jl}D^{jl}V\,d\tau$), $(\rho + p/c^2)F_i = {}^*\partial p/\partial x^i$, where V and $E = V\rho c^2$ are the ch. i. volume and energy of an element of the medium. If the medium is nonviscous ($\sigma_{ik} = 0$) and barotropic the $A_{ik}(E + pV)$ do not change in time, which indicates conservation of vortex lines and conservation of the product of the stress of vortex tubes by the relativistic thermal function (E + pV).

For motion peculiar to galaxies we may take (7) and (8) if by ξ^k we understand the departure of the gravitational-inertial force from its macroscopic value mF^k and neglect other deviations of the world metric from the macroscopic. We see clearly the effect mentioned in section 3 on the energy of the peculiar galactic motion. Neglecting this motion and confining ourselves to the macroscopic metric we consider $\Delta\omega/\omega$ in directions for which at the point of observation $D_{ij}a^i a^j \neq 0$, $F_i a^i \neq 0$. Then from (9) we find that in each given direction $\Delta\omega/\omega$ is in first approximation proportional to the distance (Δu) of the source from the point of observation, and for a given distance in any two opposite directions the half sum of the magnitudes of $\Delta\omega/\omega$ gives the magnitude of the Doppler effect, and the half difference gives the magnitude of the Einstein effect.

We introduce the nonnegative quantities $R = fV^{1/3}$, $\partial f/\partial t = 0$; $\Pi^2 = D_{jl}D^{jl} - \frac{1}{3}D^2$; $\Omega^2 = \frac{1}{2}A_{jl}A^{jl}$ ($\Pi = 0$ for an isotropic deformation, $\Omega = 0$ in the absence of rotation). Since $3R^{-1}({}^*\partial R/\partial t) = D$, we obtain from (13) and (15)

$$3R^{-1}({}^*\partial^2R/\partial t^2) + \Pi^2 - 2\Omega^2 + {}^*\nabla_j F^j - \frac{1}{c^2}F_jF^j = -\frac{\varkappa}{2}(\rho c^2 + 3p) + \Lambda c^2,$$

$$3R^{-2}({}^*\partial R/\partial t)^2 - \frac{1}{2}\Pi^2 + 3\Omega^2 - \frac{c^2}{2}C = \varkappa\rho c^2 + \Lambda c^2.$$

Let $F = 0$, $A_{ik} = 0$ for $\Lambda = 0$. Clearly, ${}^*\partial^2R/\partial t^2 < 0$ and a regular minimum of R is impossible. The increase of R is either, in some cases, monotonic and unbounded for $\tau \to \infty$ or, in other cases, continues up to a regular maximum followed by a decrease. The time interval τ from the beginning of the increase of R to any instant during this increase is smaller than the value of $R({}^*\partial R/\partial t)^{-1}$ at that instant.

P. K. Shternberg State Astronomical Institute

Received October 25, 1955

CASCADE CURVES FROM ELECTRONS AND PHOTONS IN LEAD

I. P. Ivanenko

(Presented by Academician D. V. Skobel'tsyn October 13, 1955)

The solution of the equations of cascade theory in heavy elements meets with difficulties as a result of the strong dependence of the total photon absorption coefficient $\sigma(E)$ on energy and the marked Coulomb scattering of shower electrons. The usual methods of solving cascade equations through the use of Laplace-Mellin [1] transforms are unsatisfactory in this case. In the present article we used the so-called "method of moments" which was developed in [2].

In [3] recursion formulas were obtained for the moments $\overline{t^n}(E_0, 0)$ with respect to t:

$$\overline{t^n}(E_0, 0) = \int\limits_0^\infty N(E_0, 0, t)\, t^n\, dt \Bigg/ \int\limits_0^\infty N(E_0, 0, t)\, dt,$$

where t is the thickness of the layer of matter traversed by the particles*; E_0 is the energy of the primary particle. The formulas were derived with allowance both for the energy dependence of the photon absorption coefficient $\sigma(E)$ and the Coulomb scattering of charged particles. The recursion formulas enable us, on the basis of the known function for the "equilibrium" spectrum (i.e., integrated with respect to depth) which is the zeroth moment, to calculate all succeeding moments $\overline{t^n}$.

In [4] "equilibrium" spectra averaged with respect to depth were obtained for cascade particles. To a good approximation the electron spectra were independent of the photon absorption coefficient, and the photon spectra were easily calculated taking into consideration the energy dependence of the photon absorption coefficient. In [5] the particle equilibrium spectra were calculated with allowance also for Rutherford scattering.

The moments $\overline{t}$ and $\overline{t^2}$ were first calculated approximately for lead in [6], where an attempt was also made to associate and $\overline{t^2}$ with the position and number of particles at the shower maximum. However the relationships which were obtained were approximate and correct only for very large energies.

In [7] the moments $\overline{t}$ and $\overline{t^2}$ were calculated for lead for primary electrons with allowance for the energy dependence $\sigma(E)$ of photons and approximate consideration of scattering, and from the calculated moments cascade curves were constructed. However, the approximation in [7] is very complicated and gives an unsatisfactory description of the cascade process for $t < t_{max}$ and $E_0 < 10^8$ ev. We therefore undertook a calculation of $\overline{t}$ and $\overline{t^2}$ for lead allowing for the energy dependence of $\sigma(E)$ and for scattering and ionization losses with as great accuracy as possible.

In these calculations we used an expression for the equilibrium spectrum which was obtained from [5]. However, in [5] the equations for the equilibrium spectrum allowing for scattering and ionization losses were solved approximately. The exact solution can be obtained by the method of associated equations [8]:

---

* The depth t is measured everywhere in radiation units; the radiation t-unit in lead was taken to be 5.9 g/cm².

$$N_p(\varepsilon_0, \varepsilon, \vartheta) = \sum_{n=0}^{\infty} f_n^p(\varepsilon_0, \varepsilon) P_n(\cos\theta); \quad f_n^p(\varepsilon_0, \varepsilon) =$$

$$= \frac{2n+1}{4\pi} \frac{\varepsilon_0}{q} \varepsilon e^{\sqrt{\varepsilon^2 + a_n^2}} \left(\frac{\varepsilon}{a_n + \sqrt{\varepsilon^2 + a_n^2}} \right)^{a_n} \int_{\varepsilon}^{\infty} \frac{e^{-\sqrt{x^2 + a_n^2}}}{x^2} \left(\frac{a_n + \sqrt{x^2 + a_n^2}}{x} \right)^{a_n} dx, \tag{1}$$

where $P_n(\cos\theta)$ are Legendre polynomials; $a_n = 1/2\ \epsilon_k \sqrt{n(n+1)/q}$, $\epsilon = qE/\beta$; $E_k = 21$ Mev; $q = 2.29$; β is the critical energy for a given substance*.

For $a_n = 0$ (1) goes over into the equation of Tamm and Belen'kii for the equilibrium spectrum neglecting scattering. The inaccuracy of the Tamm-Belen'kii spectrum is due to the approximate form of their initial equations, and has been estimated several times [9]. It does not exceed 4.5% for shower particles of energy $E > 10^7$ ev. On the other hand the agreement between the values of $N_p(\epsilon_0, \epsilon, \theta)$ calculated in [5] and that given by (1) is satisfactory since they agree to within 6%.

The values of the photon absorption coefficient $\sigma(E)$ were taken from [10]. The results of the calculation are given in Table 1. For small ϵ_0 the moments of the cascade curves from a primary photon are considerably larger than the moments from a primary electron; for very large $\epsilon_0 \{\overline{t^n}\}\ p \simeq \{\overline{t^n}\}\Gamma$. This difference is due to the fact that electron of small energy lose a large part of their energy by ionization instead of by the production of secondary particles which are free to continue the cascade process.

The values obtained for $\overline{t}$ and $\overline{t^2}$ were used to construct cascade curves. We have approximated the cascade curves by using the sum of the Laguerre polynomials $L_n^i(x)$:

$$N(E_0, 0, t) = (\gamma t)^i e^{-\gamma t} \sum_{n=0}^{k} A_n L_n^i(\gamma t). \tag{2}$$

The coefficients A_n were determined by the orthogonality of the $L_n^i(x)$:

$$A_n = \frac{\gamma n!}{\Gamma(n+i+1)} \int_0^{\infty} N(E_0, 0, t) L_n^i(\gamma t)\, dt. \tag{3}$$

The coefficient γ was set equal to the minimum absorption coefficient of the most penetrating part of the radiation — the photons; $\gamma = 0.24$.

The cascade curves from primary photons were approximated by using the sum of the Laguerre polynomials $L_n^1(x)$:

---

* We shall show that the solution (1) is still approximate since the initial equations are approximate; but in [4] from these equations (but with neglect of scattering) an approximate "equilibrium" spectrum was obtained which differs from the exact solution [9] by only 4%. Multiple scattering is accurately included in the equations so that (1) also differs from the exact solution by not more than 4%.

$$\{N_p(E_0, 0, t)\}^{\Gamma} = (\gamma t)\, e^{-\gamma t} \sum_{n=0}^{k} A_n L_n^1(\gamma t); \tag{4}$$

here $L_0^1(x) = 1$; $L_1^1(x) = 2-x$; $L_2^1(x) = 3-3x + x^2/2$.

The coefficients A_n are simply related to the moments $\overline{t^n}$:

$$A_0 = \gamma \frac{E_0}{\beta}; \quad A_1 = \frac{\gamma}{2} \frac{E_0}{\beta} \{2 - \gamma \{\overline{t_p}(E_0, 0)\}^{\Gamma}\};$$
$$A_2 = \frac{\gamma}{3} \frac{E_0}{\beta} \{3 - 3\gamma \{\overline{t_p}(E_0, 0)\}^{\Gamma} + \frac{\gamma^2}{2} \{\overline{t_p^2}(E_0, 0)\}^{\Gamma}\}; \ldots$$

The results of the calculations by equation (4) are given in Fig. 1. We note that the chosen form of approximation (4) satisfies exactly the boundary condition $\{N_p(E_0, 0, t)\}_{t=0}^{\Gamma} = 0$.

The cascade curves from primary electrons were approximated by using the sum of the polynomials $L_n^0(x)$:

$$\{N_p(E_0, 0, t)\}^{p} = e^{-\gamma t}\left(\sum_{n=0}^{k} A_n L_n^0(\gamma t) + C L_{k+1}^0(\gamma t)\right); \tag{5}$$

here $L_0^0(x) = 1$; $L_1^0(x) = 1-x$; $L_2^0(x) = 1-2x + x^2/2$; $L_3^0(x) = 1-3x + 1.5x^2 - x^3/6$.

The coefficient C was determined by the condition

$$\{N_p(E_0, 0, t)\}_{t=0}^{p} = 1. \tag{6}$$

The results obtained from (5) are given in Fig. 2.

The moments of the cascade curves from a primary electron for $E_0 = 10^9$ ev were taken from [2]; for $E_0 = 10^{10}$ ev they were taken from [7]. The values obtained from (5) and condition (6) for $\{N_p(E_0, 0, t)\}^p$ with E_0 equal to 10^9 and 10^{10} ev and for various values of t are given in Table 2. We note that in all the cascade curves the absorption coefficient in the "tail" i.e., were $N(E_0, 0, t)$ is of the order of unity or less, is close to the experimental value [11] $\sigma = 0.24$. The study of the approximations (4) and (5) with $\gamma = \sigma_0 = 0.773$, i.e., for light elements, shows that for $E_0/\beta \gg 1$ the approximate cascade curves differ from the exact curves by not more than

TABLE 1

		ϵ_0												E_0, ev	
		1	3	5	10	20	30	40	50	60	70	90	118.1	10^9	10^{10}
From a primary photon	$\{\overline{t_p}(E_0, 0)\}^{\Gamma}$	4.32	4.34	4.37	4.63	5.22	5.69	6.04	6.30	6.53	6.74	7.08	7.43		
	$\{\overline{t^2_p}(E_0, 0)\}^{\Gamma}$	36.1	34.8	34.8	37.1	43.8	50.3	54.3	58.5	61.8	64.7	70.3	74.6		
From a primary electron	$\{\overline{t_p}(E_0, 0)\}^{P}$	0.343	1.14	1.65	2.34	3.18	3.67	4.01	4.25	4.43	4.60	4.88	5.17	7.00	9.20
	$\{\overline{t^2_p}(E_0, 0)\}^{P}$	1.43	6.88	10.7	16.2	22.3	26.4	29.0	32.0	34.1	36.1	39.2	42.7	70.8	110.0

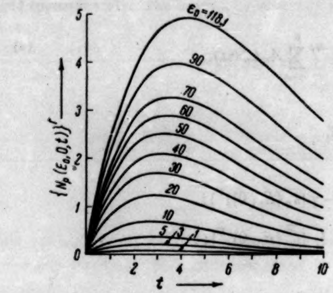

Fig. 1.

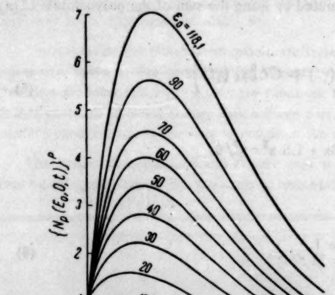

Fig. 2.

5%. Consequently, considering the inaccuracy of the "equilibrium" spectrum we may expect that the cascade curves obtained from (4) and (5) will differ from the exact curves by not more than 10%. A comparison of cascade curves (4) averaged over a photon spectrum of the form $\varphi(E) = \begin{cases} 1/E & \text{for } E < 330 \text{ Mev} \\ 0 & \text{for } E > 330 \text{ Mev} \end{cases}$ with experimental data [11] shows that the calculated and experimental curves agree to within 5%. Thus we may assume that the cascade curves in Figs. 1 and 2 satisfactorily describe the cascade process in lead.

TABLE 2

	E_0, ev	t																			
		0.1	0.5	1.0	1.4	2.0	2.6	3.0	3.5	4.0	4.5	5.0	5.5	6.0	7.0	8.0	10.0	12.0	14.0	16.0	20.0
$\{N_p(E_0, 0, t)\}^p$	10^9	2.06	5.77	9.35	11.52	13.8	15.1	15.6	15.9	15.8	15.5	15.1	14.5	13.8	12.2	10.6	7.66	5.26	3.48	2.23	0.840
	10^{10}	3.98	16.3	33.3	46.7	65.4	82.1	91.8	102.2	110.6	117.0	121.6	125.2	125.8	124.6	119.3	101.4	79.9	59.5	42.3	18.9

In [2] the method of random trials was used to obtain cascade curves for lead. However in [12] a rough approximation was used for electrons from photons below 10 Mev and for the Coulomb scattering of charged particles; thus the curves are satisfactory for $E_0/\beta \gg 1$. In this energy region the curves of [12] agree with ours within 10-15%.*

I consider it my pleasant duty to express my gratitude to Professor S. Z. Belen'kii for valuable advice and assistance, and to T. V. Klopkova who performed a considerable portion of the calculations.

M. V. Lomonosov Moscow State University

Received July 10, 1955

LITERATURE CITED

[1] L. Landau, G. Rumer, Proc. Roy. Soc. (London) 166, 213 (1938); H. Snyder, Phys. Rev. 53, 960 (1938); 76, 1563 (1949); B. Rossi and K. Greisen, The Interaction of Cosmic Rays with Matter, 1948.

[2] S. Z. Belen'kii, Cascade Processes in Cosmic Rays, 1948; S. Z. Belen'kii, J. Exptl.-Theoret. Phys (USSR) 19, 940 (1949); S. Z. Belen'kii and B. I. Maksimov, J. Exptl.-Theoret. Phys. (USSR) 22, 102 (1952).

[3] S. Z. Belen'kii, J. Exptl.-Theoret. Phys.(USSR) 19, 940 (1949); 22, 102 (1952).

[4] I. G. Tamm, and S. Belen'kii, J. Phys. (USSR) 1, 177 (1939).

[5] S. Z. Belen'kii and B. I. Maksimov, J. Exptl.-Theoret. Phys. (USSR) 22, 102 (1952).

[6] S. Z. Belen'kii, J. Exptl.-Theoret. Phys. (USSR) 14, 384 (1944).

[7] G. T. Zatsepin, Doklady Akad. Nauk SSSR 63, 243 (1948).

[8] B. Rossi, High Energy Particles, 1955.

[9] S. Z. Belen'kii, Cascade Processes in Cosmic Rays, 1948; B. Rossi, High Energy Particles, 1955.

[10] W. Heitler, The Quantum Theory of Radiation, Oxford, 1954.

[11] W. Blocker, R. W. Kenney and W. K. Panofsky, Phys. Rev. 79, 3, 419 (1950).

[12] R. R. Wilson, Phys. Rev. 86, 261 (1952).

---

* The curves of [12] averaged over the spectrum 1/E agree with experimental data [11] within the limits 2-3%. However such good agreement may be considered accidental, as is admitted by the author of [12], since he obtained curves from photons for E ≥ 20 Mev, while the spectrum from 1 to 20 Mev was treated only approximately.

SOVIET PHYSICS – "DOKLADY" VOL. 1, NO. 2 OCTOBER, 1956.

(Translation of all papers in the "Physics" Sections of the Proceedings of the Academy of Sciences of the USSR, Vol. 107, Nos. 1-6, March-April, 1956)

CONTENTS

		Russian	
	Page	Issue No.	Page
On the True Shape of X-Ray Spectra. M. A. Blokhin	145	1	33
On the Indirect Exchange Interaction. S. V. Vonsovskii and Iu. M. Seiidov	149	1	37
On the Impossibility of Explaining the Stability of Hyperons by their Large Spins. I. I. Gurevich	152	1	41
The Interaction of 300 Mev π^--Mesons with Protons, Deuterons and Nuclei in Nuclear Emulsions. L. S. Dulkova, T. A. Romanova, I. B. Sokolova, L. V. Sukhov, K. D. Tolstov and M. G. Shafronova	154	1	43
Axially Symmetric Electron Beams of a Given Shape. V. T. Ovcharov	158	1	47
Unusual V^0-Decay. E. Fridlender and S. Bercha	162	1	51
Instrumental Distortion of X-Ray Spectra. M. A. Blokhin	165	2	229
Primary Ionization by Fast Muons. G. P. Eliseev, V. A. Liubimov and A. M. Frolov	169	2	233
Diffusion Chamber Study of Negative Pion Scattering in Hydrogen. M. Kozodaev, R. Suliaev, A. Filippov and Iu. Shcherbakov	171	2	236
The Application of Fermi's Equation to the Polarization of Scattered Fast Nucleons. I. I. Levintov	175	2	240
The Diffractive Scattering of Fast Deuterons. A. I. Akhiezer and A. G. Sitenko	180	3	385
The Vertex Part at High Energies. V. Z. Blank	184	3	389
The Temperature Dependence of the Elastic Constants of Quartz. V. G. Zubov	187	3	392
The Determination of Internal Conversion Ratios for the Isomeric Transition of In^{114}. V. M. Kel'man, R. Ia. Metskhvarishvili, V. A. Romanov, L. I. Rusinov and K. A. Konoplev	189	3	394
The Effect of Quantum Fluctuations of Radiation on Electron Motion in Periodic Magnetic Systems. A. A. Kolomenskii	192	3	398
Fine and Hyperfine Structure of Paramagnetic Resonance in Bivalent Europium. A. A. Manenkov and A. M. Prokhorov	196	3	402
The Theory of the Striated Positive Column. I. M. Chapnik	199	4	529
The Sublimation of Silver Studied with Radioactive Tracers and a Mass Spectrometer. Iu. V. Kornev and E. Z. Vintaikin	203	5	661
Application of the Detailed Balancing Ratio $\frac{\sigma_{12}\sigma_{31}\cdot\sigma_{23}}{\sigma_{21}\sigma_{13}\cdot\sigma_{32}} = 1$ to an Ion Beam of Fixed Composition. M. I. Korsunskii, Kh. L. Leviant and L. I. Pivovar	206	5	664
Nuclear Reactions of High Energy Protons in Copper. N. M. Kocharian, G. S. Saakian, M. T. Aivazian, Z. A. Kirakosian and A. S. Aleksanian	209	5	668
The Effect of Radiation on Betatron Oscillations in Strong-Focusing Synchrotrons. A. N. Matveev	211	5	671

CONTENTS (continued)

		Russian	
	Page	Issue No.	Page
Opalescence in the Phase Transition of Quartz. I. A. Iakovlev, T. S. Velichkina and L. F. Mikheeva	215	5	675
The Relativistic Kinetic Equation. S. T. Beliaev and G. I. Budker	218	6	807
Shock Wave Emergence at a Stellar Surface. G. M. Gandel'man and D. A. Frank-Kamenetskii	223	6	811
Chronometric Invariants and Frames of Reference in the General Theory of Relativity. A. L. Zel'manov	227	6	815
Cascade Curves from Electrons and Photons in Lead. I. P. Ivanenko	231	6	819

The expanded program of the American Institute of Physics comprises translation of four leading Soviet physics journals, as listed below. These translations, by competent, qualified scientists, will provide all research laboratories and libraries with accurate and up-to-date information of the results of research in the U.S.S.R.

Soviet Physics — Technical Physics

A translation of the "Journal of Technical Physics" of the Academy of Sciences of the U.S.S.R. The 1956 volume, which was originally announced as containing eighteen issues, is instead being issued monthly, in expanded issues. All issues of the original Russian journal for 1956 will be translated. Approximately 4,000 Russian pages. Annually, $90.00 domestic, $95.00 foreign.

Soviet Physics — Acoustics

A translation of the "Journal of Acoustics" of the Academy of Sciences of the U.S.S.R. Four issues per year, approximately 500 Russian pages. Annually, $20.00 domestic, $22.00 foreign. The 1955 issues of "Journal of Acoustics" U.S.S.R. will also be published. Will consist of two volumes, approximately 500 pages, and the subscription price will be $20.00 for the set.

Soviet Physics "Doklady"

A translation of the "Physics Section" of the Proceedings of the Academy of Sciences of the U.S.S.R. Six issues per year, approximately 900 Russian pages. Annually $25.00 domestic, $27.50 foreign.

Soviet Physics — JETP

A translation of the "Journal of Experimental and Theoretical Physics" of the Academy of Sciences of the U.S.S.R. Twelve issues per year, approximately 2,600 Russian pages. Annually $60.00 domestic, $64.00 foreign. Back issues of Volume 1 and 2 are available at a special price of $30.00 for both to subscribers to Volume 3.

Subscriptions should be addressed to the American Institute of Physics, 57 East 55th Street, New York 22, N.Y.